HEPATIC UPTAKE OF PROTEIN-BOUND PALMITATE: ROLE OF EXTRACELLULAR BINDING PROTEIN

BY

BASSAM M. ELMADHOUN

A Thesis

Submitted to the Faculty of Graduate Studies

in Partial Fulfillment of the Requirements

for the Degree of

Doctor of Philosophy

Faculty of Pharmacy, University of Manitoba

THE UNIVERSITY OF MANITOBA

FACULTY OF GRADUATE STUDIES

*****

COPYRIGHT PERMISSION PAGE

HEPATIC UPTAKE OF PROTEIN-BOUND PALMITATE: ROLE OF EXTRACELLULAR BINDING PROTEIN

BY

BASSAM M. ELMADHOUN

A Thesis/Practicum submitted to the Faculty of Graduate Studies of The University of Manitoba in partial fulfillment of the requirements of the degree of

DOCTOR OF PHILOSOPHY

This thesis is dedicated to

My mother and my sister, for their love, encouragement, and unlimited support. I have strong believe that, without their prayer, earnest request, and please to Allah for me, I could not have accomplished this work. They are the greatest people in my life. Also I dedicate this thesis to my lovely wife Somayah Deeb, whose true love and unlimited support during my undergraduate and graduate studies, made it possible for me to overcome all difficulties encountered in my research and in my daily life.

ACKNOWLEDGMENTS

I would like to thank my supervisor Dr. **Frank Burczynski** for his advice, guidance in research, and encouragement. I am indebted to him for his contribution in my experimental work and in bringing this thesis to a successful conclusion.

I would like to acknowledge the members of my advisory committee, Dr. **Gerry Y. Minuk,** Dr. **Dan S. Sitar**, and Dr. **Keith Simons**, for their advice and critical review of this thesis.

I would like to thank Dr. **B. Luxon** for reviewing my thesis and being my external examiner.

I would like to thank **G. Q. Wang**, for teaching me various experimental techniques, for his contribution to the work in this thesis and for his friendship.

I would like to express my gratitude to Dr. **Saleh Ambah**, the chairman of Pharmaceutical Solutions Industry (PSI), Jeddah, Kingdom of Saudi Arabia, for his motivation and support in helping me complete my graduate work.

I thank Mr. **Ashok Prashar**, Novapharm Biotech Inc. Canada, for help in particle size and size distribution of lipid vesicles. Mr. **Greg Pokrajac**, Particle Sizing System, USA, for help in particle size and zeta potential determination of lipid vesicles. Dr. **Y. M. She**, Department of Physics and Astronomy, Faculty of Science, University of Manitoba, Canada, for help in analysis of mass spectra.

I would like to express my sincere gratitude to my cousin Dr. **Manal Swairjo** for her valuable personal communication and experience particularly in the achievement of the last project in my research.

This research was made possible, in part, by grants from the Medical Research Council of Canada, University of Manitoba Research Development Fund, and a University of Manitoba Graduate Fellowship.

ABSTRACT

The role of extracellular binding proteins such as albumin (ALB) on the uptake of highly protein-bound cellular substrates, e.g. long-chain fatty acids (palmitic acid, PA), has been a controversial issue for more than three decades. To gain an understanding into their role, we designed three sets of studies. The first study determined the ALB-PA high affinity constant (K_a) using the heptane-to-buffer partitioning technique. In that study, we found that the K_a was independent of binding protein concentration over a range of 0.1 to 800 μM; the equilibrium unbound ligand concentration was constant only at low ALB concentrations (< 10 μM) and low ALB-to-PA molar ratios (≤ 1:2); radiolabeled impurities in the manufacturer-supplied [^{3}H]-palmitic acid can significantly affect the cellular palmitate uptake rate, suggesting that non-[^{3}H]-palmitate radiolabeled substances are also substrates for the uptake process.

The second study determined if an ionic interaction between the protein-ligand complex and hepatocyte or cardiac myocyte surface enhanced the overall uptake of [^{3}H]-palmitate. In that study, we used α_1-acid glycoprotein, isoelectric point (pI) ≈ 2.7; conalbumin, pI ≈ 6.4; lysozyme, pI ≈ 11.0; ALB, pI ≈ 4.8 and; ALB that had been modified to yield proteins with pI values of 3.5, 4.7, 7.5 and 8.6. Our results showed a linear relationship between neonatal hepatocyte-[^{3}H]-palmitate clearance and protein pI (r^2 = 0.98). In contrast, there was an overall poor relationship between neonatal cardiac myocyte-[^{3}H]-palmitate clearance and protein pI (r^2 = 0.48). We suggested that an ionic interaction between the

extracellular protein and cell surface might be responsible for supplying more ligand to cells for uptake.

The third study examined the rate and mechanism of transfer of anthroyloxy labeled palmitic acid (AOPA) from ALB and a modified ALB (ALB_{E1}, pI $\approx$ 7.5) to model membranes (neutral and charged lipid vesicles). In that study, we determined that the rate of AOPA transfer from both proteins decreased nonlinearly when ionic strength increased. Maximum transfer occurred at neutral pH (7.4). Transfer was directly dependent on concentration of acceptor lipid vesicles, increased by increasing protein-bound concentration, and was affected by the lipid membrane surface charge. We suggested that AOPA transfer from binding proteins to lipid membranes occurred through two concomitant processes, an aqueous diffusion of the free ligand and a collisional interaction between the protein-ligand complex and membranes. The latter study strengthened our hypothesis that charged amino acid residues on proteins are important for a collisional interaction between ligand-protein complexes and cell surface. Collectively, results from this thesis provide evidence that uptake from the protein-bound fraction contributes a significant portion to the overall cellular palmitate uptake mechanism.

LIST OF FIGURES

LIST OF TABLES

ABBREVIATIONS

AGP	α_1-acid glycoprotein
ALB	bovine serum albumin
ALB_E	ALB reacted with ethylenediamine for 2 hours
ALB_{E1}	ALB reacted with ethylenediamine for 10 minutes
ALBm	ALB reacted with maleic anhydride
ALBs	ALB reacted with succinic acid
ANOVA	analysis of variance
AOPA	16-(9-anthroyloxy) palmitic acid
B	buffer
BSA	bovine serum albumin
CONALB	conalbumin
dl	deciliter
DOPC	synthetic 1,2-dioleoyl-sn-glycero-3-phosphocholine
DOPE	synthetic 1,2-dioleoyl-sn-glycero-3-phosphoethanolamine
DOPS	synthetic 1,2-dioleoyl-sn-glycero-3-phosphoserine
DPH	1,6-diphenyl-1,3,5-hexatriene
EDTA	ethylenediamine tetraacetic acid
EMP	electrophoretic mobility
FAs	fatty acids
FFA	free fatty acid

Hr	hour
H	heptane
I-FABP	Intestinal fatty acid-binding protein
K_a	high-affinity equilibrium binding constant
K_d	equilibrium dissociation constant
KD_a	kilodalton
K_{off}	dissociation rate constant
LCFA	long-chain fatty acid
L-FABP	liver fatty acid-binding protein
LYS	lysozyme
MEM	minimum essential medium
ml	milliliter
M_w	molecular weight
n	number of samples
NBD-DOPE	1,2-dioleoyl-sn-glycero-3-phosphoethanolamine-N-(7-nitro-2,1,3-benzoxadiazole-4-yl)
PBS	phosphate buffer saline
P_c	partition coefficient
pI	isoelectric point
PR^+	heptane-to-buffer partition ratio in the presence of protein
PR^-	heptane-to-buffer partition ratio in the absence of protein

rpm	round per minute
sec	second
SA	stearylamine
SD	standard deviation
SEM	standard error of the mean
μl	microliter
α	free (unbound) fraction
neuLUVs	neutral large unilamellar vesicles
-veLUVs	negatively charged large unilamellar vesicles
+veLUVs	positively charged large unilamellar vesicles

TABLE OF CONTENTS

Chapter one

Literature review

Fatty acids (FAs) are essential substrates for every living cell. Their multiple physiological functions make them critical for the regulation of a broad spectrum of metabolic activities inside living cells as well as in the plasma compartment of blood. They are available to cells as circulating free fatty acids (FFA), bound to serum albumin, or as triglycerides. LCFA are preferred substrates for energy production particularly in the heart [1, 2]. In addition to their cellular oxidation as fuel, free fatty acids have various important biological functions such as (a) energy storage in the form of triglycerides; (b) essential substrates for the production of phospholipid components of plasma membranes; (c) precursors for the synthesis of important biological mediators such as eicosanoids and (d) recently, as important intracellular mediators for gene expression [3, 4]. These biological functions require the continuous supply of a sufficient amount of fatty acids. The following outlined the role of fatty aids in normal physiology.

A.1. Fatty acids and energy supply

Fatty acids from dietary fats or released from adipose tissue stores, circulate in the blood as bound to albumin and are highly extracted by muscle, liver, heart, and many other tissues. Inside the cell, FAs are bound to cytosolic fatty acid binding protein (FABP), which transports them to the site of action. They are oxidized in mitochondria by β-oxidation. They have a higher energy density than carbohydrates and are stored in the form of triglycerides in large quantities in fat tissues. Most of cells cannot synthesize or store fatty acids in

sufficient amounts for oxidative energy requirements. Cardiac myocytes, for example, depend more on a continuous supply of fatty acids for contractile activity of the heart than can be supplied from triglycerides stores inside the cell [1, 2].

Inside the cell, FAs are activated to their CoA derivatives (fatty acyl CoA) on the outer mitochondrial membrane by the help of carnitine carrier. Carnitine acyltransferase (the key enzyme that attaches the fatty acyl group to carnitine carrier) is an important regulator of fatty acid oxidation and ketone bodies synthesis. Further oxidation of acetyl CoA in tricarboxylic acid cycle (TCA) yields additional high-energy bound phosphate (ATP). The net energy yields from tricarboxylic acid cycle and oxidative phosphorylation are 12 ATP for each acetyl group oxidized. In the liver, much of the acetyl CoA is converted to ketone bodies, which are released into circulation and used as fuels by some tissues such as muscle, kidney, and brain. In addition to FAs β-oxidation in mitochondria, α-, ω-, and peroxisomal oxidation of FAs also occurs [3].

FAs with 20 or more carbon atoms or branched fatty acids may be oxidized by a process involving the α-carbon (α-oxidation). Oxidation of this carbon results in release of carboxyl group in the form of CO_2. This process takes place mainly in the brain and nervous tissue. ω-oxidation is a process where FAs are oxidized at the ω-carbon of the chain by enzymes located in the endoplasmic reticulum. In this process, the methyl group at the end of fatty acid chain is converted to a carboxyl group; thus a dicarboxylic acid is produced.

Normally, this process is a minor oxidation pathway except in conditions that interfere with β-oxidation such as a deficiency in β-oxidation key enzymes at which dicarboxylic acids are produced in high amounts [3].

In peroxisomes, long-chain fatty acids (20-26 carbons) are oxidized through a pathway called peroxisomal oxidation. This process is similar to β-oxidation; however, it differs in that hydrogen peroxide is produced which can generate oxygen free radicals. Hydrogen peroxide is converted to water and oxygen by the effect of catalase enzyme. No ATP is produced in peroxisomal oxidation [3].

A.2. Fatty acids and biosynthesis.

Endogenous fatty acids (produced in cells) or exogenous fatty acids (obtained from diet) are used for the synthesis of triglycerides (fatty acid storage from); phospholipids, sphingolipids, cholesterol (building blocks of cell membrane) and eicosanoids (important regulators of cell function). In the liver, the activated form of fatty acid (fatty acyl CoA) reacts with glycerol-3 phosphate to form phosphatidic acid. The latter is converted to diacylglycerol by a process of dephosphorylation. Another fatty acyl CoA reacts with the diacylglycerol to form triacylglycerol. Triacylglycerols are not stored in the liver but secreted into the circulation packaged with cholesterol, phospholipids, and proteins to form low density lipoproteins [3, 5].

Phospholipids are synthesized from fatty acid. Fatty acyl CoA reacts with glycerol 3-phosphate producing phosphatidic acid. Various polar groups are

added to phosphatidic acid at carbon 3 of the glycerol 3-phophate moiety. The latter process yields amphipathic molecules such as phosphatidylcholine, phosphatidylinositol, and cardiolipin [3].

Sphingolipids, which are the membrane components of central nervous system, are also synthesized from fatty acids. Synthesis of sphingolipids is similar to synthesis of glycerophospholipids but differ in that acetyl CoA e.g. palmitoyl CoA reacts with serine rather than glycerol [3].

Cholesterol, which is circulating in blood in lipoproteins, is synthesized by a pathway that requires acetyl CoA. Liver and the intestine are the main sites of cholesterol biosynthesis. Pathway for cholesterol synthesis involves three major and complicated steps. Because cholesterol is a precursor of bile salts, the liver has the highest rate of cholesterol biosynthesis than other tissues [3].

Prostaglandins, thromboxanes, and leukotrines (eicosanoids) are important regulators of cell function. They participate in many processes such as inflammatory response, control of bleeding, regulation of smooth muscle contraction, and regulation of water and sodium excretion by the kidney. They are also regulating bronchoconstriction and bronchodilation. These molecules are synthesized from polyunsaturated fatty acids containing 20 carbon atoms such as arachidonic acid (the most common precursor of the eicosanoids), linoleate and α-linolenate. Arachidonic acid cannot be synthesized in the body and therefore, it can be obtained from the diet or other fatty aids from which arachidonic acid can be synthesized e.g. the essential fatty acid linoleate [3].

A.3. Fatty acids and membrane proteins

of fatty acids on Cl^- channel is not dependent on fatty acid metabolism; thus it is

It is reported that some cytoplasmic proteins can be modified post-translationaly by fatty acids. Palmitic acid (a long-chain fatty acid) is covalently attached to proteins through thioester linkage at cysteine residues. This acylation (palmitoylation) is known to be a reversible process and can determine the extent to which a protein is associated with membrane. The palmitoyl groups on the membrane-bound protein are rapidly exchanged between other neighboring proteins. The process of acylation and deacylation of proteins can affect their binding and localization to membranes. Deacylation process results in removing the protein from the membrane and the dissociated protein can act as a component of signal transducing pathway. Rab protein, Src-family members, and G-proteins are examples of lipid-modified proteins [6, 7].

A.4. Fatty acids and ion channels

Studies on the effect of fatty acids on apical membrane Cl^- channel in airway epithelia have shown that unsaturated fatty acids e.g. arachidonic acid, linoelaidic acid, myristoleic acid, and oleic acids can reversibly inhibit apical membrane Cl^- channel. Arachidonic acid, for example, is one of the major fatty acid components of membrane phospholipids that under certain conditions can be released into extracellular environment and act as a signaling molecule. This fatty acid may have regulatory effect on Cl^- channel and control the rate of transepithelial Cl^- secretion. Further studies showed that the inactivation effect

possible that fatty acids directly interact with protein associated with Cl^- channel and alter its function [8, 9].

Fatty acids also stimulate Na^+-Ca^{++} exchange and passive Ca^{++} permeability of cardiac sarcolemmal vesicles [10]. Such effect requires anionic charge. This effect may have a significant implication when the level of fatty acids increases during myocardial ischemia. A number of studies showed that free fatty acids can act as messenger molecules that regulate many ion channels such as Na^+, K^+, Ca^{++}, and Cl^- channels. In all cases, the effect of fatty acids on ion channels is believed to be direct and not mediated by cellular signaling pathway. The action of fatty acids on ion channel suggests that these molecules may have an important regulatory effect on various cell functions [11].

A.5. Fatty acids as signal transducers

Action of fatty acids has been shown to be involved in more complex interaction with cell signaling pathway than the direct effects as described on ion channel. Amri, et al. [12] showed that LCFAs have a regulatory role on the expression of adipose-related genes during differentiation of preadipose cells to adipose cells. Many other investigators have suggested that fatty acids can act as intermediates in controlling differentiation and / or proliferation of mammary epithelial cells [13, 14]. Grimaldi, et al. [15] showed that nonmetabolized long-chain fatty acids e.g. α-bromopalmitate exerts the same induction effect on adipose-related gene as native fatty acid.

A.6. Fatty acids and biogenesis

Because fatty acids constitute the basic structure of cell membrane and the membrane of intracellular compartments, it is reasonable to believe that DNA synthesis and regeneration could be regulated by fatty acid concentration inside the cell. Linoleic acid increases DNA synthesis in hepatoma cells transfected with liver fatty acid binding protein. Metabolic products of linoleic acid are important since the inhibition of cyclooxygenase (enzyme responsible for linoleic acid metabolism) by indomethacin completely stops the growth stimulation. Increasing delivery of fatty acids may enhance cell proliferation and modulation of organ growth. On the other hand, decreasing delivery of fatty acids would retard organ growth. In either case, the clinical benefit of increasing or decreasing fatty acid uptake is evident. The latter case may be important in the treatment of cancer [16].

A.7. Other roles of fatty acids in normal physiology

1- Fatty acids can influence the binding of low density lipoprotein (LDL) to its receptors [17]. Fatty acids inhibit binding and uptake of LDL; thus they may be important modulators of LDL metabolism.

2- Fatty acids can reverse arrhythmias in cardiac myocytes [18]. This effect is confined to polyunsaturated long-chain fatty acids. Monounsaturated or saturated fatty acids have no such effect. Polyunsaturated fatty acids could be useful antiarrhythmic agents similar to class I antiarrhythmic drugs such as lidocaine. The mechanism through which fatty acids

reverse arrhythmias remains speculative. It is possible that the effect of those fatty acids on activity of various ion channels may be partially responsible for the observed effect [19].

3- Fatty acids can regulate the expression of some enzymes involved in their catabolism such as lipoprotein lipase [20, 21]. It is possibly that the regulation of lipoprotein lipase activity by fatty acid has an important implication in control of uptake and metabolism of these substrates by adipocytes during starvation.

4- Fatty acids accumulation in the lipoproteins has a stimulatory effect on cholesteryl ester transfer protein (CETP). This protein mediates the transfer of cholesteryl esters from high density lipoprotein (HDL) to very low density lipoprotein (VLDL). The accumulation of fatty acids on lipoproteins is seen particularly during lipolysis [22].

5- An essential fatty acid such as linoleic acid has a protective role on various skin disorders. This fatty acid binds covalently with another fatty acid attached to cerebrosides in the skin to produce acylglucosylceramide, which prevent water's evaporation from skin. Linoleic acid is also a precursor for the synthesis of arachidonic acid (an important precursor of eicosanoids)[3].

6- Fatty acids have an important regulatory effect on intracellular pH. The magnitude of pH change depends on fatty acid level [23]. The effect of fatty acid on intracellular pH may be important in the regulation of various

cell functions such as pH sensitivity of certain ion channels and enzymes, inhibition of glycolysis, secretion of insulin, and cellular fuel homeostasis [24].

In addition to their important biological functions, long-chain fatty acids have been shown to be involved in various pathophysiological conditions. For example, free fatty acid and glycerol plasma concentrations and turn over rates are elevated in patients with various types of cancers [25]. Elevated plasma levels of LCFA have been shown to contribute to the suppression of immune function in patient with acute leukemia [26]. Development of insulin resistance and fasting hyperglycemia in non-insulin dependent diabetic patients has been shown to be a result of elevated plasma free fatty acid [27, 28]. Elevated plasma concentrations of LCFA are common in a number of diseases such as in coronary heart disease, atherosclerosis, cholestatic liver disease, gallstones, obesity and nephrotic syndrome [29-32]. Excessive free fatty acid uptake by muscle cells has been suggested to be involved in the early stage of the development of human myopathy [33]. Based on this information, careful regulation of all aspects of long-chain fatty acid disposition including cellular uptake would be of great clinical benefit.

In plasma, fatty acids are highly bound to circulating albumin. Despite their extensive protein binding (unbound fraction is less than 0.01 %) [34], the liver (extraction ratio > 90%) [35-37] and the heart (extraction ratio 40 to 70 %) [38-40] are extremely efficient in extracting them from the circulation.

The route of fatty acid transport from the circulation to the cytoplasm of the cell involves several discrete but interrelated events [41, 42]. These events could be summarized as follows:

Extracellular transport of fatty acids

Fatty acids in plasma are transported in the form of triglycerides in chylomicrons and lipoproteins or tightly bound to serum albumin. On their way from the capillary to the extravascular space, fatty acids have to pass the capillary wall. At this point, the liberated fatty acid from triglycerides (by the action of endothelial lipoprotein lipase) may be taken by the endothelial cells and transferred to the interstitial space. Albumin-fatty acid complexes may also pass the endothelium through clefts or by carrier-mediated transcytosis.

Cellular uptake of fatty acids

In the interstitial fluid, fatty acids and other albumin-bound ligands are taken up by the cell in their unbound forms. This means that the albumin-fatty acid complex must dissociate prior to ligand uptake. Whether spontaneous dissociation of albumin-ligand complexes is capable of supplying the required free ligands or albumin-bound ligands take part in the uptake process is controversial. The under lying mechanism(s) remain unclear. Following dissociation from albumin, fatty acids traverse cell membrane to their site of action. Several models have been proposed to explain the cellular uptake mechanism. Some investigators strongly believe that cellular fatty acid uptake is a simple passive process regulated mainly by lipid physical properties. This

belief is supported by the reports that the ionization properties of fatty acids in lipid bilayers, at physiological pH, result in a high population of the un-ionized form, which spontaneously flip-flops to the inner leaflet.

On the other hand, some investigators argue strongly that carrier proteins in the cell membrane are required for the transfer of fatty acid across the lipid bilayer. This belief is supported by the reports that the cellular uptake of fatty acid displays features compatible with carrier mediated transport. To date, three fatty acid transporters have been cloned and characterized. These include the plasma membrane fatty acid binding protein ($FABP_{pm}$), fatty acid transporter (FAT), and fatty acid transport protein (FATP). The contribution of these carriers to the overall uptake process and factors regulating the transport process of these substrates across cell membrane is currently undergoing much investigation.

Intracellular transport of fatty acids

Following desorption from the inner membrane leaflet, fatty acids enter the cytosol as monomer or bound to 14 KDa cytosolic fatty acid binding proteins (FABP). Similar to albumin, cytosolic FABP increases the aqueous solubility of fatty acids in the cytoplasm. Through protein binding, the overall diffusional flux of fatty acids in the cytoplasm is increased several fold. Several lines of evidence suggest that different FABPs in different tissues may transport fatty acids by different mechanisms. For example, it is believed that fatty acid transfer from L-FABP to lipid membranes occurs by diffusional process; whereas a membrane–

protein collisional interaction may occur for transfer from I-FABP. This suggests that, the movement of fatty acid in intestinal enterocytes is subject to regulation.

Many studies designed to elucidate facilitated uptake (defined as membrane mediated enhanced protein-ligand dissociation rate) support the view that a facilitation process is operative in hepatocytes isolated from adult rats [43-45]. The facilitation process expressed by hepatocytes was not seen in cardiac myocytes isolated from adult rats [46]. Some reports suggest that specific recognition sites exist on the cell surface of neonatal cardiac myocytes that may mediate the dissociation of albumin-fatty acid complex and thereby enhance substrate uptake [47, 48]. Total rather than the unbound concentration of fatty acid was shown to account for the uptake rate. The authors speculated that serum albumin, in an unknown way, may play a role in the cellular uptake mechanism [48]. Whether cellular uptake of these substrates occurs only from the unbound pool or whether extracellular binding proteins play an important role in the overall uptake is controversial.

Of the proponents who speculate that a facilitation process is operative, several mechanisms have been postulated to explain the dependence of uptake on the protein-bound complex. One of the proposed theories is that contact of the protein-ligand complex on the cell surface induces a conformational change in the complex and releases the bound ligand which makes it available for uptake [49, 50]. A second possibility is that site specific collisional exchanges

might be responsible for the direct off loading of protein-bound ligands at the cell surface. Such a process occurs for enzyme reaction. [51].

The most plausible mechanism proposed to explain how uptake can occur from the protein-ligand fraction includes an ionic field effect associated with the cell surface charge [52]. Recent studies by Burczynski, et al. examined the effect of protein surface charge on the uptake of long-chain fatty acid such as palmitic acid by hepatocyte suspension. In that study, the authors used binding proteins of different surface charge characteristics (different isoelectric points). The observed hepatocyte-palmitate clearance was greatest when the basic protein lysozyme (pI=11) was used and lowest in the presence of the acidic protein α_1-acid glycoprotein (pI=2.7). They concluded that an ionic interaction between extracellular binding protein and the hepatocyte surface was responsible for providing more unbound ligand than expected.

Many reports of protein-membrane interactions have been described in the literature. Wadhwani, et al [53] showed that the blood nerve barrier and blood brain barrier preferentially transported cationized albumin (pI more than 7) over native albumin (pI = 4.9). The authors explained this enhancement by the presence of anionic microdomains on the basal lamina of the perineurial cells, which preferentially attracted the oppositely charged macromolecules. Nishida, et al. [54] tested the interaction of bovine serum albumin, as a model protein, with aluminum oxide hydroxide (microcrystalline structure which may be used for the treatment of phosphatemia). They found that the interaction of bovine serum

albumin occurred rapidly, maximum at pH 6.4, was significantly reduced by the presence of phosphate, and depended on the amount of adsorbent. The authors found that bovine serum albumin is negatively charged and aluminum oxide hydroxide is positively charged at near neutral pH; thus the electrostatic attraction between them is strong. Ghitescu, et al. [55] showed that the net electrical charges of circulating molecules play important roles in the permeability of such molecules through the cells. They studied renal permeability of anionic, neutral and cationic albumins and found that cationic albumin was cleared from the circulation faster than neutral or anionic albumin. This enhancement at the basement membrane was due to the presence of anionic sites on the membrane. Norde and Lyklema [56] studied the effect of charge, ionic strength, and temperature on the adsorption of human plasma albumin at negatively charged polystyrene surfaces. They demonstrated that the net surface charge on both protein molecules and adsorbent material has a significant effect on the adsorption process. Galis, et al. [57] and Raicu, et al. [58] showed that uptake and transcytosis of albumin when carrying fatty acids is increased when compared with delipidated albumin. It was suggested that binding of fatty acid to albumin promotes the albumin-fatty acid-membrane interaction.

Many other reports outlined in the literature showed that the protein surface charge has a significant role on the protein influx rate across various types of cells such as proximal tubular cells [59], hepatocytes [60] and endothelial cells [61]. Collectively, these studies as well as many others

describing the ionic interactions between cellular macromolecules and plasma membrane showed that protein surface charge could be an important factor to be taken into account in studying uptake processes.

Research goal

The purpose of our research work is to further our knowledge for the role of extracellular binding proteins particularly serum albumin on the cellular uptake process of long-chain fatty acids. Our main research goal was to provide evidence supporting the notion that serum albumin not only functions as a carrier of long-chain fatty acids throughout the circulation but also has a direct role in fatty acid uptake through an interaction with the cell surface.

Research objectives

In order to achieve our research goal we designed our work into three studies. **The objective of the first study** was to determine the high affinity binding constant (K_a) of albumin-palmitate complex and to test the hypothesis that the determined K_a is independent of protein concentration. This was necessary to accurately calculate the unbound fraction and interpret the property of uptake studies. **The objective of the second study** was to test the hypothesis that cellular uptake of long-chain fatty acid (e.g. [^{3}H]-palmitic acid) occurred from both the unbound and protein-bound fractions. In this study we investigated the effect of protein surface charge on the uptake of highly purified [^{3}H]-palmitic acid by hepatocyte and cardiac myocytes isolated from neonatal rats. **The objective of the third study** was to test the hypothesis that transfer of

fatty acid from binding protein to cell membranes is enhanced through a collisional interaction of the complex with the membrane surface. In this study we determined the kinetics of a long-chain fatty acid (e.g. anthroyloxy labeled palmitic acid; AOPA) transfer from binding proteins to model membranes of different surface charge. In this study we also determined the effect of acceptor lipid vesicle concentration, aqueous ligand solubility, and the binding protein concentration on transfer rate.

Chapter two

Binding of [^{3}H]-palmitate to bovine serum albumin: Effect of radiolabeled impurities on binding constant and hepatocyte-[^{3}H]-palmitate uptake studies

B.1. Introduction

The hepatic uptake process is typically studied in the presence of binding proteins such as ALB and tracer ligand concentration. Studies make use of ALB concentrations ranging from a low of 5μM to physiological (500 μM) and tracer ligand concentration [44]. Use of tracer ligand concentration ensures that binding occurs to the single high-affinity site of ALB. This allows investigators to calculate an apparent high-affinity equilibrium binding constant (K_a) for that site. Other investigators [62] choose to conduct uptake studies using constant ligand-to-ALB molar ratios such as 0.01:1, 0.1:1, 1:1, 2:1 over a wide range of ALB concentrations (16 to 600 μM). For all studies, the precise determination of unbound fraction is critical in elucidating the uptake process.

Calculating an unbound fraction requires knowledge of the K_a value for the ALB-ligand complex. There are several methods currently available for determining the unbound long-chain fatty acid concentration in the presence of binding proteins. Some methods use spectrophotometric titration or utilize a fluorescent probe such as acrylodan-derivatized intestinal fatty acid binding protein [63] or doxorubicin-ALB as a free fatty acid sensor protein [64]. The former probe undergoes a wavelength shift when binding fatty acids and as such is easy to analyze. The later probe shows a decrease in absorption band at 600 nm with increasing fatty acid concentration. Third method involves equilibrium dialysis. Protein-bound ligands are separated from the unbound ligands by a physical barrier such as polyethylene sheeting [65, 66]. A drawback of this

method is that it cannot be used to determine the unbound fatty acid fraction in the presence of high ALB concentrations, e.g. greater than 50 μM [67]. These methods result in estimates of K_a that ranged from a low of 0.3 X 10^8 M^{-1} [68] to a high of 4.6 X 10^8 M^{-1} [69, 70]. Use of the lower estimates leads one to calculate higher unbound fractions, whereas using the higher K_a values leads to much lower calculated unbound fractions.

The simplest and most widely used technique employs partitioning of long-chain fatty acids between an organic and an aqueous phase. However, this technique results in K_a values from 0.2 X 10^8 M^{-1} [71] to 1.4 X 10^8 M^{-1} [43]. The order of magnitude difference in K_a makes interpretation of uptake data difficult. Moreover, this technique requires calibration. Burczynski, et al. previously described [72] potential problems that occur in calibrating this method due to radiolabeled impurities. In this study, we repeated and extended those initial observations to determine the effect of both hydrophilic and lipophilic impurities on the K_a for the ALB-palmitate complex. This method was used to test the hypothesis that the ALB-palmitate K_a is a constant value at all ALB concentrations. It has been suggested that K_a for the ALB-long-chain fatty acid complex may not be a constant but may be dependent on ALB concentration [73]. We extended those studies to determine the unbound palmitate concentration at different ALB concentrations when the protein-to-ligand molar ratio was kept constant.

B.2. Materials

[9,10-^{3}H]-palmitic acid (56.5 Ci / mmol) with a radiochemical purity of 97.8% was obtained from New England Nuclear, Boston, MA, USA. ALB (essentially fatty acid-free) was obtained from Sigma Chemical Co. (St. Louis, MO). All other chemicals were obtained from Sigma Chemical Co. with the exception of heptane, which was purchased from Fisher Scientific (Pittsburg, PA). The aqueous buffer used throughout all experiments was phosphate buffer saline (PBS), which had a composition of (in mM) 137 NaCl, 2.68 KCl, 1.65 KH_2PO_4, 8.92 Na_2HPO_4, 3 NaN_3, with pH adjusted to 7.4 using 0.1 N NaOH.

B.3. Methods

B.3.1. Construction of incubation vessel

Glass scintillation vials (20-ml borosilicate glass with white urea screw caps; Fisher), 150-ml Erlenmeyer flasks, and 500- and 1000-ml glass bottles (Wheaton, USA) with black urea screw caps were used. For the 150- ml Erlenmeyer flasks, we used plastic stoppers instead of urea screw caps. A sampling tube (1.6- mm ID capillary tubes; catalog number 7980A, Corning, U.S.A.) was inserted through a predrilled hole in the cap of each vessel. The capillary tube was secured to the cap using Press-Tite contact cement (no. 6; LePage, Ontario, Canada). A Sure-cap (Cat. #B4422, Baxter Scientific Products) was used to cover the outer end of each capillary tube.

B.3.2. Purification of [^{3}H]-palmitic acid

[^{3}H] Palmitic acid was purified as previously described [74]. A 1 ml sample of the manufacturer-supplied solution of [^{3}H]-palmitic acid was added to 0.98 ml research quality distilled water (18mΩ.cm^2) containing 0.1 N NaOH and approximately 1 mg thymol blue. Heptane (1.2 ml) was layered onto the aqueous phase, and the mixture was vortex-mixed for 60 s. After separation, the heptane phase was discarded, fresh heptane was added, and the procedure repeated. After two such extractions, the aqueous phase was acidified using two drops of 6 N HCl, heptane added, and the mixture vortex-mixed for 60 s. The purified palmitate contained in the heptane phase was harvested, fresh heptane added to the acidified aqueous phase, and the extraction procedure was repeated. The second heptane phase was combined with the first. The harvested heptane was evaporated until approximately 20 μl heptane remained, at which time 1 ml of 100% ethanol was added. The purified [^{3}H]-palmitic acid was stored in ethanol at -20°C until used.

B.3.3. H:B partitioning of [^{3}H]-palmitic acid

The partitioning of [^{3}H]-palmitate between heptane and buffer was determined as described previously [72, 75]. Vessels were incubated at 37°C in an oscillating [120 round per minute (rpm)] water bath (New Brunswick Scientific, model G760, USA) for up to 120 hours (hr). The buffer phase was sampled by

inserting a Hamilton syringe (100 μL) through the capillary tube. The contents of the syringe were

added directly to a scintillation vial. The heptane phase was directly sampled using an Eppendorf pipette. The outsides of the pipette tips were wiped with a tissue prewetted with heptane. Both the pipette tip and its contents were added to a scintillation vial for determination of radioactivity. Radioactivity was determined using an LS6500 liquid scintillation counter (Beckman Instruments) with automatic quench correction after the addition of ReadySafe (Beckman) scintillate.

The following six protocols were followed to determine the effect of radiolabeled impurities on the [^{3}H]-palmitate heptane-to-buffer partition ratio in the absence and presence of ALB.

Protocol 1. Experiments were conducted to investigate the effect of incubation time on the partitioning of [^{3}H]-palmitic acid between heptane and buffer in the absence of ALB.

Protocol 2. Experiments were conducted to investigate the effect of organic and aqueous phase volumes on the [^{3}H]-palmitate heptane-to-buffer partition ratio. The heptane-to-buffer volume ratio ranged from 1 to 0.005.

Protocol 3. Experiments were conducted to investigate the effect of the initial addition of [^{3}H]-palmitic acid (tracer concentration $\approx$ 2 nM) to heptane phase, to heptane phase with subsequent evaporation and the addition of fresh heptane and to aqueous phase. Adding the [^{3}H] palmitic acid to the heptane

phase with subsequent evaporation of the heptane prevented the initial high concentration that would be expected if the [^{3}H]-palmitic acid was added directly to the aqueous phase, thus reducing the chance of aggregate formation. Adding the [^{3}H]-palmitic acid directly to the aqueous phase may be expected to be associated with the lowest heptane-to-buffer partition ratio by virtue of the fact that the high [^{3}H]-palmitic acid concentration in the aqueous phase may form aggregates.

Protocol 4. Experiments were conducted to determine the partition ratio when hydrophilic radiolabeled impurities were minimized through a series of extractions. After equilibration of [^{3}H]-palmitate, the heptane phase was harvested and layered over fresh buffer. This maneuver was repeated several times in an attempt to reduce the hydrophilic radiolabeled impurities. It may be expected that this set of experiments represented the highest partition ratio (owing to the minimal hydrophilic radiolabeled impurities).

Protocol 5. Experiments were designed to investigate the heptane-to-buffer partition ratio in the presence of ALB (concentration range 0.1 - 800 μM). A series of extraction steps was followed that reduced the contribution of both hydrophilic and lipophilic radiolabeled impurities to the partition ratio values (PR^+). Table 1 outlines the initial conditions and successive extraction procedure. The initial conditions show the volume of heptane and buffer phase used. Table 1 also indicates the volume of heptane and buffer phase that, after equilibration, was sampled and replaced with the same volume of fresh heptane

ALB (μM)	Initial	Conditions	Extraction	1	Extraction	2	Extraction	3	Extraction	4	Extraction	5	Extraction	6
	H ml	B ml	ΔH ml	ΔB ml	ΔH ml	ΔB ml	ΔH ml	ΔB ml	ΔH ml	ΔB ml	ΔH ml	ΔB ml	ΔH ml	ΔB ml
0.1	3	17	NR	8.5	NR	1.7	NR	NR	NR	NR	NR	NR	NR	NR
1	3	17	NR	3.4	NR	1.7	NR	NR	NR	NR	NR	NR	NR	NR
3	5	15	NR	1.5	NR	1.5	NR	NR	NR	NR	NR	NR	NR	NR
5	5	15	5	NR	5	NR	NR	NR	NR	NR	NR	NR	NR	NR
10	10	10	10	NR	10	NR	NR	NR	NR	NR	NR	NR	NR	NR
30	10	10	10	NR	10	NR	NR	NR	NR	NR	NR	NR	NR	NR
50	10	10	10	NR	10	NR	NR	NR	NR	NR	NR	NR	NR	NR
100	10	10	10	NR	10	NR	NR	NR	NR	NR	NR	NR	NR	NR
300	10	10	10	NR	10	NR	10	NR	10	NR	NR	NR	NR	NR
500	10	10	10	NR	10	NR	10	NR	10	NR	10	NR	NR	NR
800	10	10	10	NR	10	NR	10	NR	10	NR	10	NR	10	NR

Table 1. Method for extracting hydrophilic and lipophilic radiolabeled impurities from buffer and heptane phases. Six extractions were performed. ΔH, change in heptane phase, i.e., volume of organic phase that was replaced with fresh heptane. ΔB, change in buffer phase, i.e., volume of aqueous phase that was replaced with fresh buffer. NR, no replacement of heptane or aqueous phase. H, heptane; B, buffer.

and / or buffer for extraction 1. Following equilibration a second extraction procedure was performed. The extraction procedures were repeated six times. For each ALB concentration, the [^{3}H]-palmitic acid was initially added to the aqueous phase.

Protocol 6. The unbound [^{3}H]-palmitate fraction was determined at various ALB concentrations, while the ALB-to-palmitate molar ratio was kept constant.

B.3.4 Uptake studies

B.3.4.1 Hepatocyte isolation

Studies were carried out in accordance with the University of Manitoba Animal Care Committee. Hepatocytes were isolated from female Sprague-Dawley rats (body wt, 125-150 g), as previously described [43]. Rats were housed in a temperature- and light-controlled room (22°C; 12:12-h light-dark cycle starting at 0600) and allowed Prolab animal diet (Agway County Foods) and water ad libitum. Livers were perfused in situ at 20 ml / min initially with oxygenated Swim's S-77 medium containing 5 mM EDTA and finally with Swim's S-77 medium containing 25 mg / dl collagenase and 5 mM $CaCl_2$ after an intraperitoneal injection of pentobarbital (50 mg / Kg). Perfused livers were excised, combed free of connective tissue, and filtered through 50 mesh followed by 200 mesh stainless steel filters (Sigma Chemical). The isolated hepatocytes were suspended in Swim's S-77 medium and centrifuged three to four times (each at 300 rpm) to eliminate any nonviable cells. The viable isolated hepatocytes were stored in Swim's S-77 medium at room temperature and used

within 2 hr of isolation. Immediately before experiments, cells were equilibrated to 37°C. The preparation was considered suitable when more than 90% of the cells excluded the Trypan blue dye before and after the uptake studies.

B.3.4.2 Uptake procedure

The final cell count in the uptake environment was always maintained at ≈ 5 x 10^6 / ml. This was achieved by adding constant volumes of cell suspension e.g. 50 μl to 5 ml solutions of PBS (37^0C) containing fatty acid-free ALB and tracer concentration of either the purified [^{3}H]-palmitic acid or the manufacturer-supplied [^{3}H]-palmitic acid. At specified times, a 1.0-ml aliquot of cell suspension was sampled, immediately filtered through GF/C glass microfiber filters (Fisher Scientific) by vacuum aid filtration, and washed with 5 ml ice-cold PBS to stop uptake and to remove any adherent extracellular fluid. Cell-associated radioactivity was assessed by liquid scintillation counting (Beckman LS6500TA) using Ready Safe scintillate (Beckman).

B.3.5. Data analysis

The heptane-to-buffer partition ratio was calculated as the total radioactivity in the heptane phase divided by the total radioactivity in the buffer phase. The predicted [^{3}H]-palmitic acid heptane-to-buffer partition ratio in the absence of a protein (PR^-) was expressed as:

$$PR^- = P_c \; / \; 1 \; + \; (K_d \; / \; [H^+]) \qquad (1)$$

where P_c is the fatty acid partition coefficient (=$10^{5.64}$) [76], K_d is the dissociation constant [66] for palmitic acid (=$10^{-4.9}$ M) , and $[H^+]$ is the hydrogen ion

concentration of the aqueous phase ($10^{-7.4}$ M). The predicted heptane-to-buffer partition ratio was calculated to be 1,376.

The unbound [^{3}H] palmitic acid fraction (α) was calculated using:

$$\alpha = \frac{PR^+}{PR^-} \qquad (2)$$

where PR^+ is the heptane-to-buffer partition ratio of [^{3}H]-palmitic acid in the presence of ALB and PR^- is the experimentally determined heptane-to-buffer partition ratio in the absence of ALB.

The apparent equilibrium binding constant (K_a) was calculated using:

$$K_a = \frac{1-\alpha}{\alpha C_a} \qquad (3)$$

where C_a is the ALB concentration [66].

Hepatocyte [^{3}H]-palmitate space was calculated from the ratio of the cell-associated radioactivity to the concentration of radioactivity in the bathing medium. The [^{3}H]-palmitate clearance was calculated from the least-squares linear regression coefficient for the slope of the plot [^{3}H]- palmitate space divided by the uptake interval. Data were analyzed using ANOVA and Tukey's multiple comparison test [77] and are reported as means ± SD, unless otherwise specified.

B.4. Results

B.4.1. [^{3}H]-palmitic acid partition ratio in the absence of ALB

The time required to reach equilibrium for the partitioning of [^{3}H]-palmitic acid between 3.5 ml heptane and 700 ml buffer (volume ratio 0.005) is shown in Fig. 1. When the [^{3}H]-palmitic acid was initially added to the heptane phase, the partition ratio value at 24 hr (878±46; n=6) was significantly greater ($p< 0.01$) than the 48-hr value (695±40; n=6), which was not statistically different from the values at 72, 96 or 120 hr. Organic and aqueous phases were therefore sampled at 48 hr in all subsequent experiments that used a 0.005 heptane-to-buffer volume ratio. For other volume ratios such as 1, 0.1 and 0.01 samples were obtained after 24 hours since our preliminary experiments and previous work have shown that equilibrium was achieved within 24-hr [72].

With the addition of [^{3}H]-palmitic acid to the heptane phase and the subsequent evaporation of heptane (allowing the [^{3}H]-palmitic acid to be slowly incorporated into the aqueous phase), the heptane-to-buffer partition ratio at 24 hr was much lower (259±88; n=3) than when the [^{3}H]-palmitic acid was initially added to the heptane phase without heptane evaporation (878±46; n=6). Equilibrium was reached after 48 hr of incubation (545±49; n=6). When the [^{3}H]-palmitic acid was added directly to the aqueous phase, the 24-hr heptane-to-buffer partition ratio was only (44±15; n=4). Equilibrium was reached after 96 hr of incubation (237±8; n=11). The partition ratio value in this case was statistically lower than the other two values, suggesting that formation of dimers or some other [^{3}H]-palmitate aggregate form may be responsible for the lower partition ratio values (see Figure 1).

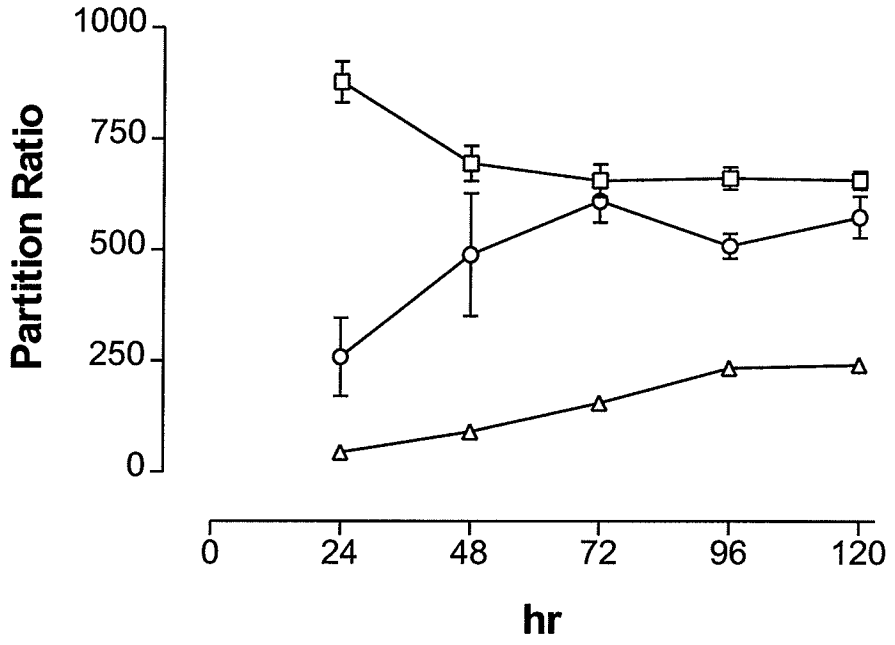

Figure 1. Heptane-to-buffer [^{3}H]-palmitic acid partition ratio vs. time using a constant heptane-to-buffer volume ratio of 0.005. Data shown represent mean ± SD, n=6. □, [^{3}H]-palmitic acid was initially added to the heptane phase; O, [^{3}H]-palmitic acid was initially added to the heptane phase, heptane allowed to evaporate, followed by the addition of fresh heptane. △, [^{3}H]-palmitic acid initially added to the aqueous phase.

Table 2 shows the dependence of the partition ratio on the heptane-to-buffer volume ratio. As the volume of the aqueous phase increased (decreasing volume ratio), the partition ratio increased. This is compatible with the notion of hydrophilic radiolabeled substances that become less important (diluted) as the volume of the aqueous phase increases [72].

Because radiolabeled impurities greatly affect the equilibrium binding constant value [43], we attempted to further decrease the degree of contamination. To this end, we performed a series of aqueous extractions. In these experiments, the [^{3}H]-palmitic acid was initially added to the heptane phase. After 24 hr of incubation, the heptane phase was harvested and added to fresh buffer (extraction 1). After the second 24-hr incubation, the heptane phase was again harvested and added to fresh buffer (extraction 2). This maneuver was repeated until the observed [^{3}H]-palmitic acid partition ratio did not change after further extraction. The heptane-to-buffer volume ratio in this series of experiments was kept constant at 0.3. Figure 2 shows that the initial heptane-to-buffer partition ratio value was 61±0.6 (n=6) and increased to a maximum of 702±19 (n=6).

B.4.2. [^{3}H]-palmitic acid partition ratio in the presence of ALB

Figure 3 depicts the [^{3}H]-palmitic acid buffer-to-heptane partition ratio values following successive extractions of radiolabeled impurities (see Table 1; note that Fig. 3 shows buffer/heptane, not heptane/buffer, values). Initially (no extraction), we observed that the partition ratio was independent on ALB

Volume Ratio	PR^-
1.0	25.3 ± 0.8
0.1	187 ± 12
0.01	550 ± 35
0.005	695 ± 40

Table 2. Heptane-to-buffer [^{3}H]-palmitic acid partition ratio in the absence of any binding protein at various heptane-to-buffer volume ratios. Values are mean ± SD; n = 4. Samples were incubated for 24-48 h at 37°C in an oscillating water bath (120-rpm). [^{3}H]-palmitic acid was purified by alkaline ethanol extraction (see METHODS) and added to the organic phase. PR^-, heptane-to-buffer partition ratio in the absence of binding protein.

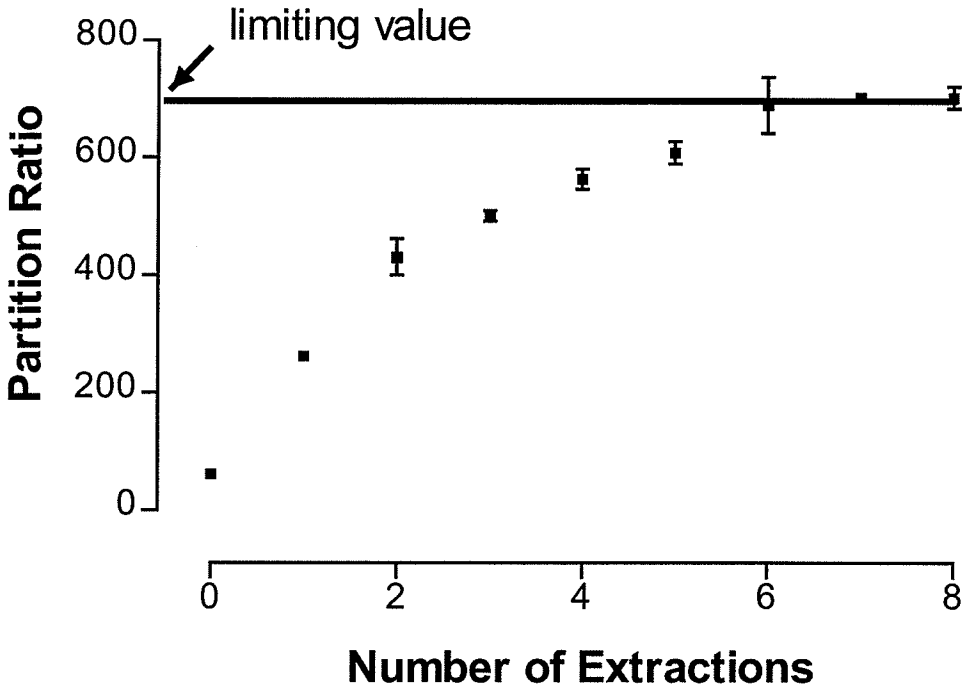

Figure 2. Heptane-to-buffer [^{3}H]-palmitic acid partition ratio vs. number of extractions. Heptane-to-buffer volume ratio was 0.3. Data shown represent means ± SD, n = 6.

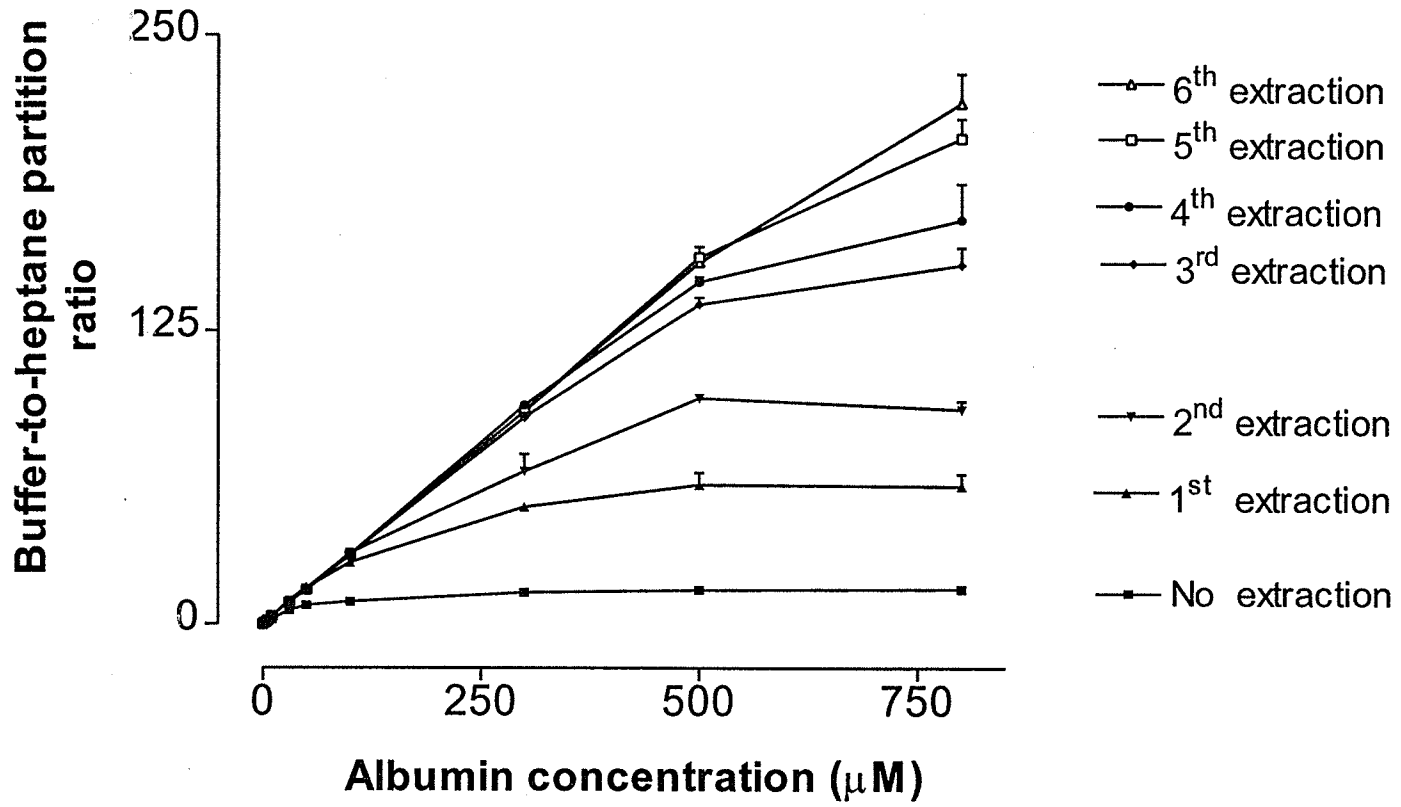

Figure 3. Buffer-to-heptane [^{3}H]-palmitic acid partition ratio vs. ALB concentration. Extraction procedure followed is as described in Table 1. Data shown represent mean ± SD, n=6.

concentration. The deviation from linearity in Figure 3 became less apparent with successive extractions. After extraction 6, the [^{3}H]-palmitic acid buffer-to-heptane partition ratio was linearly related to ALB concentration (with the exception of the highest albumin concentration tested). At 800 μM ALB there existed a slight but statistically insignificant deviation from linearity.

Table 3 shows that K_a, calculated by Eq. 3 and using our experimentally determined $\overline{PR}$ value of 702, remained constant at all ALB concentrations.

B.4.3. Unbound [^{3}H]-palmitate concentration

Table 4 shows the [^{3}H]-palmitic acid concentration at various ALB concentrations, using different ALB-to-ligand molar ratios. In all cases, the unbound ligand fraction decreased with an increase in the ALB concentration. The unbound [^{3}H]-palmitic acid concentration was not statistically different at low ALB concentration (i.e., $\leq$ 10 μM) when the ALB-to-ligand molar ratio was 1:1 and 1:2. At higher ALB-to-ligand molar ratios (i.e., 3:1 and 4:1) the unbound ligand concentration increased with an increase in ALB concentration. In all cases, at ALB concentrations between 40 and 800 μM, the unbound ligand concentration increased with an increase in ALB concentration.

B.4.4. Hepatocyte-[^{3}H]-palmitate clearance

Uptake of purified and manufacturing-supplied [^{3}H]-palmitate by hepatocytes isolated from female rates in the presence of 5, 50, 500 μM ALB are shown in Fig. 4A and 4B, respectively. [^{3}H]-palmitate hepatocyte clearances are

Albumin (μM)	α	K_a (M^{-1})
0.1	$(4.2 \pm 0.1) \times 10^{-2}$	$(2.3 \pm 0.1) \times 10^{8}$
1	$(4.4 \pm 0.1) \times 10^{-3}$	$(2.2 \pm 0.1) \times 10^{8}$
3	$(1.5 \pm 0.1) \times 10^{-3}$	$(2.2 \pm 0.1) \times 10^{8}$
5	$(9.0 \pm 1.0) \times 10^{-4}$	$(2.2 \pm 0.1) \times 10^{8}$
10	$(4.0 \pm 0.2) \times 10^{-4}$	$(2.3 \pm 0.1) \times 10^{8}$
30	$(1.5 \pm 0.1) \times 10^{-4}$	$(2.3 \pm 0.1) \times 10^{8}$
50	$(9.5 \pm 0.3) \times 10^{-5}$	$(2.1 \pm 0.1) \times 10^{8}$
100	$(4.8 \pm 0.1) \times 10^{-5}$	$(2.1 \pm 0.1) \times 10^{8}$
300	$(1.6 \pm 0.1) \times 10^{-5}$	$(2.1 \pm 0.1) \times 10^{8}$
500	$(9.0 \pm 0.3) \times 10^{-6}$	$(2.2 \pm 0.1) \times 10^{8}$
800	$(6.5 \pm 0.4) \times 10^{-6}$	$(2.0 \pm 0.10) \times 10^{8}$

Table 3. [^{3}H]-Palmitate free fraction and calculated apparent equilibrium binding constant for albumin-[^{3}H]-palmitate complex at varying albumin concentrations. Values are mean $\pm$ SD; n = 6. [^{3}H]-Palmitate free fraction (α) was calculated using PR^{-} = 702. K_a calculated apparent equilibrium binding constant.

Unbound Palmitate Concentration, nM

Albumin, μM	1 : 1*	2 : 1*	3 : 1*	4 : 1*
0.1	4.9 ± 0.3	10.2 ± 0.3	14 ± 1	20 ± 2
1	5.1 ± 0.5	10.2 ± 0.3	20 ± 1	27 ± 1
10	5.0 ± 0.2	12.6 ± 02	31 ± 2	50 ± 1
40	7.8 ± 0.3	20.6 ± 0.4	50 ± 1	87 ± 2
400	11.4 ± 0.5	50.4 ± 1.4	120 ± 20	245 ± 11
800	13.9 ± 1.1	59.3 ± 3.8	200 ± 1	444 ± 23

Table 4. Unbound palmitate concentration at various palmitate-to-albumin molar ratios. Values are means ± SD. * Molar ratio.

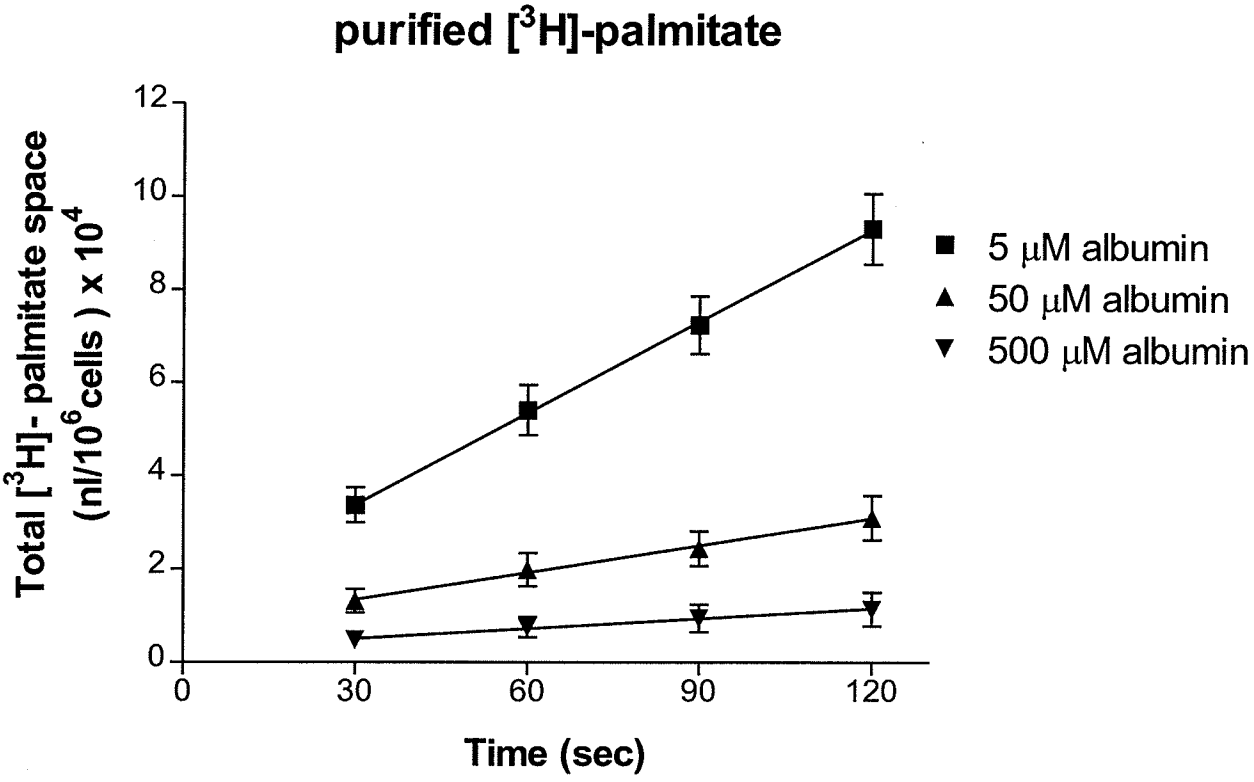

Figure 4A. Plot of total [^{3}H]-palmitate space for each concentration of albumin. Purified palmitate was used. The total palmitate clearance was calculated as the slope of each plot by use of linear regression analysis. Data are means ± SEM (n=6 to 8).

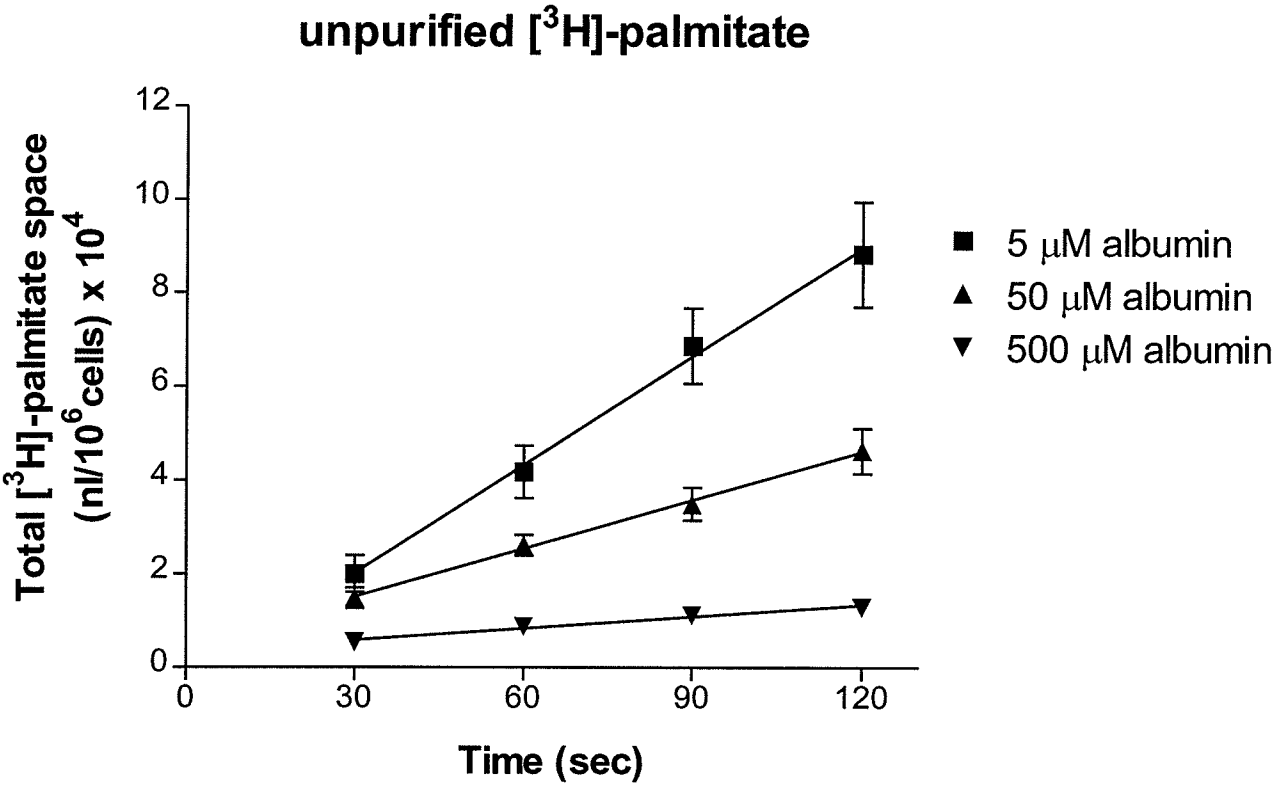

Figure 4B. Plot of total [^{3}H]-palmitate space for each concentration of albumin. Manufacturer-supplied palmitate was used. The total palmitate clearance was calculated as the slope of each plot by use of linear regression analysis. Data are means ± SEM (n=6 to 8).

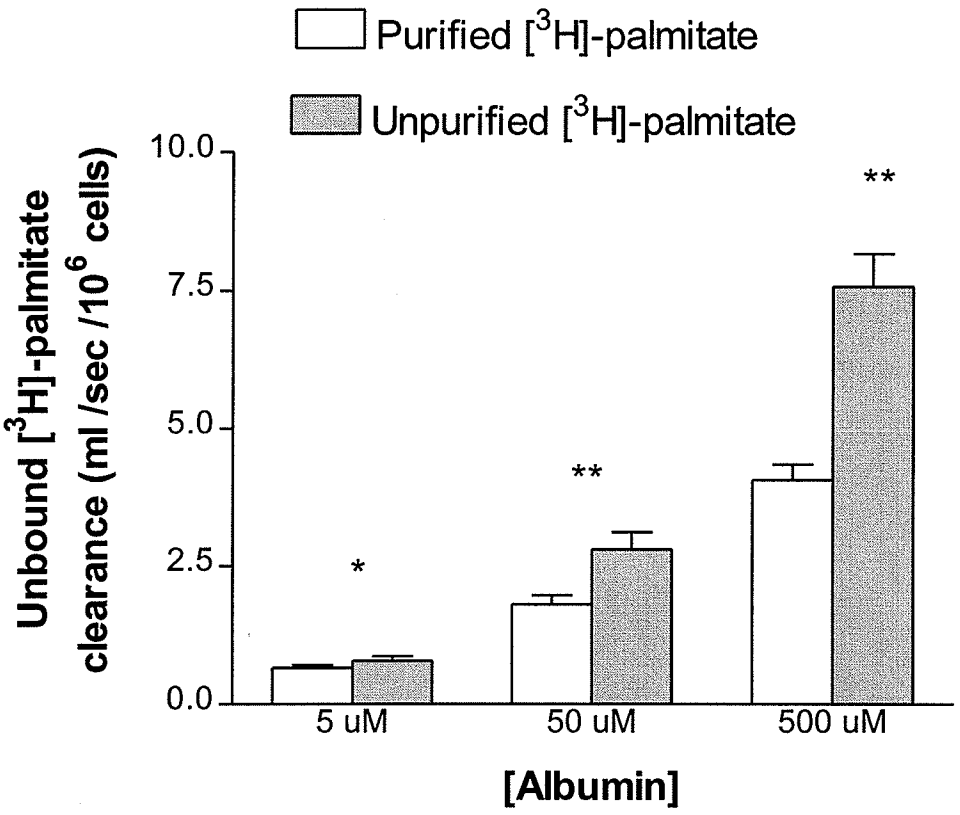

Figure 4C. Purified and manufacturer-supplied unbound [^{3}H]-palmitate-hepatocyte clearance at 5, 50, and 500 μM ALB. Data are means ± SEM, n = 6 to 8. * $p < 0.05$, ** $p < 0.01$

shown in Fig. 4C. The apparent intrinsic clearances (defined as the total clearance divided by the equilibrium unbound ligand concentration) using purified [^{3}H]-palmitate were statistically lower than those using the manufacturer-supplied radiolabel. The total [^{3}H]-palmitate clearances (in means ± SE) using purified [^{3}H]-palmitate were (5.9 ± 0.4) X 10^{-1}, (1.6 ± 0.1) X10^{-1}, and (3.7 ± 0.5) X 10^{-2} μl. s^{-1}. 10^6 $cells^{-1}$ for 5, 50, and 500 μM ALB, respectively; and for manufacturer-supplied [^{3}H]-palmitate were (7.1 ± 0.7) X10^{-1}, (2.5 ± 0.3) X10^{-1}, and (6.8 ± 0.5) X 10^{-2} μl. s^{-1}. 10^6 $cells^{-1}$ for 5, 50, and 500 μM ALB, respectively.

B.5. Discussion

Heptane-buffer partitioning of long-chain fatty acids has been widely used for determining the unbound fraction of long-chain fatty acids in the presence of binding proteins. This technique is particularly well suited for use at physiological ALB concentrations owing to the increased solubility of palmitate in the heptane phase. However, because there is a difference in solubility of long-chain fatty acids between the aqueous and organic phases, this technique requires calibration. Burczynski, et al. have evaluated this method [72] and reported that calibration is difficult, making the technique unreliable unless precautions are taken. The presence of hydrophilic and lipophilic radiolabeled impurities makes estimation of the partition ratio, in the absence of binding proteins, difficult. Partition ratio values may vary by an order of magnitude and, indeed, this is what has been reported in the literature [72, 75, 78]. Lower heptane-to-buffer partition ratio (PR^-) values were reported by Smith and Tanford

[76] and Fleischer et al. [71] of ≈ 100, while higher values of ≈ 1,400 were reported by Simpson et al. [78]. Although some of the problems associated with radiolabeled impurities may be overcome, the presence of low-level lipophilic radiolabeled impurities makes this technique unreliable for use with higher albumin concentrations, i.e. >100 μM [43]. Hence, it is difficult to test the hypothesis that K_a for the ALB-long-chain fatty acid complex is constant [73].

In the present study we confirmed our earlier report [72] showing the [^{3}H]-palmitic acid heptane-to-buffer partition ratio dependence on heptane-to-buffer volume ratio. This dependence suggested the presence of radiolabeled impurities. Our experimentally determined PR^- maximum value was much lower (702 ± 19) than the predicted maximum of 1,376, despite efforts to minimize the hydrophilic radiolabeled substances by using a small heptane-to-buffer volume ratio (0.005). Thus radiolabeled impurities and / or [^{3}H]-palmitate aggregates must be present despite our purification and dilution efforts. Previous work [72] using gas chromatography / mass spectrometry analysis showed the presence of glycerol monopalmitate and glycerol monostearate as major lipophilic radiolabels. However, the monoglycerides seem unlikely to be responsible for the difference observed in Fig. 1. Hydrophilic radiolabeled substances could not be analyzed with gas chromatography because they were below detection limits. Because the partition ratio values were dependent on which phase initially contained the radiolabel (Fig. 1), the possibility of [^{3}H]-palmitic acid aggregates is likely. These aggregates may function as the initial phase of micelle formation.

The presence of long-chain fatty acid dimers has been postulated by Goodman [75] and a dimerization constant has been calculated by Mukerjee [79] to explain the low partition ratio values. It is unlikely that micelle formation offers an alternative explanation for our low partition ratio results, since the unbound long-chain fatty acid concentration in the aqueous phase (< 1 nM) was much lower than the critical micellar concentration.

In the presence of binding proteins radiolabeled impurities greatly affect the PR^+ value, because small amounts of impurity can become large relative to unbound [^{3}H]-palmitate. At low ALB concentrations (i.e., < 5 μM) a large portion of the [^{3}H]-palmitate is present in the heptane phase. Hydrophilic radiolabeled substances may significantly affect the resulting PR^+ value, whereas lipophilic radiolabeled impurities do not affect the PR^+ value. At higher protein concentrations, the reverse occurs. Much more of the [^{3}H]-palmitate is present in the aqueous phase by virtue of its binding to ALB. Hydrophilic radiolabeled impurities are not expected to affect PR^+, but lipophilic radiolabeled impurities may significantly affect PR^+ values because a much smaller amount of [^{3}H]-palmitic acid is present in the organic phase. Thus in the case of high concentration of binding protein, the PR^+ values could be artificially high.

Our method for removing hydrophilic and lipophilic radiolabeled impurities (Table 1) resulted in buffer-to-heptane partition ratios that were linearly related to ALB concentration (Fig. 3), suggesting that K_a is indeed a constant. At 800 μM ALB there was a slight (statistically insignificant) deviation from linearity. The

procedure outlined in Table 1, i.e., the selected heptane and buffer volumes and the volumes removed for each ALB concentration, is not steadfast. Any suitable heptane-to-buffer volumes ratio will help reduce the contribution of radiolabeled impurities). We calculated K_a from our data using the equation $K_a = (1-\alpha) / (\alpha C_a)$. The free fraction ($\alpha$) was calculated using our experimentally determined PR^+ value (from Fig. 3) and PR^- of 702. Using $PR^- = 702$ to calculate α rather than the expected value (1,376) assumed that all radiolabeled constituents are candidates for protein binding. This assumption may be valid, since reports have shown that when two carbon-18 fatty acids are covalently bound in the middle (thus having free carboxyl groups) they act as a single-chain fatty acid (monomer) but with lower protein binding properties [23, 24]. Thus, if [^{3}H]-palmitic acid aggregates occur, it also may behave as a monomer and bind to ALB.

The present studies gave important experimental evidence showing that the equilibrium binding constant for the ALB-palmitate complex is independent of protein concentration. Previous work designed to investigate the role of binding protein on the drug uptake process has determined the apparent K_a using low protein concentrations and assuming it to be the same at higher protein concentrations [43, 44, 62]. To date, no study has critically assessed this assumption for long-chain fatty acids. Through reducing the radiolabeled contaminants in the manufacturer-supplied [^{3}H]-palmitate, we offer the experimental evidence that supports this assumption. Moreover, the average equilibrium binding constant value obtained at all ALB concentrations [$K_a = (2.2 \pm$

0.1) X 10^8 M^{-1}; mean ± SE] agrees with the values reported by Pond et al. [70] [(4.6 ± 0.3) X 10^8 M^{-1}; mean ± SE] and Bojesen and Bojesen [80] [1.0x10^8 M^{-1}]. The unbound fractions in the latter studies were determined using erythrocyte ghosts. Richieri et al. [63] reported K_a values of 1.45 X 10^8 M^{-1} and 1.22 X 10^8 M^{-1} for the binding of palmitate to human serum albumin and ALB, respectively, using fluorescence emission of acrylodan-derivatized intestinal fatty acid binding protein. Compared with other accepted methods, heptane-to-buffer partitioning is the only method sensitive enough to measure the unbound fatty acid concentration using high ALB (i.e., physiological) and tracer palmitate concentration.

Previous reports suggest [62, 81] that the binding of a long-chain fatty acid to ALB at a given ALB-to-ligand molar ratio results in a constant unbound ligand concentration over a range of ALB concentrations. Our studies show (Table 4) that the unbound ligand concentration is constant only at low ALB concentrations (≤ 10 μM) and only at low ALB-to-palmitate molar ratio (i.e., 1:1 and 1:2). At higher ALB concentrations and higher molar ratios, the unbound ligand concentration increased with an increase in protein concentration. This observation was reported by Spector et al. [81], using acidic buffer solutions (pH 6.0). Our results are of particular importance to studies using ALB-to-ligand constant molar ratios, which may require reinterpretation given the present evidence.

We further investigated whether the radiolabeled impurities are extracted by hepatocytes. Figure 4 shows that uptake was greater for the unpurified [^{3}H]-palmitate than the purified ligand. Clearly, these impurities are substrates for the cellular uptake process. These substances become much more important at higher binding protein concentrations. As the ALB concentration was increased from 5 to 500 μM, the extent of uptake attributable to radiolabel impurities also increased. At 5, 50, and 500 μM ALB, ≈ 20%, 56%, and 84% of total uptake was attributable to the impurities, respectively. Thus studies designed to investigate the uptake process of highly lipophilic protein-bound ligands such as [^{3}H]-palmitic acid must purify the manufacturer-supplied radiolabel before use. An overestimate of the uptake rates may otherwise be obtained.

Chapter three

Palmitate uptake by neonatal rat myocytes and hepatocytes: role of extracellular protein

C.1. Introduction

Given that many different intracellular and extracellular processes are regulated by nonesterified long-chain fatty acids levels (see chapter four), it is important to further our understanding on the initial step(s) in the overall cellular uptake process of these important physiological substrates. Many investigators have studied the role of plasma proteins in the uptake process. Some believe that uptake is driven solely by the unbound fraction [44, 62] while others argue that the protein-bound fraction contributes a significant portion of the total amount extracted [52, 82].

Paris et al [48] investigated long-chain fatty acid uptake by cultured cardiac cells isolated from chick embryos. They showed that albumin actually increased the rate of palmitate uptake. One possible explanation for the observed enhancement by albumin was that the serum albumin-fatty acid complex was the preferred substrate through specific recognition by some components of the outer surface of the cardiac cell than the unbound fatty acid. The authors suggested that albumin cannot be replaced by other serum long-chain fatty acid binding proteins. In the present study we were interested to determine if the cellular uptake rate of a radiolabeled long-chain fatty acid, [^{3}H]-palmitate, indeed occurred from both the unbound and protein-bound fractions in rat neonatal hepatocytes and cardiac myocytes. Our study further investigated whether the uptake process was specific to albumin or whether it was nonspecific and other extracellular binding proteins could take part in the uptake

process. Finally, results of this study will show if the observed facilitated uptake in adult hepatocytes reflects the developmental stage of the animal or if it is also present in newborn animals.

C.2. Materials

[9,10-^{3}H] Palmitic acid (56.5 Ci/mmol) with a radiochemical purity of 97.8% was obtained from New England Nuclear. Bovine serum albumin (ALB, essentially fatty acid-free), α_1-acid glycoprotein (AGP), conalbumin (CONALB) and lysozyme (LYS) were obtained from Sigma Chemical (St. Louis, MO.). All other chemicals were obtained from Sigma Chemical with the exception of heptane, which was supplied by Fisher Scientific (Pittsburg, PA). Dulbecco's modified Eagle's medium / Ham's nutrient mixture F12 (DF; 1:1; Gibe Laboratories), minimum essential medium (MEM, GibcoBRL), fetal bovine serum (FBS, Hyclone Laboratories), trypsin, collagenase, and DNAse were obtained from Worthington Biochemical Corporation, Halls Mill Road, Treehold, New Jersey, USA. Percoll was obtained from Pharmacia. The aqueous buffer used throughout all experiments was phosphate buffer saline (PBS), which had a composition of (in mM: 137 NaCl, 2.68 KCl, 1.65 KH_2PO_4, 8.92 Na_2HPO_4 and 3 NaN_3), with pH adjusted to 7.4 using 0.1 N NaOH.

C.3. Methods

C.3.1. Chemical modification of albumin.

C.3.1.1.Succinylation of albumin.

Albumin was reacted with succinic anhydride as previously described [83]. Briefly, albumin was dissolved in 100 ml distilled water (pH 7) to a concentration of 20 mg / ml. The pH was maintained at 7 by addition of 0.2 M NaOH and the solution was continuously stirred as 1.6 g succinic anhydride was added in small portions over 30 minutes. The succinylated albumin (ALBs) was extensively dialyzed for 24-48 hours at 4°C against several changes of distilled water. The modified albumin was lyophilized and stored at - 20°C until used.

C.3.1.2. Cationization of albumin.

Albumin was first activated by carbodiimide and then reacted with ethylenediamine as described in detail [84]. Briefly, 500-ml solution of ethylenediamine (13.32% v/v) in distilled water was prepared and the pH was adjusted to 4.75 using ≈ 350 ml 6 N HCl. To this solution, (2 g) albumin was added followed by the addition of (0.725 g) of 1-ethyl-3 (3-dimethyl-amino propyl)-carbodiimide. The reaction was quenched after 2 hours (in case of ALB_E) or 10 minutes (in case of ALB_{E1}) by adding 30 ml 4 M acetate buffer, pH 4.75.

The resulting modified protein was dialyzed overnight against distilled water at 4°C, concentrated, lyophilized, and stored at –20° C until used.

C.3.1.3. Maleylation of albumin.

Albumin was modified with maleic anhydride as previously reported [85]. Briefly, albumin was dissolved in 100 ml distilled water (pH 8.5) to a concentration of 10 mg / ml. The pH was maintained at 8.5 by addition of 2 M NaOH and the solution was continuously stirred as solid maleic anhydride (50 molar excess over albumin) was added in small increments over 30 minutes at 4^0C. Completion of the reaction was determined when the pH dropped and remained constant at 7.0. The maleylated albumin (ALBm) was extensively dialyzed for 24-48 hours at 4^0C against several changes of distilled water. The modified albumin solution was concentrated, lyophilized and stored at -20^0C until used

C.3.2. Determination of the extent of albumin modification

We examined the modified albumins by assessing: (a) the extent of modification of their lysine residues in case of ALBs and ALBm, (b) the extent of modification of their carboxyl groups in case of ALB_E and ALB_{E1}.

For ALBs and ALBm, the extent of acylation of amino groups of the protein was determined by ninhydrin reaction as previously described [86, 87]. Briefly, a range of protein concentrations (mg %: 2, 4, 8, 16, 32, and 64) was prepared in distilled water. To one-ml protein solution in test tube, one ml of 4 M

sodium acetate buffer, pH 5.5 and one ml of 0.1 M ninhydrin reagent were added. Test tubes were placed in boiling water bath for 20 min. then cooled under tab water to below 30°C followed by the addition of 5 ml 50% ethanol and thoroughly shaken (about 30 sec) before being read at 570 nm against an appropriate blank. For both modified albumins, native albumin was used as standard. The slopes of the drawn straight lines obtained from the plots between the protein concentration and absorbance were used in the following equation [86, 87]:

$$\% \text{ Modification} = 100\ (1-S_m / S_n) \qquad (4)$$

where S_m and S_n represent slopes of the straight lines drawn for modified and native albumin, respectively.

For ALB_E and ALB_{E1}, the extent of modification of their carboxyl groups was determined by mass spectrometry as previously described [88]. Amino acid modifications were identified by peptide mapping on a SCIEX prototype tandem quadrupole/TOF mass spectrometer (QqTOF) coupled to a matrix assisted laser desorption ionization (MALDI) ion source. The tryptic digestions were conducted in 25 mM ammonium bicarbonate solution (1% trypsin, w/w) at 37°C for 24 hours. The resulting peptide fragments were detected by MALDI/TOF mass spectrometry. A 2,5 dihydrobenzoic acid (DHB) solution (100 mg/ml in acetone) was used as the matrix. Peptide fragment sequence identifications were performed by the collision gas and collision energies of 50-180 eV.

C.3.3. Determination of (pI) and (M_W) of proteins

The isoelectric points (pI) of CONALB, ALB, ALB_E, ALB_{E1}, ALBs, and ALBm were determined using a Model 111 Mini IEF-cell (BIO-RAD) and BioLyte 3/10 obtained from BIO-RAD Laboratories (California, USA). Gels were stained with Coomassie blue R-250. The pI of AGP and LYS was previously determined to be 2.7 and 11, respectively, [52] and found to be similar to the values reported in literature [89].

Mass measurements of modified proteins were conducted on an orthogonal injection electrospray ionization time-of-flight mass spectrometer (ESI/TOF III). Prior to analysis residual sodium, potassium, and phosphate were removed from proteins by ultrafiltration using 25-mM ammonium bicarbonate buffer. Following ultrafiltration the protein was dissolved in 5 % acetic acid in methanol/water (1:1 v/v). Analysis was performed at the declustering voltage of 190 eV. Protein concentrations were determined using the Bradford method [90] or ultraviolet method [91]. For both methods, albumin was used as the standard.

C.3.4. Purification of [^{3}H]-Palmitic acid

Palmitate was purified by a modified ethanol extraction procedure [74]. Purification of the manufacturer supplied [^{3}H]-palmitate is of primary concern when using very small unbound ligand fractions. We have shown that without further purification the apparent cellular [^{3}H]-palmitate-clearance may be

overestimated because of the presence of radiolabeled contaminants [34]. Thus, in all our experiments, we routinely purify the manufacturer-supplied [^{3}H]-palmitate using a heptane/buffer extraction procedure. Briefly, A 1-ml sample of manufacturer-supplied solution of [^{3}H]- palmitic acid was added to 0.98 ml research quality distilled water (18 MΩ. cm) containing 0.1 N NaOH and approximately 1 mg thymol blue. Heptane (1.2 ml) was layered onto the aqueous phase, and the mixture was vortex-mixed for 60 s. After separation, the heptane phase was discarded, fresh heptane was added, and the procedure was repeated. After four such extractions, the aqueous phase was acidified using two drops of 6 N HCl, heptane was added, and the mixture was vortex-mixed for 60 s. The purified palmitate contained in the heptane phase was harvested, fresh heptane was added to the acidified aqueous phase, and the procedure was repeated four times. The harvested heptane phase evaporated until approximately 20 μl heptane remained, at which time 1 ml of 100% ethanol was added. The purified [^{3}H]-palmitic acid was stored in ethanol at -20°C until used.

C.3.5. Determination of unbound palmitate fraction (α) and the protein-palmitate equilibrium binding constant (K_a)

Unless otherwise indicated all protein solutions were prepared in PBS buffer. The purified [^{3}H]-palmitate (≈2 nM) was added to solutions of phosphate buffer saline containing AGP, LYS, CONALB, ALB, ALBs, ALB_E, ALB_{E1} or ALBm. The unbound palmitate fractions in the presence of each protein were measured

at different concentrations (range from 0.1 μM to 2100 μM) using heptane: buffer partitioning technique as previously described [34]. The equilibrium association constant for the different palmitate-protein complexes was calculated using equation 3 (see chapter two)

C.3.6. Determination of protein-palmitate dissociation rate constant (K_{off})

The method used to measure the K_{off} rate was based on the transfer rate measurements of [^{3}H]-palmitate from binding protein to a solid phase acceptor such as albumin-agarose. This method has been utilized by other investigators [36, 92, 93] and a comparative review to other available methods was reported [94]. Briefly, the different protein-[^{3}H]-palmitate complexes (concentrations similar to that used in the uptake experiments) were added to albumin-agarose acceptor bead solutions (10 ml, 30% wet gel by volume) at 37°C. At specified time intervals (3 to 5 s), 1000 μl aliquots were immediately filtered through GF/C glass microfiber filters (Fisher Scientific) by vacuum assisted filtration. Aliquots (100 μl) of the filtrate and incubation mixture were sampled for radioactivity determination. The natural logarithm of the ratio of filtrate radioactivity to the total radioactivity was plotted against time. The slope of the regression line was taken as being indicative of the K_{off} value. Control experiments using [^{125}I] - radiolabeled proteins showed that there was no detectable binding of the different proteins to the albumin-agarose acceptor beads. Our studies were completed following 20 sec. of reaction. This time frame has been shown to be sufficient to determine the initial exponential transfer rate (K_{off}) of the protein-fatty

acid complex to the acceptor [36]. Longer reaction time periods were not necessary since the interpretation of the second exponent is ambiguous and may include reassociation to albumin and/or dissociation from the albumin-agarose binding sites back into the superfusate.

C.3.7. Determination of protein solution viscosity

Viscosity of each protein solution used in this study was measured using the Wells-Brookfield Cone / Plate Digital Viscometer (Model CP-40). Measurements were made using the same spindle at different speeds. Briefly, solutions of PBS containing 0.23 μM ALB, 0.28 μM ALBs, 0.4 μM ALB_E, 0.22 μM ALB_{E1}, 0.36 μM ALBm, 2100 μM LYS, 1.41 μM CONALB, or 322 μM AGP were prepared. A 1 ml protein solution was placed and spread evenly over the surface of the viscometer cup. Sufficient time was allowed for the sample fluid to reach the desired temperature (37°C). Viscosity of each protein solution was measured and reported as Centipoise; mean ± SEM.

C.3.8. Preparation of cardiac myocytes from 1-3 day-old rat pups

This study was performed in accordance to the University of Manitoba Animal Care Committee. Cardiac myocytes were isolated from 1-3 day-old rats of either gender [95]. Excised hearts were placed in 4°C glucose (10 g/L) containing PBS solution. Hearts were minced with scissors in a minimum volume of PBS, washed 2-3 times with the same buffer to remove blood and excess tissue. Minced hearts were washed once with PBS (37°C). Hearts were then

transferred to a sterile top stirrer flask and the volume was increased to 17.5 ml PBS. A DNAse (0.5% w/v)/ collagenase (2% w/v) combined solution (2 ml) and 0.5 ml of a 2% w/v trypsin solution were added. The mixture was agitated moderately on a rotary shaker at 37° C for 10 minutes. Myocytes were released by pipetting the digested mixture 2 to 3 times with a 25-ml pipette. The supernatant containing the isolated myocytes was transferred to a fresh tube and PBS (37°C) was added and the mixture pipetted two or three times, left to stand for one minute and the free myocytes in the supernatant were again collected. This maneuver was repeated 6 times. To the combined supernatant, 20 ml dulbecco's modified eagle's medium supplemented with 20% serum were added. The mixture was centrifuged at 1150 rpm (145x g) for 5 minutes. Non-myocyte cells were removed using a discontinuous Percoll gradient. The resulting preparation (Fig. 5) contained more than 95% viable cardiac myocytes as assessed by trypan blue (0.2%) exclusion.

C.3.9. Preparation of parenchymal hepatocytes from 1-3 day-old rat pups

Neonatal rat hepatocytes were isolated from 1-3 day old rats as previously described [96, 97]. Livers were isolated from 1-3 day old rat pups of either gender and placed in Ca^{2+} and Mg^{2+} free PBS at 4°C, pH 7.4, rinsed three times with the same buffer, cleaned of extraneous tissues, and minced (pieces were approximately 0.5 mm in length). The buffer was aspirated and the minced livers were rinsed three times with PBS containing 500 μM EDTA and left to stand for 5 minutes at 37°C. Tissue was then rinsed three times with EDTA-free PBS. Liver

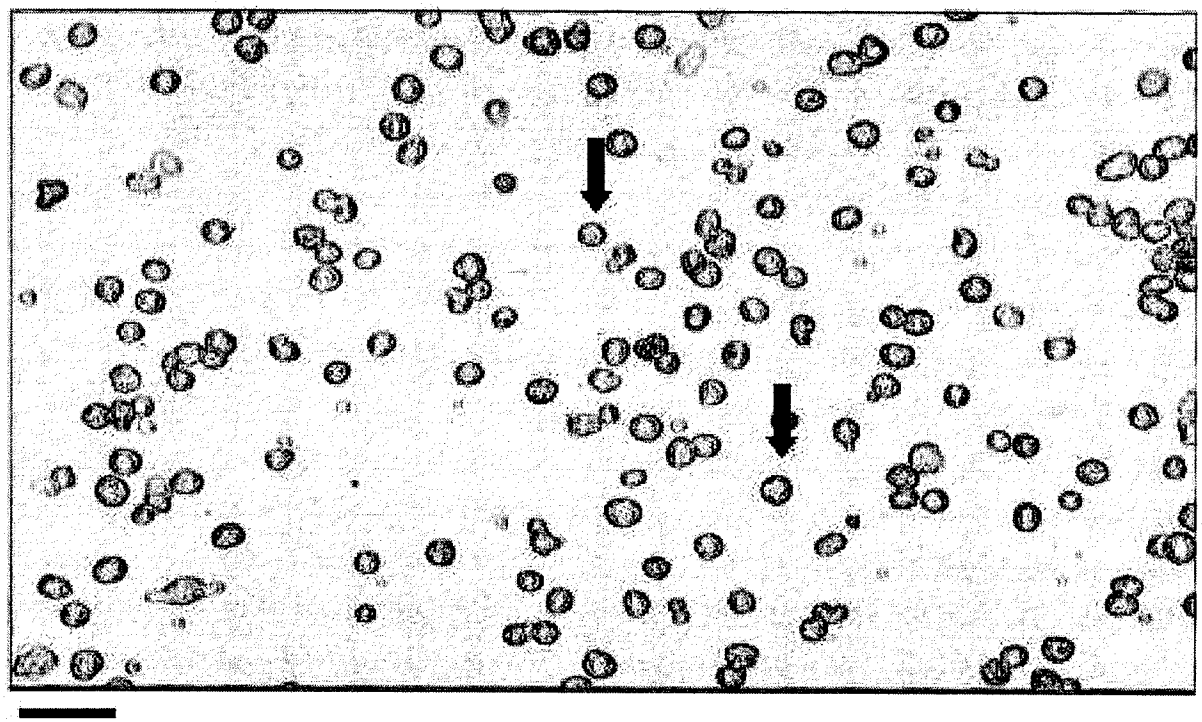

Figure 5. Myocyte-rich fraction obtained after purification by a Percoll gradient from hearts of 1-3 day-old rats. Cells (arrows) are round with viability of > 95 %. The cell diameter of cardiac myocytes from newborn rats was approximately 12 μm. Bar represents 30 μm..

tissue was then incubated in a solution of collagenase (MEM containing 0.35 mg / ml collagenase) for 10 minutes at 37°C stirring at moderate speed with a magnetic stirrer. This process was repeated six times. After each digestion the supernatant was collected. The combined supernatants were filtered through a 50 μm-pore size nylon mesh. Hepatocytes were separated from nonhepatocytes by centrifugation twice at 50g for 3 minutes. The supernatant was a mixture of hepatocytes and haemopoietic cells. To isolate the hepatocytes the supernatant was centrifuged twice at 30g for 1 min and twice at 15g for 1 min using MEM. Haemopoietic cells Fig. 6 were recognized by light microscopy. The final pellet contained mostly hepatocytes (Fig. 7; >90%). Cell number and viability were assessed using 0.2 % trypan blue.

C.3.10. Uptake procedure

Myocytes or hepatocytes were added to solutions of PBS (37° C) containing [^{3}H]-palmitate (≈ 5.0 nM) and either 0.23 μM ALB, 0.28 μM ALBs, 0.4 μM ALBe, 0.22 μM ALB_{E1}, 0.36 μM ALBm, 2100 μM LYS, 1.41 μM CONALB, or 322 μM AAG. These protein concentrations resulted in an unbound palmitate fraction of α = 0.03. All uptake studies were performed using the same unbound palmitate fraction. Myocyte and hepatocytes density in the uptake medium was 3.0×10^5 cells / ml or 5.0×10^5 cells / ml, respectively. Cells were gently agitated to prevent their sedimentation in the incubation solution. At 30 sec intervals, 0.4 ml aliquots of the cell suspension were immediately filtered (by aid of vacuum)

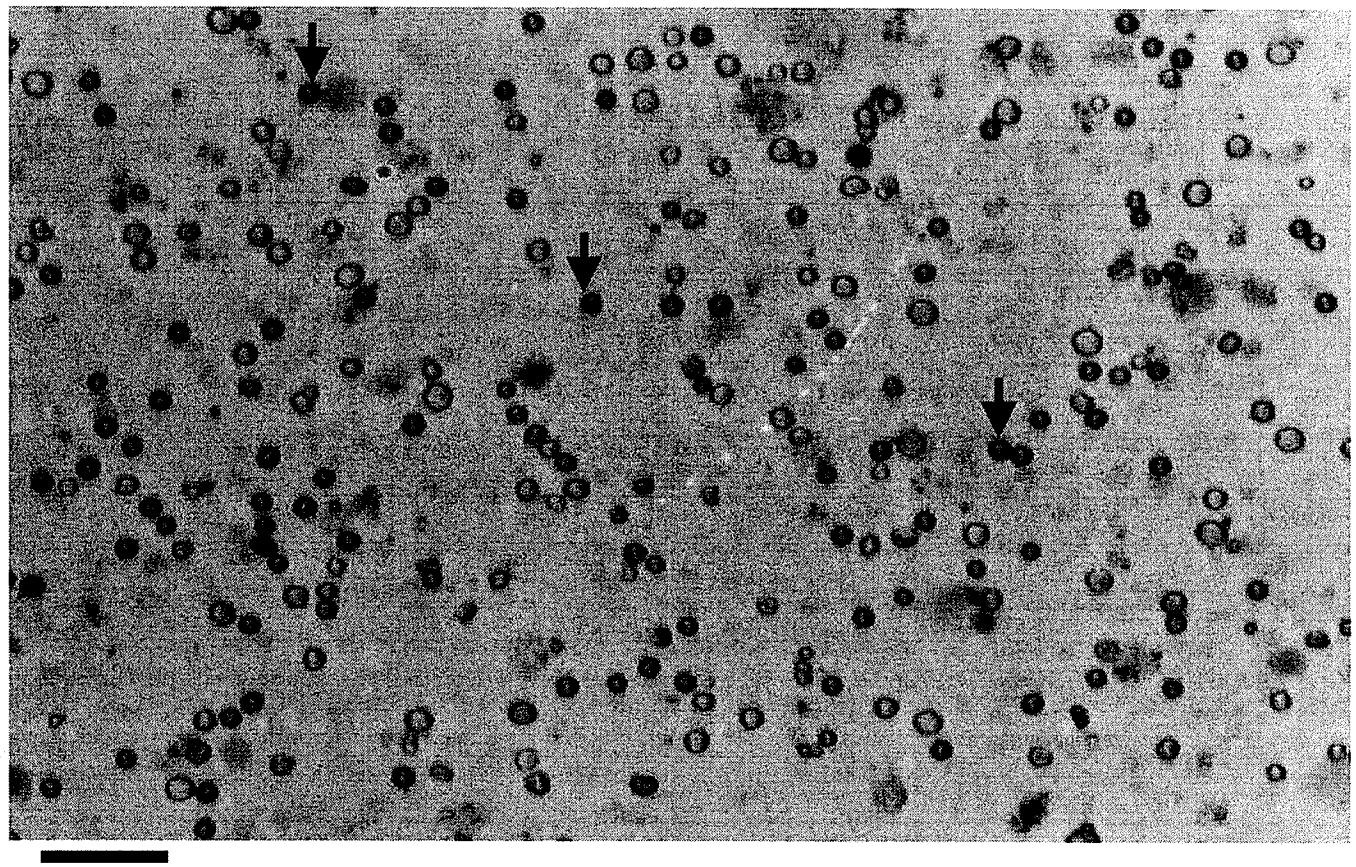

Figure 6. Haemopoietic-rich fraction obtained from the supernatant after sequential centrifugation of hepatocytes (see materials and methods). Haemopoietic cells (arrows) are round with dark edge and clearly smaller than hepatocytes ($\approx$ 4 μm). Bar represents 20 μm.

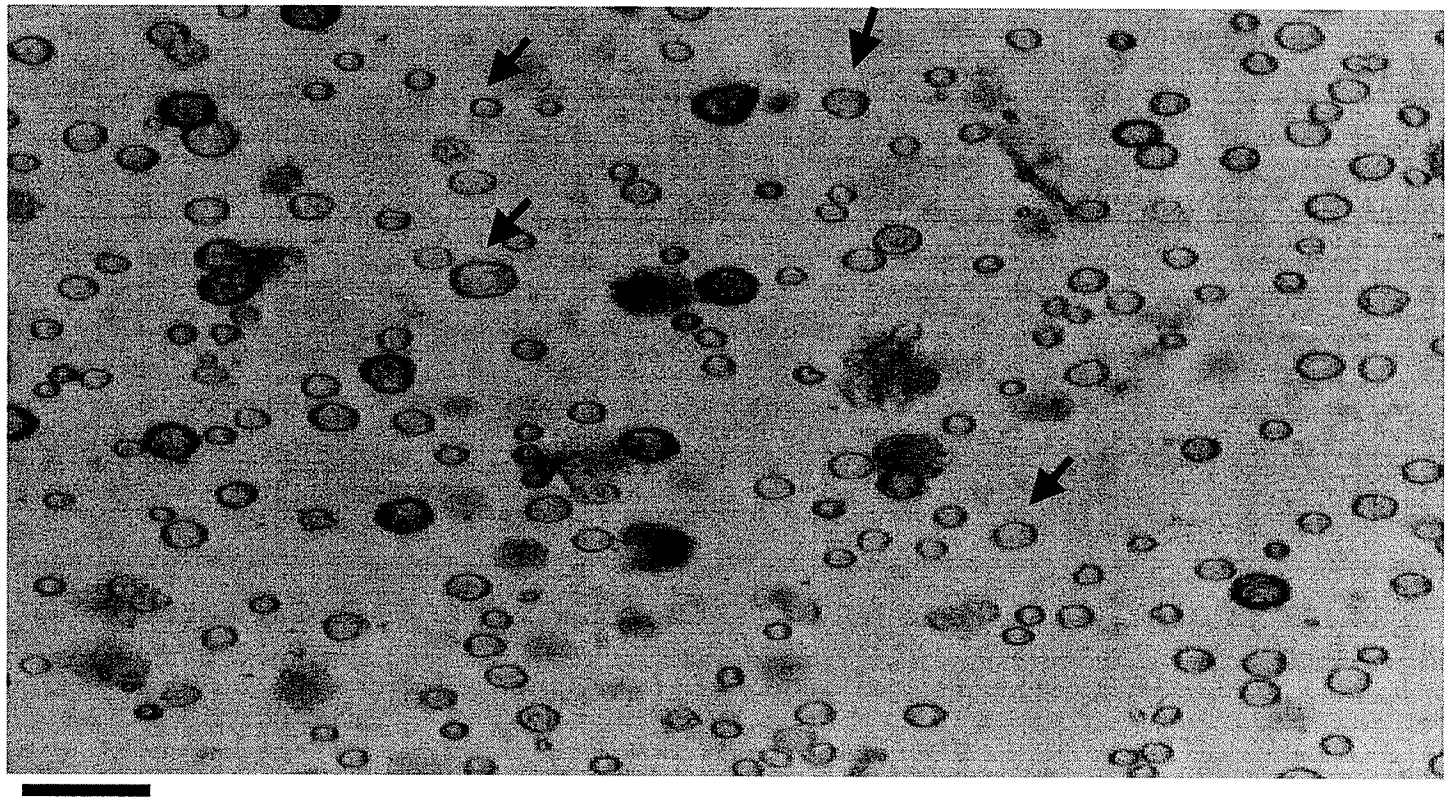

Figure 7. Hepatocyte-rich fraction obtained by sequential centrifugation of two cell population (haemopoietic and hepatocytes) from livers of 1-3 day-old rats. Hepatocytes (arrows) are rounded and occasionally adhered to each other. The cell viability and purity are > 90%. The average cell diameter of hepatocytes from newborn rats was approximately 10 μm (range 8-12 μm). Bar represents 24 μm.

using GF/C filters and washed with 8 ml of ice-cold PBS. The wash step has been shown to prevent the transmembrane flux of [^{3}H]-palmitate and to wash any adhered extracellular [^{3}H]-palmitate containing solution [44]. The uptake procedure did not change cell viability. In all studies cell viability was greater than 95%.

C.3.11. Data analysis

Cells associated radioactivity was determined by scintillation counting using LS6500 liquid scintillation counter (Beckman Instruments) with automatic quench correction after the addition of Ready Safe (Beckman). Total palmitate space was calculated as the ratio of recovered cell-associated radioactivity to the concentration of radioactivity in the uptake solution.Total palmitate clearances (μl / s. 10^6 cells) were obtained from the slope of the plot of palmitate space (μl / 10^6 cells) vs. uptake interval. The data are presented as means $\pm$ SEM and the n value represents the number of animals used (in case of hepatocytes or cardiac myocytes uptake experiments) or number of replicates performed for other experiments. Data were analyzed by student t-test or one-way analysis of variance (ANOVA) and Tukey's multiple comparison test to test if there are any significant differences among mean palmitate clearances as well as for other experiments. The ratio of palmitate clearance in the presence of different binding proteins to the palmitate clearance in the presence of ALB was calculated and the plot of this ratio vs. protein isoelectric point was analyzed by regression analysis. A p value of < 0.05 was considered statistically significant.

C.4. Results

C.4.1. Molecular weight (M_W) and isoelectric point (pI) of proteins

The molecular weights of ALB, ALBm, ALBs, ALB_E, and ALB_{E1} were determined to be 66400, 69400, 67400, 68800, and 67300, respectively. The molecular weighst of LYS, AGP, and CONALB were obtained from the manufacturer specification and were reported to be 14400, 45000, and 77000, respectively, (Table 5). Protein concentrations for heptane: buffer partitioning and uptake experiments were confirmed either by the Bradford assay or by a spectrophotometric method using ALB as a standard. The isoelectric point of ALBm, ALBs, ALB, CONALB, $ALB_{E1,}$ and ALB_E are shown in Table 5. Based on these pI values, AGP, ALBm, ALBs, and ALB were designated as anionic binding proteins; CONALB, and ALB_{E1} were designated as neutral binding proteins; ALB_E and LYS were designated as cationic binding proteins.

C.4.2. Extent of ALB modification

Results of ninhydrin color reaction for native as well as ALBs and ALBm are shown in Figure 8. The decreased absorption in the ninhydrin color reaction provided evidence that the reaction had mainly occurred at amino groups of albumin. Figure 8 inset shows the percent modification for each preparation calculated from equation 4. Fifty one percent of the positively charged free amino groups of lysine residue were modified with the negatively charged maleyl residues, resulting in ALBm. Only 10 % of the free amino groups of lysine were modified with the negatively charged succinyl residues, which resulted in the

Parameter	AGP	ALBm	ALBs	ALB	CON-ALB	ALB_{E1}	ALB_E	LYS
Ka (10^8 M^{-1}) (n=4)	0.001 ± 0.0001	0.90 ± 0.01	1.18 ± 0.03	2.2 ± 0.10	0.23 ± 0.10	1.49 ± 0.19	0.86 ± 0.06	0.00016 ± 0.00001
K_{off} (sec^{-1}) (n=4-6)	0.081 ± 0.024	0.069 ± 0.010	0.061 ± 0.005	0.070 ± 0.016	0.054 ± 0.006	0.064 ± 0.011	0.070 ± 0.007	0.130 ± 0.022
PI range	2.9[a]	3-4.5	4.5-4.7	4.9	6.2–6.6	7.0–7.5	8.6	11.0[b]
Cardiac Myocyte Clearance Rate (µl / s. 10^6 cells)	0.83 ± 0.15 (n=4)	0.78 ± 0.06 (n=7)	0.99 ± 0.050 (n=14)	0.93 ± 0.06 (n=31)	1.53 ± 0.10 (n=7)	1.58 ± 0.18 (n=8)	1.82 ± 0.10 (n=16)	1.90 ± 0.07 (n=10)
Hepatocyte Clearance Rate (µl / s. 10^6 cells)	0.20 ± 0.02 (n=4)	0.40 ± 0.04 (n=6)	0.50 ± 0.04 (n=6)	0.72 ± 0.07 (n=8)	0.85 ± 0.03 (n=6)	0.98 ± 0.05 (n=6)	1.4 ± 0.22 (n=6)	1.87 ± 0.10 (n=6)
Average M_w	45000	69400	67400	66400	77000	67300	68800	14400
Viscosity at 37°C mPa.s (n=4)	0.83 ± 0.03	0.82 ± 0.04	0.84 ± 0.04	0.87 ± 0.01	0.98 ± 0.01	0.84 ± 0.04	0.78 ± 0.01	2.4 ± 0.40

Table 5. Summary of physiochemical characteristics of the eight binding proteins investigated. K_a, high-affinity equilibrium binding constant; K_{off}, dissociation rate constant; pI, isoelectric point; M_w, molecular weight; AGP, α_1-acid glycoprotein; ALBm, ALB reacted with maleic anhydride; ALBs, ALB reacted with succinic acid; ALB, bovine serum albumin; CONALB, conalbumin; ALB_{E1}, ALB reacted with ethylenediamine for 10 minutes; ALB_E, ALB reacted with ethylenediamine for 2 hours; LYS, lysozyme. [a] pI of AGP was taken from the literature. [b] pI of LYS was taken from the literature. Data presented as means ± SEM, where n indicates the sample size.

Protein	% Modification
Native ALB	0
ALBm	51.0
ALBs	10.0

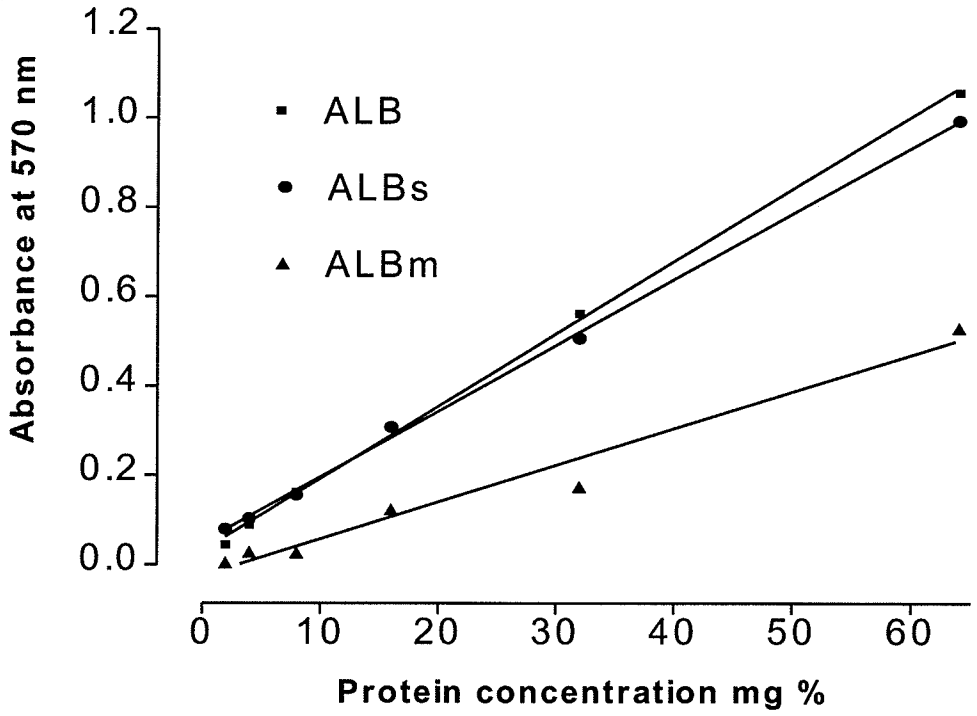

Figure 8. Plot of ninhydrin color intensity vs. protein concentration. The protein preparations are native ALB, ALBs, and ALBm. Least square regression analysis was used to draw straight lines. Inset shows the extent of acylation of amino groups in native ALB treated with succinic or maleic anhydride.

formation of ALBs. Peptide mapping of ALB_E and ALB_{E1} compared to native ALB showed that approximately 97% and 37% of the glutamic acid residues were modified by the addition of the ethylenediamine groups, respectively.

C.4.3. Determination of unbound palmitate fraction (α) and the protein-palmitate equilibrium binding constant (K_a).

The unbound palmitate fraction in the presence of each binding protein at different concentration was measured using heptane-to-buffer partitioning. Using protein concentrations of 0.1 μM for ALB, ALBs, ALB_E, ALB_{E1}, ALBm, and CONALB; 20 μM for AGP and; 50 μM for LYS. Unbound fractions were determined to be 0.042 ± 0.001, 0.078 ± 0.011, 0.110 ± 0.004, 0.061 ± 0.009, 0.105 ± 0.001, 0.224 ± 0.004, 0.330 ± 0.03, 0.59 ± 0.046 (mean ± SEM, n = 4), respectively. The calculated K_a value for each protein is shown in Table 5. We used those K_a values to calculate the protein concentration required yielding an unbound palmitate fraction of 0.03 for the uptake experiments.

C.4.4. Determination of protein-palmitate dissociation constant (K_{off})

The calculated k_{off} values from regression analysis results for the slope of the plot ratio of filtrate radioactivity to total radioactivity versus time for the different protein-[^{3}H]-palmitate complexes are shown in Table 5. Figure 9 shows the data from all experiments (n=4-6). Variability in the data reflects the day-to-day variability observed in the transfer experiments. In all individual experiments the correlation coefficient for the plot of natural logarithm of the ratio of filtrate

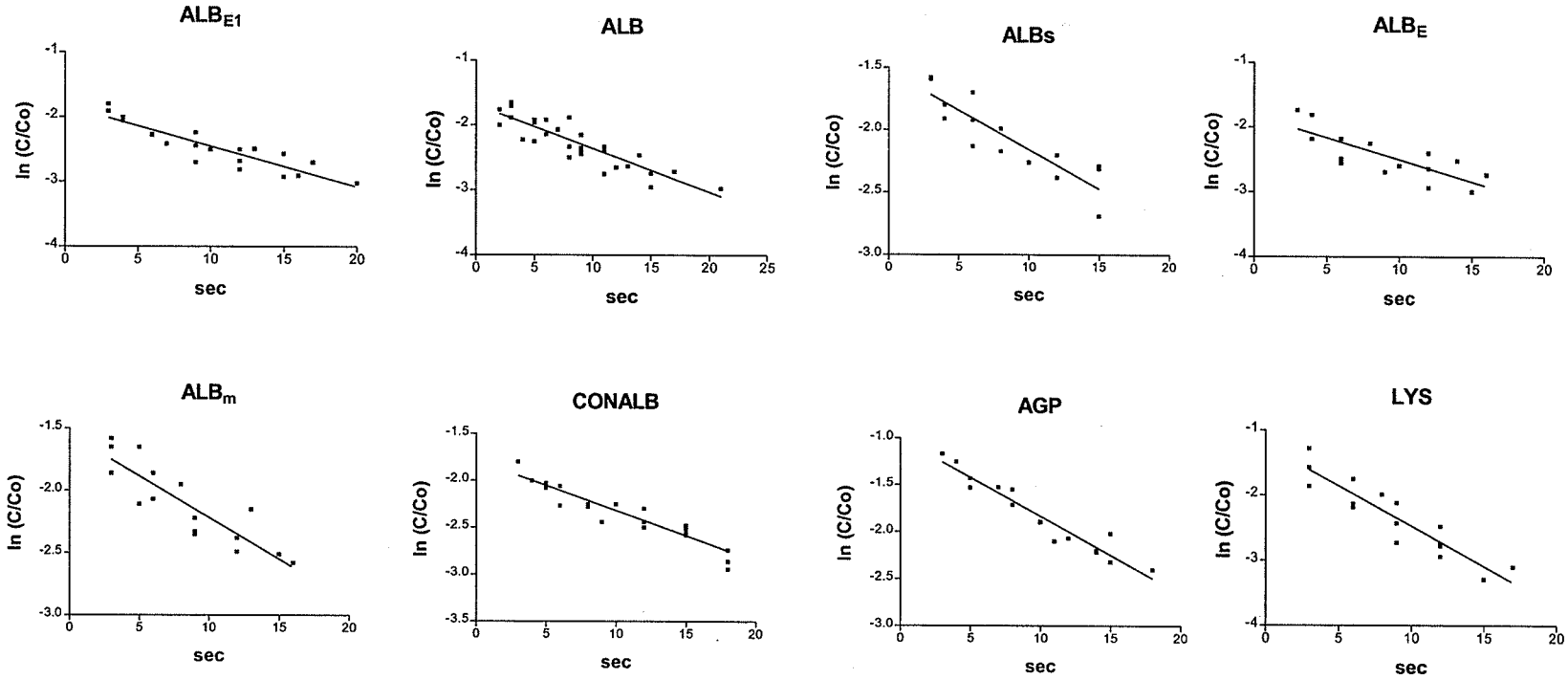

Figure 9. Transfer of [^{3}H]-palmitate from the different proteins to albumin-agarose at 37°C (four to six separate experiments, data from all experiments). The ordinate shows the natural logarithmic ratio of filtrate radioactivity to total radioactivity. Graphs show the individual data points obtained from all experiments conducted. The variability in the different plots also portrays the day-to-day variability in experiments.

radioactivity to the total radioactivity versus time was approximately 0.9. There was no statistically significant difference in K_{off} values obtained for all binding proteins with the exception of lysozyme-palmitate, which was significantly higher than the other proteins ($p < 0.05$).

C.4.5. Viscosity of protein solutions

Because viscosity affects the diffusion of proteins and ligands, differences in the protein concentrations may influence overall clearance by affecting solution viscosity. Table 5 shows the viscosity of each protein solution measured at 37^{0}C. Measurements were made using the same protein concentration used in the uptake studies. There were no statistical differences between the viscosity values for AGP, ALBm, ALBs, ALB, CONALB, ALB_{E1}, and ALB_E. However, the viscosity of LYS was significantly greater than the other proteins ($p<0.001$).

C.4.6. Myocyte- [^{3}H]-palmitate clearance

A summary of the [^{3}H] palmitate clearances by neonatal cardiac myocytes in the presence of the eight binding proteins is shown in Figure 10 (clear bars). In all individual uptake experiments the correlation coefficient for the plot of [^{3}H]-palmitate space vs. time was greater than 0.90. The [^{3}H]-palmitate clearance in the presence of CONALB (1.53 $\pm$ 0.10 μl / s. 10^6 cells; mean $\pm$ SEM; n=7), ALB_{E1} (1.58 $\pm$ 0.18 μl / s. 10^6 cells; mean $\pm$ SEM; n=8), ALB_E (1.82 $\pm$ 0.10 μl / s. 10^6 cells; mean $\pm$ SEM; n=16), or LYS (1.90 $\pm$ 0.07 μl / s. 10^6 cells; mean $\pm$ SEM; n=10) was significantly different ($p<0.05$) than ALB (0.93 $\pm$ 0.06 μl / s. 10^6 cells;

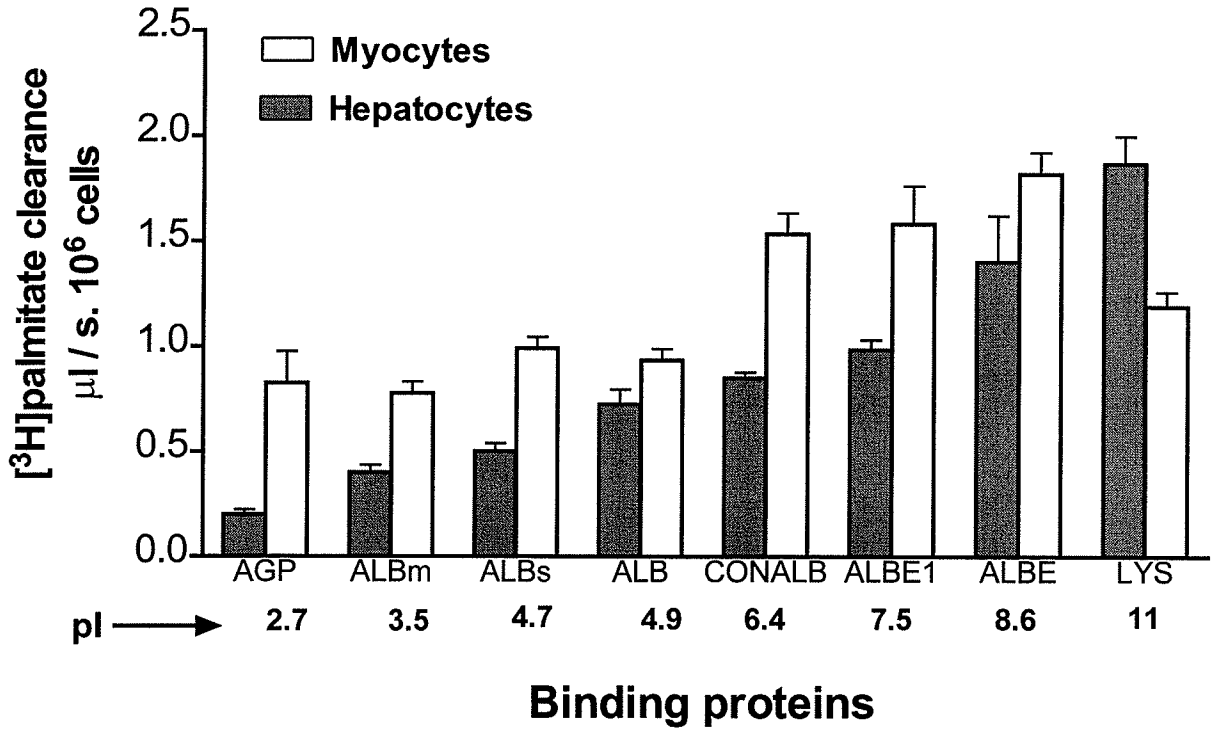

Figure 10. Myocyte- [^{3}H]-palmitate clearances (clear bars) and hepatocyte-[^{3}H]-palmitate clearances (solid bars). Clear and solid bars represent AGP, ALBm, ALBs, ALB, CONALB, ALB_{E1}, ALB_E, and LYS. Data are means ± SEM; n = 4 to 30. In each case the free fraction (α) = 0.03

mean ± SEM; n=31). In contrast, there was no significant difference in [^{3}H]-palmitate clearance when AGP (0.83 ± 0.15 μl / s. 10^6 cells; mean ± SEM; n=4), ALBm (0.78 ± 0.06 μl / s. 10^6 cells; mean ± SEM; n=7) or ALBs (0.99 ± 0.05 μl / s. 10^6 cells; mean ± SEM; n=14) was used as binding protein compared to ALB ($p > 0.05$). The relationship between isoelectric point and the ratio of [^{3}H] palmitate clearance in the presence of each binding protein to that of ALB is shown in Figure 11. Regression analysis showed that there was an overall poor correlation between neonatal cardiac myocyte-[^{3}H]-palmitate clearance and protein pI ($r^2 = 0.48$). The slope of the regression line in Fig. 11 showed that for each unit increase in pI value there was a 15 ± 6% increase in the [^{3}H]-palmitate clearance. However, when only the albumin and albumin modified binding proteins were considered there was a much better correlation between [^{3}H]-palmitate clearance and protein pI (r^2=0.90, Fig. 12). Regression analysis result using the nonalbumins is shown in Figure 13.

C.4.7. Hepatocyte- [^{3}H] palmitate clearance

[^{3}H]-palmitate clearance by neonatal hepatocytes in the presence of eight binding proteins is shown in Figure 10 (dark bars). As with the myocyte study, in all individual uptake experiments the correlation coefficient for the plot of hepatocyte [^{3}H]-palmitate uptake vs. time was greater than 0.90. [^{3}H]-palmitate clearance differed significantly (compared to albumin; 0.72 ± 0.07 μl / s.10^6 cells; mean ± SEM; n=8; $P < 0.05$) when, AGP (0.20 ± 0.02 μl / s. 10^6 cells; mean

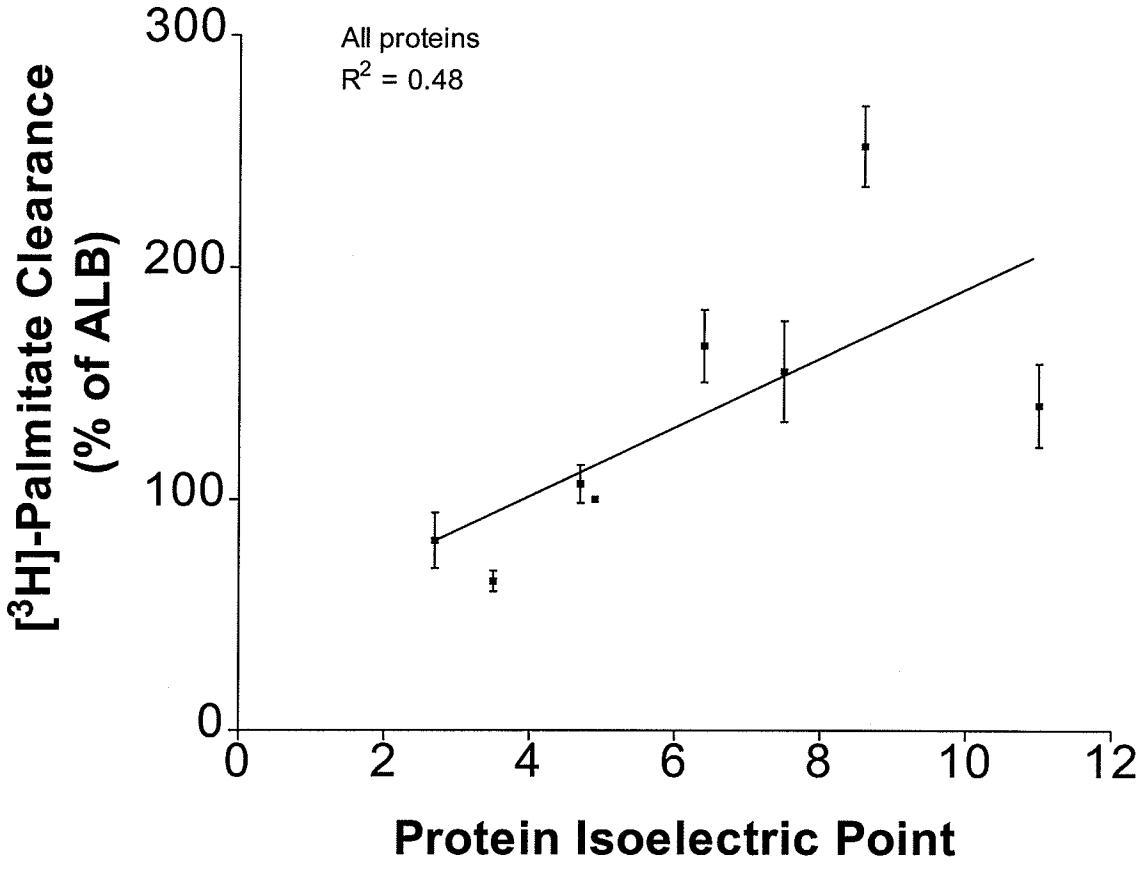

Figure 11. Relationship between myocytes-[^{3}H[-palmitate clearance relative to albumin and protein isoelectric point. Data represent the ratio of [^{3}H]-palmitate clearances in the presence of AGP, ALBm, ALBs, CONALB, ALB_{E1}, ALB_E, or LYS to those obtained with ALB. (R^2 = 0.48). Where no bar is indicated, SEM value is smaller than symbol size.

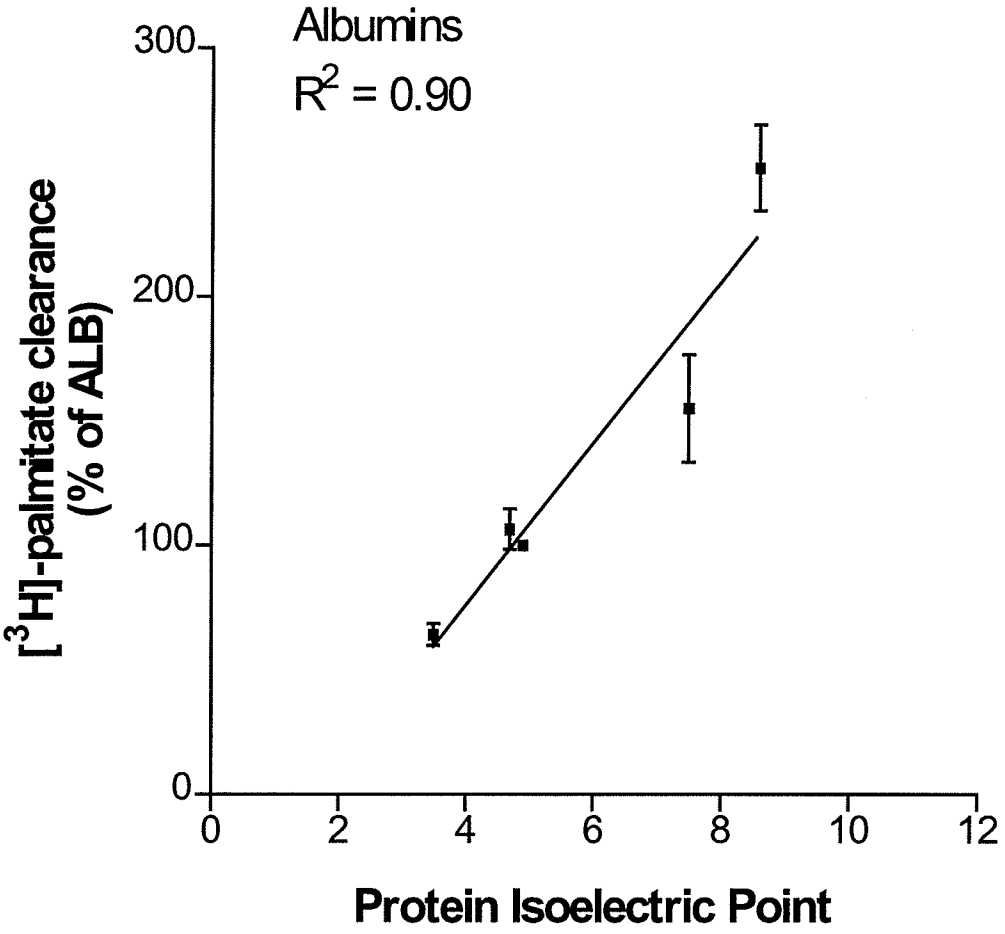

Figure 12. Relationship between myocyte-[^{3}H]-palmitate clearance relative to albumin and modified albumins isoelectric point. Data represent the ratio of [^{3}H]-palmitate clearances in the presence of ALBm, ALBs, ALB_{E1}, or ALB_E to those obtained with ALB. (R^2 = 0.90).

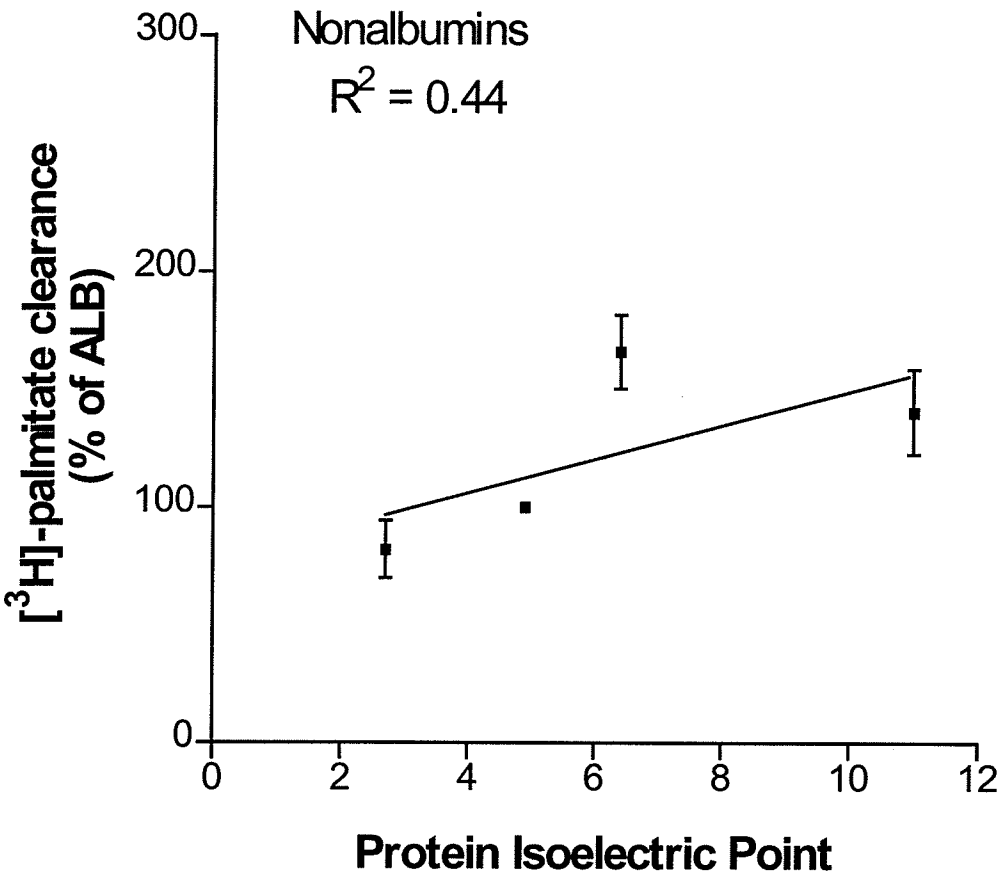

Figure 13. Relationship between myocyte-[^{3}H]-palmitate clearance relative to albumin and nonalbumins isoelectric point. Data represent the ratio of [^{3}H]-palmitate clearances in the presence of AGP, CONALB, or LYS to those obtained with ALB. (R^2 = 0.44).

± SEM; n=4), ALBm (0.40 ± 0.04 μl / s. 10^6 cells; mean ± SEM; n=6), ALBs (0.50 ± 0.04 μl / s. 10^6 cells; mean ± SEM; n=6), ALB_{E1} (0.98 ± 0.05 μl / s. 10^6 cells; mean ± SEM; n=6), ALB_E (1.40 ± 0.22 μl / s. 10^6 cells; mean ± SEM; n=6), or LYS (1.87 ± 0.10 μl / s. 10^6 cells; mean ± SEM; n=6) was used as binding protein. In contrast, there was no significant difference when CONALB (0.85 ± 0.03 μl / s. 10^6 cells; mean ± SEM; n=6) was used as binding protein compared to ALB ($p>0.05$). The relationship between isoelectric point and the ratio of [^{3}H] palmitate clearance in the presence of each protein to that of ALB is shown in Figure 14. Regression analysis showed that there is a strong correlation between neonatal hepatocyte- [^{3}H] palmitate clearance and protein pI (r^2 = 0.99). The slope of the regression line showed that for each unit increase in pI value, there was 25 ±1 % increases in the [^{3}H]-palmitate clearance. This relationship in the presence of albumin and modified albumins is shown in Figure 15 while the relationship in the presence of nonalbumin proteins is shown in Figure 16.

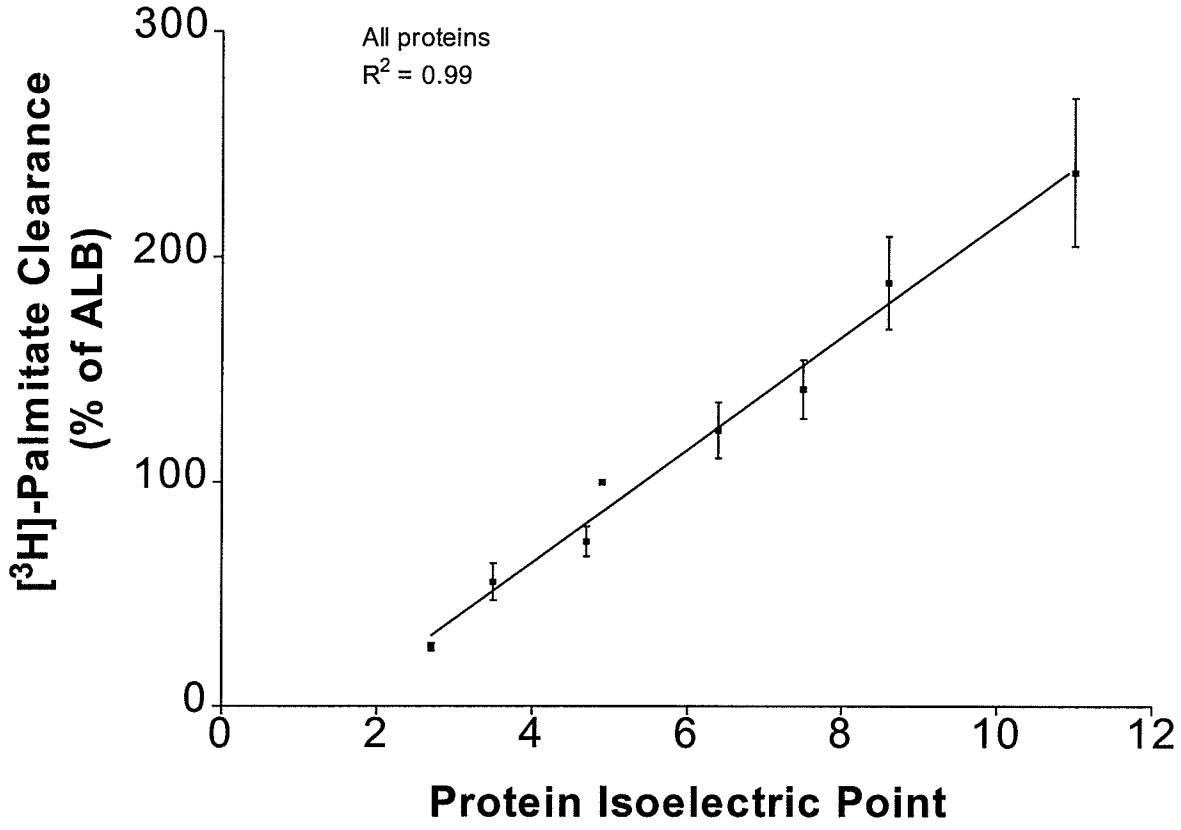

Figure 14. Relationship between hepatocyte-[^{3}H]-palmitate clearance relative to albumin and protein isoelectric point. Data represent the ratio of [^{3}H]-palmitate clearances in the presence of AGP, ALBm, ALBs, CONALB, ALB_{E1}, ALB_E, or LYS to those obtained with ALB. (R^2=0.99). Where no bar is indicated, SEM value is smaller than symbol size.

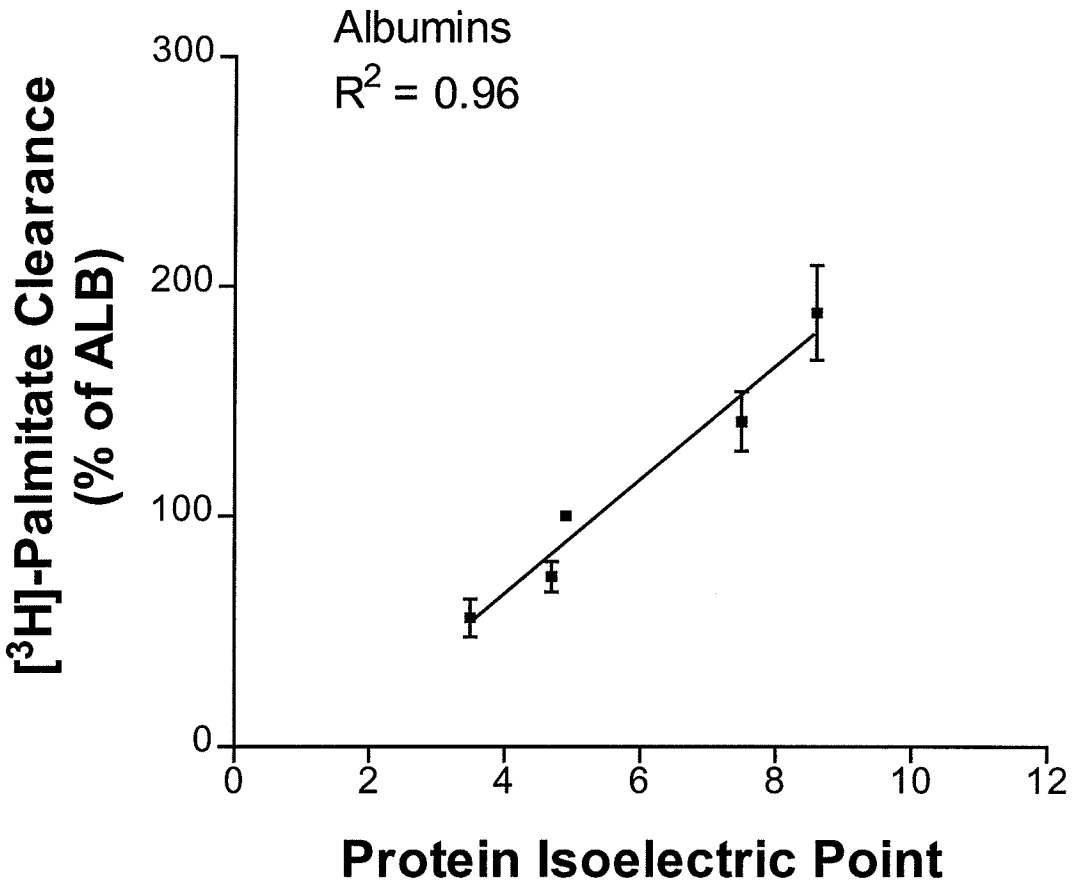

Figure 15. Relationship between hepatocyte-[^{3}H]-palmitate clearance relative to albumin and modified albumins isoelectric point. Data represent the ratio of [^{3}H]-palmitate clearances in the presence of ALBm, ALBs, ALB_{E1}, or ALB_E to those obtained with ALB. (R^2 = 0.96).

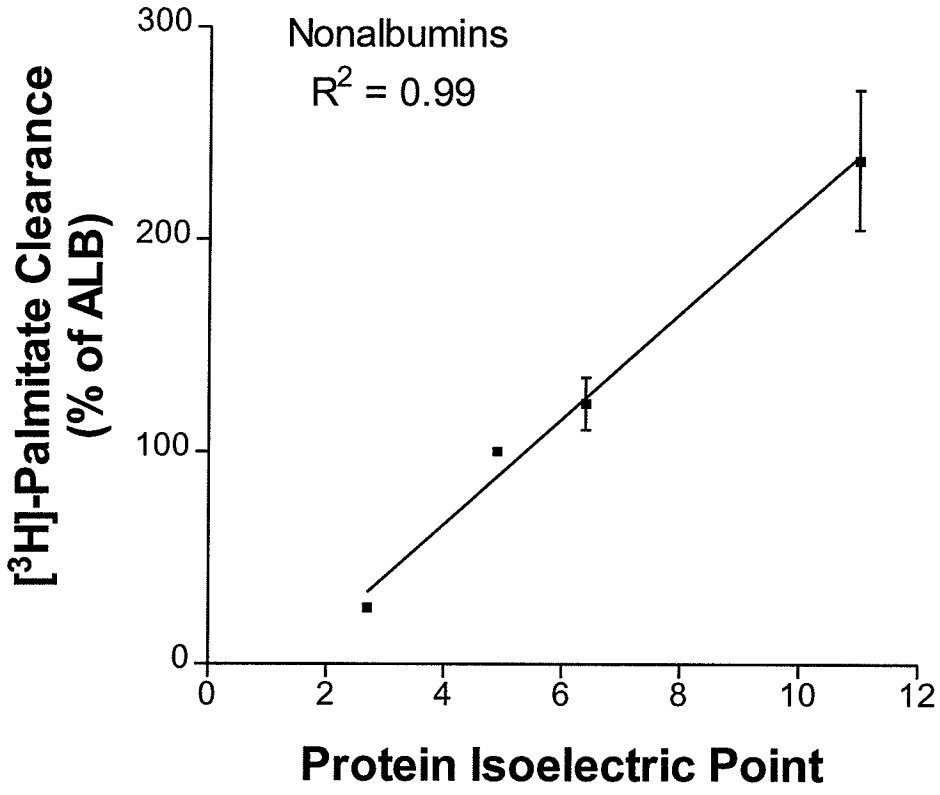

Figure 16. Relationship between hepatocyte-[^{3}H]-palmitate clearance relative to albumin and nonalbumins isoelectric point. Data represent the ratio of [^{3}H]-palmitate clearances in the presence of AGP, CONALB, or LYS to those obtained with ALB. (R^2 = 0.99).

C.5. Discussion

Investigators have reported that albumin facilitates the uptake of albumin-bound ligands and that this facilitation process was specific to albumin [48]. That work has led others [37, 98] to suggest that specific albumin receptors on the surface of hepatocytes and cardiac myocytes enhance the dissociation rate of the albumin-ligand complex thus facilitating the overall uptake rate. Contrary to the suggestion of albumin mediated ligand uptake, others believe that extracellular binding proteins do not participate in the uptake process. Circumstantial evidence favours the view that uptake occurs solely from the unbound fraction and the protein bound fraction serves only to replenish that amount of unbound ligand extracted by cells [62]. The present study provides evidence for the former argument i.e., extracellular protein mediated uptake of the protein-bound ligand (also termed facilitated uptake).

In the present study binding proteins with much different surface charge characteristics were used to test the hypothesis that an ionic interaction between extracellular proteins and the surface of hepatocytes and cardiac myocytes isolated from neonatal animals facilitates the uptake of the unbound ligand. The relationship between the [^{3}H]-palmitate clearance ratio and protein isoelectric point (surface charge) shown in Figure 14 provides evidence that extracellular proteins are indeed involved in the uptake process. This relationship leads us to conclude that one potential mechanism for facilitated uptake of protein-bound ligands is an ionic interaction between the protein-palmitate complexes and the

hepatocyte surface. Ionic interactions have been reported to be involved in the uptake and transcytosis of albumin-bound long-chain fatty acids by endothelial cells [57] as well as enhanced adsorption of human plasma albumin at negatively charged surfaces [56]. At the outer cell membrane leaflet, polar groups such as phospholipids and glycoproteins exist in various states of ionization. At physiological pH most of these polar groups are negatively charged [99-102]. An increased charge density in neonatal heart ventricular and liver cells has been reported to occur between pH 4 and 9 with hepatocytes showing a much greater charge density than cardiac myocytes [99]. Thus, we speculate that the positively charged binding proteins may be attracted to the negatively charged hepatocyte surface. The ionic attraction would be expected to result in a marked reduction in the diffusional distance of the protein-ligand complex. In this manner uptake is enhanced beyond that predicted by conventional theory. Moreover, the acidic microenvironment associated with the cell surface charged groups also would result in an increased unbound fraction. Previous work has shown that acidic environments lead to a decrease in the Ka of albumin-ligand complexes [103, 104] as well as modulating the conformational change in albumin (neutral-base, neutral-fast transition) [105, 106]. Furthermore, albumin is known to undergo a conformation change when it collides with surfaces that can lead to enhanced ligand dissociation [50]. The net result of those changes is that more ligand becomes unbound and available for uptake.

Whether specific 'albumin receptors' on the surface of hepatocytes

explain the present data is not clear. Our data do not disprove the existence of specific albumin receptors but we suggest that ionic recognition sites exist on the surface of hepatocytes. Those recognition sites may be receptors although not specific to albumin since a very good correlation existed between [^{3}H]-palmitate clearance in the presence of the nonalbumin binding proteins and protein surface charge (Figure 14).

Unlike the data for neonatal hepatocytes, evidence favoring the view that protein-bound ligands are involved in the uptake process was not that clear for rat neonatal cardiac myocytes (Figure 11). However, if we separate the albumin binding proteins from the nonalbumin binding proteins (Figure 12), a relationship between the [^{3}H]-palmitate clearance in the presence of the different extracellular modified albumins and protein surface charge becomes evident. The coefficient of determination shows a very good fit of the data between [^{3}H]-palmitate clearance ratio and albumin surface charge (r^2=0.90). The coefficient of determination for the [^{3}H]-palmitate clearance in the presence of the nonalbumin binding proteins and protein surface charge, however, was poor (Figure 13; r^2=0.44). Thus, based upon regression analysis the present data are consistent with the notion that the surface of neonatal cardiac myocytes may contain sites specific for albumin and albumin-like proteins that catalyze the dissociation of the albumin-palmitate complex. The liberated palmitate is then free to interact with the cell surface to become extracted [98].

We took several precautions in our study design. First, purity of the [^{3}H]-

palmitate is of primary concern when using very small-unbound ligand fractions. The manufacturer-supplied [^{3}H]-palmitate must be further purified prior to use or data interpretation may lead to incorrect conclusion. As I stated in chapter two, radiolabeled impurities are also extracted by cell. The extent of uptake attributable to radiolabeled impurities increased by increasing binding protein concentration. Uptake of impurities may reach up to 84% at physiological albumin concentration. Thus, in all our experiments we routinely purify the supplied [^{3}H]-palmitate using a heptane:buffer extraction procedure.

Second, to ensure that the driving force for uptake was similar for all proteins investigated we conducted our studies using similar unbound fractions. The amount of protein required to provide an unbound palmitate fraction of 0.03 was calculated using the equilibrium binding constant for the different protein-[^{3}H]-palmitate complexes determined by the heptane:buffer partition ratio. As outlined in chapter two, when radiolabeled impurities were eliminated the calculated K_a was independent of protein concentration and thus use of equation 3 is a valid approach towards calculating protein concentration to yield a predetermined unbound fraction.

Third, we chose to conduct our studies using a high albumin:[^{3}H]-palmitate molar ratio. Using this molar ratio the majority of ligand binding would occur to the highest affinity protein binding site and the calculated values (K_a, K_{off}, and α) would be representative of the values for ligand binding to that site.

Because significant differences in the dissociation rates for the different

proteins could affect the overall [^{3}H]-palmitate clearance, i.e., higher dissociation rate may be expected to be associated with higher clearances [52], it was necessary to assess the protein-ligand dissociation rate for each binding protein. It is interesting to note that while the K_a differed considerably between the different protein-[^{3}H]-palmitate complexes, the dissociation rate constants for the different proteins were similar with the exception of lysozyme. It is generally thought that changes in K_a are reflected by changes in K_{off}. However, that reasoning assumes that the association process (K_{on}) is a constant for all proteins and expected to be diffusion limited (diffusion through the aqueous phase to the protein binding site). If the rate-limiting step for the protein-palmitate association rate is not ligand diffusion through the unstirred fluid surrounding the protein but rather ligand diffusion through the protein matrix to the binding site, k_{on} also could differ considerably. Such reactions have been shown for carbon monoxide binding to myogloblin and haemoglobin [107, 108], suggesting that similarities in k_{off} for the different proteins may be possible. Since the dissociation rate constants were similar for the different protein-[^{3}H]-palmitate complexes, it is unlikely that our conclusion for extracellular protein mediated uptake was affected by changes in the dissociation rate constant.

It is well known that diffusion through the adjacent extracellular unstirred fluid layer has the potential to affect the overall uptake rate [109] Diffusion is affected by solution viscosity. An increased viscosity would decrease the diffusion coefficient of both the protein-bound and unbound ligands and lower the uptake

rate. Table 5, however, showed that there were no significant differences in the viscosity of different protein solutions with the exception of LYS. LYS was associated with a significantly higher viscosity than the other protein solutions. A higher viscosity is expected to lower the overall clearance since it would take longer to traverse the adjacent unstirred fluid layer. However, for both cardiac myocyte and hepatocyte experiments [^{3}H]-palmitate clearances in the presence of LYS were greater than the observed [^{3}H]-palmitate clearances in the presence of ALB. Thus, we conclude that viscosity was not a factor in our conclusion.

Taking into consideration our testing criteria, the marked differences in myocyte or hepatocyte-palmitate uptake rates among various proteins could not be explained by the difference in protein viscosity, protein-palmitate dissociation rate, presence of radiolabeled impurities, or in the unbound fraction available for the uptake. Our results were consistent with the notion that ionic interactions between protein-ligand complexes and the cell surface facilitate ligand uptake by decreasing the diffusional distance of the unbound ligand and / or facilitate the protein-ligand dissociation rate.

Based on the regression analysis of the data in Figure 14 (in case of hepatocytes) and Figure 11 (in case of cardiac myocytes), the slope of the regression lines showed that hepatocyte-[^{3}H]-palmitate clearance increased by 25 % with a unit increase in pI while cardiac myocyte-[^{3}H]-palmitate clearance increased by 15% with a unit increase in pI. The significant difference in

palmitate delivery between hepatocyte and cardiac myocytes suggests that significant differences may exist in the outer membrane leaflet of hepatocyte and cardiac myocyte and / or difference in the cell microenvironment.

Collins, et al. [99] examined the pH-mobility relationship of cells derived from chick embryo heart ventricle and liver. He found that there is an increase in charge density on these cells between pH 4 and 9. In addition, liver cells showed much greater charge densities than heart cells at pH above 4. The author concluded that the difference in charge density between hepatocyte and myocyte surface suggests that these cell surfaces have similar ionogenic groups and that they differ only in their relative quantities. Also this indicates that the higher net negative charge density on liver cells may be due to the presence of comparatively larger number of aniongenic groups than to a relative deficiency of cationgenic ones [110].

Further analysis was made by comparing the adult hepatocyte-[^{3}H] palmitate uptake data taken from our previous study [52] with our neonatal hepatocyte- [^{3}H]-palmitate uptake data from this study after correcting the uptake data from μl / s. 10^6 cells to μl / s . mg protein (adult rat hepatocyte contains 4 fold more protein than neonatal rat hepatocyte) [111]. Our finding (Table 6) showed that the neonatal hepatocyte-[^{3}H]-palmitate clearance in the presence of albumin was greater than the adult hepatocyte-[^{3}H]-palmitate clearance. The difference in the observed clearances between adult and neonatal hepatocytes may reflect the difference in their electrophoretic mobility (EMP, the mobility of

Binding protein	[^{3}H]-palmitate clearance [1] mean ±SEM, n=8 neonatal rat hepatocyte	[^{3}H]-palmitate clearance[2] mean ±SEM, n=13 adult rat hepatocyte
ALB	2.25 ± 0.22 µl / s. mg protein	1.79 ± 0.24 µl / s. mg protein

Table 6. [^{3}H]-palmitate clearance by neonatal and adult rat hepatocyte. [1]= result from this study. [2] = result from previous study (52).

the cells under the effect of an electric current towards the anode). EMP of hepatocytes isolated from adult and neonatal rat liver was reported to be -0.761 ± 0.01 and -0.942 ± 0.015 $\mu m\ sec^{-1}\ V^{-1}$. cm, respectively [100].

The present data support the literature reports describing the developmental aspects of neonatal hepatocytes. For example, in neonates, cholesterol synthesis in the liver is reduced and consequently, neonatal hepatocytes synthesize and translocate lipoprotein lipase very actively compared to adult hepatocytes. This adaptation was made so that the neonatal liver can extract cholesterol effectively from plasma lipoproteins, as it is the major source of cholesterol for cell needs [112]. Similar to this adaptation, the surface of neonatal hepatocyte has a greater negative charge density than the surface of adult hepatocytes, thus attracting oppositely charged endogenous bound substrates.

In conclusion, our study shows that there was a linear relationship between neonatal hepatocyte [^{3}H]-palmitate clearance and protein pI. In contrast, there was an overall poor relationship between neonatal cardiac myocyte [^{3}H]-palmitate clearance and protein surface charge. The relationship improved when the [^{3}H]-palmitate clearance data were analyzed in the presence of the modified albumins. Our study leads us to conclude that an ionic interaction between extracellular proteins and the hepatocyte surface enhances the overall uptake of [^{3}H]-palmitate in neonatal hepatocytes. Such an interaction was not present in cardiac myocytes. Uptake of [^{3}H]-palmitate in cardiac

myocytes was, however, consistent with the notion of albumin receptor mediated uptake.

Overall our study shows that hepatic drug uptake from physiological proteins (albumin, α_1-acid glycoprotein, conalbumin, etc.) is higher if the protein contains a net positive charge. Thus, hepatic clearance of lipophilic drugs bound to albumin would be expected to be higher than the same drug bound to α_1-acid glycoprotein. It is known that α_1-acid glycoprotein generally binds cationic drugs while anionic compounds are normally bound to albumin. The present data allow us to speculate that the clearance (efficiency of uptake) of anionic drugs would be expected to be higher than cationic drugs. Thus binding of drugs to proteins containing higher positive surface charged groups would be expected to enhance the hepatic uptake process.

Chapter four

Kinetics of fatty acid transfer from serum albumin to phospholipid vesicles

D.1. Introduction

Results from chapter three lead us to believe that cellular LCFA uptake must occur from both free and protein bound fractions (at least in case of hepatocytes and cardiac myocytes). In this chapter we extended our investigation to determine the kinetics of LCFA transfer from albumin to model membranes.

Using a fluorescence resonance energy transfer assay, we examined the transfer rate of anthroyloxy labeled palmitic acid (AOPA) bound to ALB (isoelectric point, pI=4.8) or modified ALB (ALB_{E1}, pI=7.5) to negative, positive, and neutral lipid vesicles. This technique has been successfully used to study the rate and mechanism of transfer of many important physiological substrates such as cholesterol [113]; phospholipids [114]; sphingomyelin [115]; short-chain fatty acids [116]; and long-chain fatty acids [117, 118] between various binding proteins and phospholipid vesicles.

The kinetics of fatty acid transfer from binding protein to model membranes has been investigated using NMR spectroscopy and fluorescence techniques. Using ^{13}C NMR technique, the chemical shifts of carboxyl carbon were followed to characterize binding, partitioning, and transfer of fatty acid in a mixture of albumin and vesicles. One limitation of this method was that the kinetics of transfer could not be accurately determined. Hamilton and Cistola showed that the exchange of oleic acid between lipid and protein was slow on the NMR time scale [119]. Using the fluorescence technique, the rate and

mechanism of fatty acid transfer between binding protein, lipoprotein and vesicles were investigated. The most widely studied binding proteins were fatty acid binding proteins isolated from liver, adipocyte, heart and intestine. The change in the intrinsic fluorescence of albumin (upon fatty acid binding) or change in fluorescence of anthroyloxy labeled-fatty acid (upon dissociation from albumin) with time was followed to measure the transfer rate.

Daniels, et al. [120] showed that the rate constants for desorption of fatty acids from albumin to small unilamellar vesicles varied between 0.12 s^{-1} for myristate to 0.01 s^{-1} for stearate. Desorption rates were shown to be dependent on fatty acid chain length and degree of saturation a characteristic consistent with transfer through aqueous diffusion. Recent studies have suggested that desorption rates of long-chain fatty acid from bovine serum albumin or fatty acid binding proteins are faster than previously reported. In addition, the transfer process has been shown to be affected by the type of fatty acid, albumin to fatty acid molar ratio, albumin and vesicle concentration, membrane composition, pH, and temperature [116-118, 121-125]. Kinetic analysis of bilirubin transfer from albumin to membrane vesicles revealed that the delivery of albumin-bound bilirubin to hepatocyte surface occurs through aqueous diffusion rather than a collisional-mediated process [126].

Our objective in the present study was to elucidate how the transfer rate of free fatty acids bound to proteins that differ only in their surface charge characteristic is affected by the acceptor membrane surface charge, the acceptor

vesicle concentration, and the properties of the aqueous phase.

D.2. Materials

Fluorescently labeled 16-(9-anthroyloxy) palmitic acid (AOPA) was purchased from Molecular Probes, Inc. (Eugene, OR). Synthetic 1,2-dioleoyl-sn-glycero-3-phosphocholine (DOPC), synthetic 1,2-dioleoyl-sn-glycero-3-phosphoserine (DOPS), synthetic 1,2-dioleoyl-sn-glycero-3-phosphoethanolamine (DOPE), 1,2-dioleoyl-sn-glycero-3-phosphoethanolamine-N- (7-nitro-2,1,3-benzoxadiazole-4-yl) (NBD-DOPE) are of high purity and were obtained from Avanti Polar Lipids (Birmingham, AL). Bovine serum albumin (ALB, essentially fatty acid-free), and stearylamine (SA) were purchased from Sigma Chemical Co. (St. Louis, MO.). The aqueous buffer used throughout all experiments was phosphate buffer saline (PBS), which had a composition of (in mM: 137 NaCl, 2.68 KCl, 1.65 KH_2PO_4, 8.92 Na_2HPO_4 and 3 NaN_3) with pH adjusted to 7.4 using 0.1 N NaOH. All other chemicals were reagent grade or better.

D.3. Methods

D.3.1. Chemical modification of albumin.

Albumin was modified by activating the carboxyl groups with carbodiimide treatment and then aminating them with ethylenediamine as previously described (see C.3.1; chapter three).

D.3.2. Determination of molecular weights (M_W), the extent of albumin modification, and isoelectric (pI)

Mass measurements of ALB and ALB_{E1} were conducted on an orthogonal injection electrospray ionization time-of-flight (ESI/TOF III) mass spectrometer as previously described (see C.3.4; chapter three). Amino acid modification was identified by peptide mapping as previously described (see C.3.2; chapter three). The (pI) values for ALB and ALB_{E1} were determined using a model 111 Mini IEF-cell (BIO-RAD) and BioLyte 3/10 obtained from Bio-Rad Laboratories (California, USA). Gels were stained with Coomassie blue R-250.

D.3.3. Preparation of large unilamellar vesicles (LUVs)

Lipid vesicles were prepared by the mechanical dispersion method as described previously [127, 128]. Briefly, 65 mol % synthetic 1,2-dioleoyl-sn-glycero-3-phosphocholine (DOPC), 10 mol % 1,2-dioleoyl-sn-glycero-3-phosphoethanolamine-N-(7-nitro-2,1,3-benzoxadiaz-ole-4-yl) (NBD-DOPE), and 25 mol % 1,2-dioleoyl-sn-glycero-3-phospho-L-serine sodium salt (DOPS, in case of negatively charged lipid vesicles, -veLUVs), or stearylamine (SA, in case of positively charged lipid vesicles, +veLUVs), or 1,2-dioleoyl-sn-glycero-3-phosphoethanolamine (DOPE, in case of neutral lipid vesicles, neuLUVs) in chloroform were evaporated in a rotary evaporator under nitrogen gas to form a thin lipid film on the inner wall of the rounded-bottom flask. PBS containing 0.02% sodium azide (NaN_3), 0.1 mM dithiothreitol (DTT), and 0.1 mM

ethylenediamine-tetraacetic acid (EDTA) was added to a final concentration of 10-13 mM total lipids. The liposome dispersion was extruded 11 times through a polycarbonate membrane, (Nuclepore, catalogue # 61000, 200-nm pore size) using a mini-extruder (Avanti polar Lipids, Alabaster, AL, USA) to obtain a homogenous population of large unilamellar vesicles. Lipid vesicles preparations were stored at room temperature and used within four weeks. Phospholipid and NBD-DOPE concentrations were checked by determination of total inorganic phosphate [129] and UV-spectrophotometer using an extinction coefficient 21,700 cm^{-1} M^{-1}, respectively.

D.3.4. LUVs quality assessment

Determination of zeta potential, mean vesicle size and size distribution were performed using Nicomp 380 ZLS Submicron Particle Sizer / Zeta Potential Analyzer (Particle Sizing Systems, Langhorne, PA, USA). The Nicomp 380 ZLS uses dynamic light scattering (DLS) methods to determine particle size distributions. The Nicomp 380 ZLS uses electrophoretic techniques to measure the zeta potential of a dispersed system. Electron microscopy was used to determine unilamellarity of lipid vesicles.

D.3.5. Binding of AOPA to ALB and ALB_{E1}

Binding of AOPA to ALB or ALB_{E1} was analyzed by fluorimetric titration according to Cogan et al. [130]. Briefly, fluorescently labeled AOPA from a concentrated ethanolic stock solution was added to PBS containing 1 μM ALB or

ALB_{E1} . The molar ratio of AOPA to protein in PBS varied between 0.1 and 3.0. The total ethanol concentration was less than 1.5% (v/v) at the end of the titration. An increase in the fluorescence intensity was observed with increasing AOPA concentration at 37°C. No correction for background levels of AOPA in PBS was necessary since the contribution of AOPA blank to the observed fluorescence intensity in the presence of protein was less than 5%.

D.3.6. Equilibrium partitioning of AOPA between binding proteins and acceptor vesicles.

ALB or ALB_{E1} (1 μM) in PBS, pH 7.4, was incubated with 0.1 μM AOPA at 37°C for 10 minutes and the fluorescence intensity monitored. The protein-AOPA complex was then mixed with positive LUVs, negative LUVs, or neutral LUVs and the mixture was incubated for 20 minutes. This time period was sufficient to achieve equilibrium partitioning of AOPA. At equilibrium, the measured fluorescence reflected only the AOPA bound to protein. The relative partition ratio of AOPA between protein and each lipid vesicle preparation (PR_{AOPA}, mol / mol) was calculated as follows [121]:

$$PR_{AOPA} = \frac{(\%\,\text{Protein-bound AOPA})/\text{mM protein}}{(100-\%\,\text{Protein-bound AOPA})/\text{mM phospholipid}} \qquad (5)$$

where the numerator is the fluorescence intensity measured after addition of lipid vesicles divided by the fluorescence intensity measured before the addition of lipid vesicles.

D.3.7. Transfer assay

Transfer kinetics of AOPA from ALB or ALB_{E1} to different acceptor vesicles were measured using a resonance energy transfer assay as described by Wootan et al. [122]. Briefly, 1 μM ALB or ALB_{E1} was incubated with 0.1 μM AOPA at 37°C until binding equilibrium was reached (as measured by maximum fluorescence intensity). AOPA was stored as a concentrated solution containing ethanol. The ethanol concentration in the incubation mixture was < 0.1 % (v/v). Lipid vesicles were added to the protein-palmitate complex so that the final molar ratio of lipid vesicles to protein was 100. Upon mixing for less than 5 seconds, the decrease in AOPA fluorescence with time was monitored with RF-5000 Recording Spectrofluorometer P/N 206-12400 (Shimadzu Scientific Instrument Inc., Columbia, Maryland). Excitation was at 361 nm and emission was monitored at 470 nm. At equilibrium, the remaining fluorescence signal reflected the remaining protein-bound AOPA. There was no detectable intensity for the binding protein alone, vesicles alone, or unbound AOPA in PBS at the concentrations used.

Pre-equilibrium data were collected in photon counting mode at 10 sec intervals for 600 to 1000 sec and analyzed by plotting the variation of fluorescence intensity versus time, fitting to a single exponential equation [122]:

$$F(t) = C_o \exp^{-Kt} + C \qquad (6)$$

where, C_o is the initial (maximum) fluorescence intensity, K is the transfer rate of AOPA from binding protein to acceptor vesicles (units of sec^{-1}), t is the time

interval (sec), and C is the fluorescence intensity of AOPA which remained bound to the protein at equilibrium.

D.3.8. Data analysis

Data are represented as mean ± SEM unless otherwise mentioned. n is the number of replicates performed for each experiment. Whenever appropriate, data were analyzed using non-linear least square regression analysis or linear regression analysis. Goodness of fit was assessed by the coefficient of determination (r^2) which was > 0.9, and absolute sum of squares which was < 0.1. For statistical differences, data were analyzed using student t-test and taking $p < 0.05$ as the level for significance.

D.4. Results

D.4.1. Molecular weights (M_W), extent of albumin modification and (pI).

See C.4.1, C.4.2, and Table 5 in chapter three.

D.4.2. LUVs physical properties

The physical characteristics of the lipid vesicles are shown in Table 7. The zeta potential calculated for each lipid vesicle preparation revealed that the lipid vesicles had appropriate charges (Figures 17-19). Vesicle size and unilamellarity were confirmed by negative-stain and cryoelectron microscopy. There was no significant difference between the mean vesicle sizes of the three-lipid vesicle preparations (Figures 20-22).

Physical properties	Negatively charged vesicles (-veLUVs)	Neutral vesicles (neuLUVs)	Positively charged vesicles (+veLUVs)
Average zeta potential (mV)	-18	-5	+10
Mean diameter (nm ± SD)	199 ± 37*	200 ± 39* 232 ± 66**	222 ± 35*

Table 7. Physical properties of lipid vesicles. Average zeta potential, and mean particle size were measured using Nicomp 380 ZLS submicron Particle Sizer / Zeta Potential Analyzer. * = LUVs in PBS and **= neuLUVs incubated for 48 hours in PBS containing 1 M NaCl.

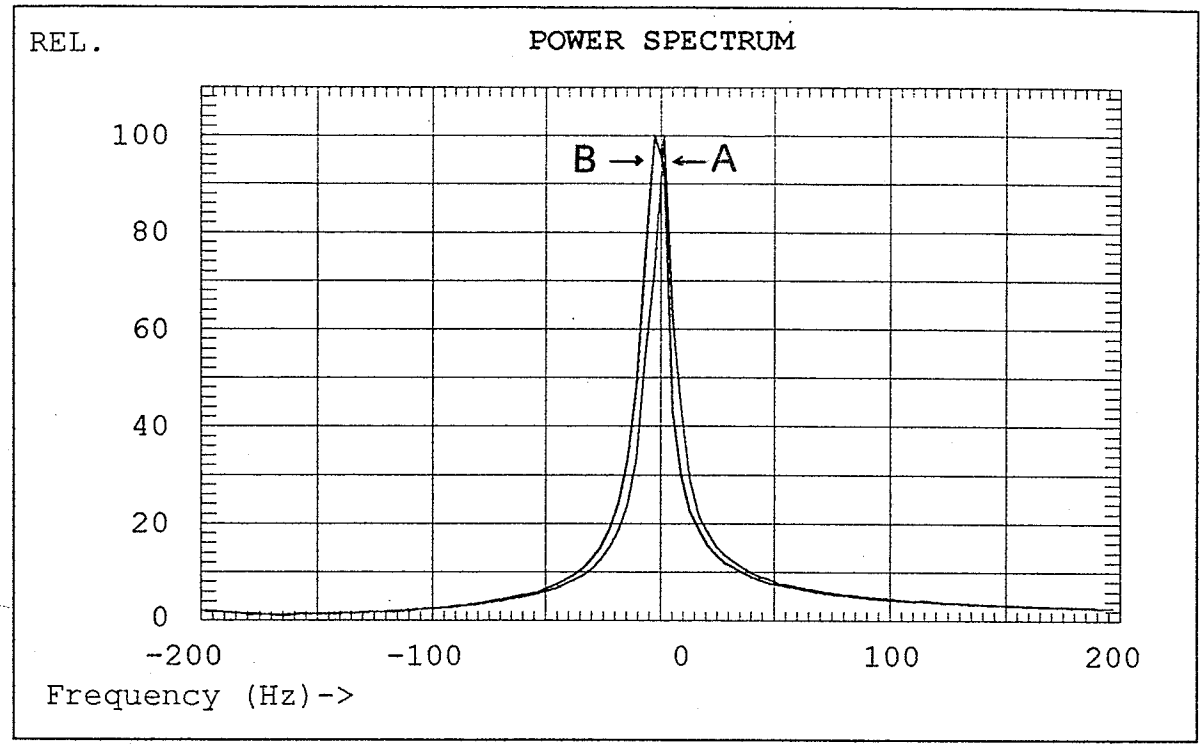

Figure 17. Power spectrum from a Nicomp 380 ZLS Submicron Particle Sizer/Zeta Potential Analyzer used for zeta potential measurement of negatively charged lipid vesicles (-veLUVs). Peak A is the reference (zero mobility). Peak B is the lipid vesicle sample, which was shifted by –3.46 Hz with respect to the reference peak due to the velocity of the vesicles moving along the electric field. The calculated average zeta potential was - 18.13 mV.

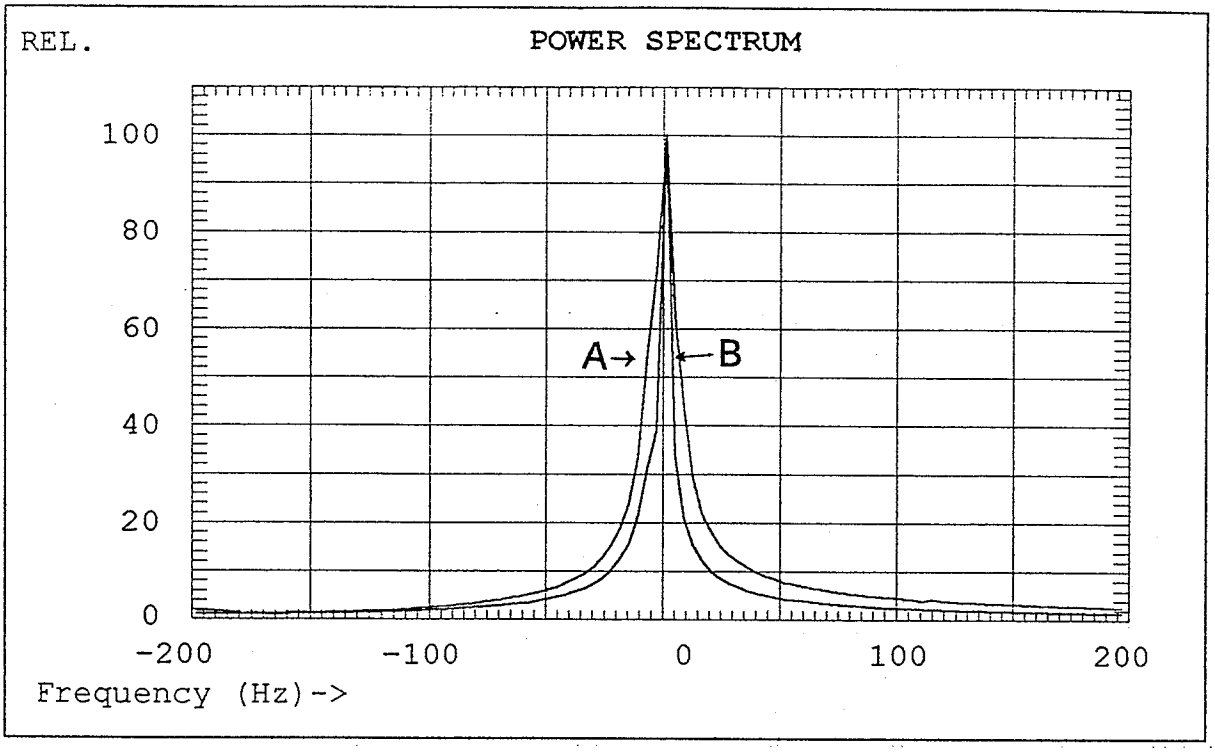
REL.
POWER SPECTRUM
100
80
60
40
20
0
A→
←B
-200
-100
0
100
200
Frequency (Hz)->
Figure 18. Power spectrum from a Nicomp 380 ZLS Submicron Particle Sizer/Zeta Potential Analyzer used for zeta potential measurement of neutral lipid vesicles (neuLUVs). Peak A is the reference. Peak B is the lipid vesicles sample, which is comparable to peak A (zero mobility).

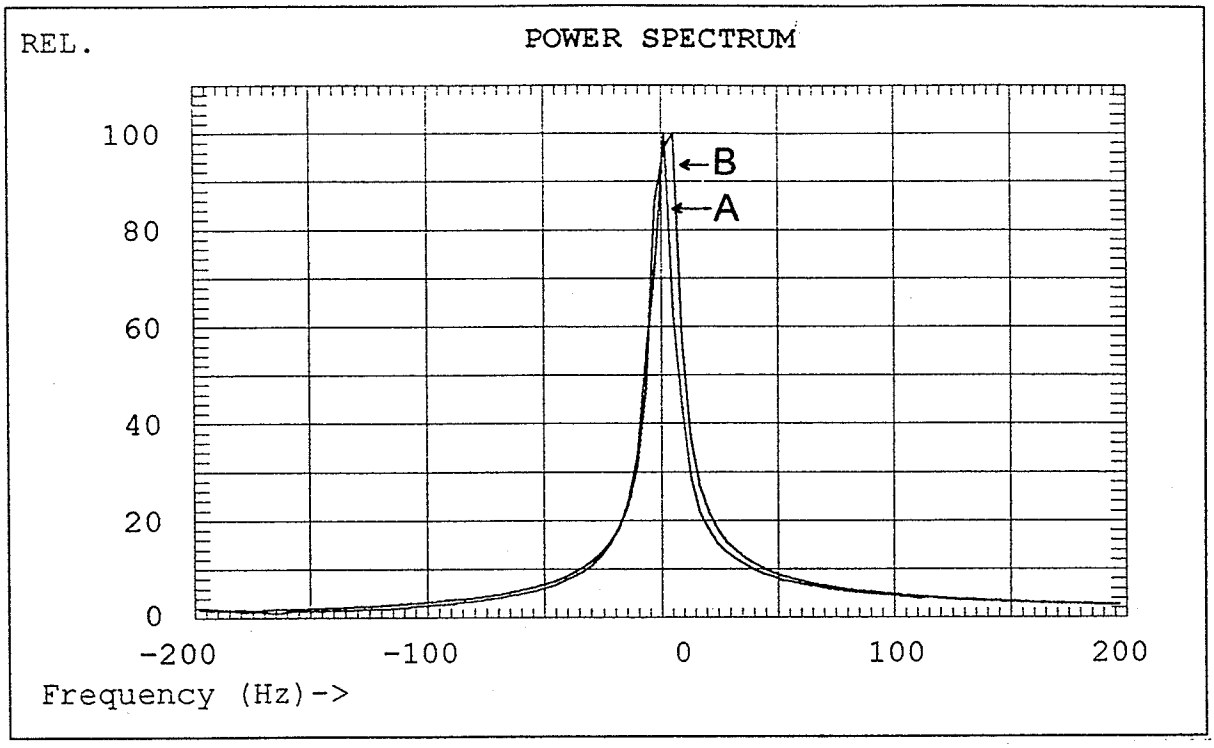

Figure 19. Power spectrum from a Nicomp 380 ZLS Submicron Particle Sizer / Zeta Potential Analyzer used for zeta potential measurement of positively charged lipid vesicles (+veLUVs). Peak A is the reference (zero mobility). Peak B is the lipid vesicle sample, which is shifted by 1.83 Hz with respect to reference peak due to the velocity of the vesicles moving along the electric field. The calculated average zeta potential was + 9.58 mV.

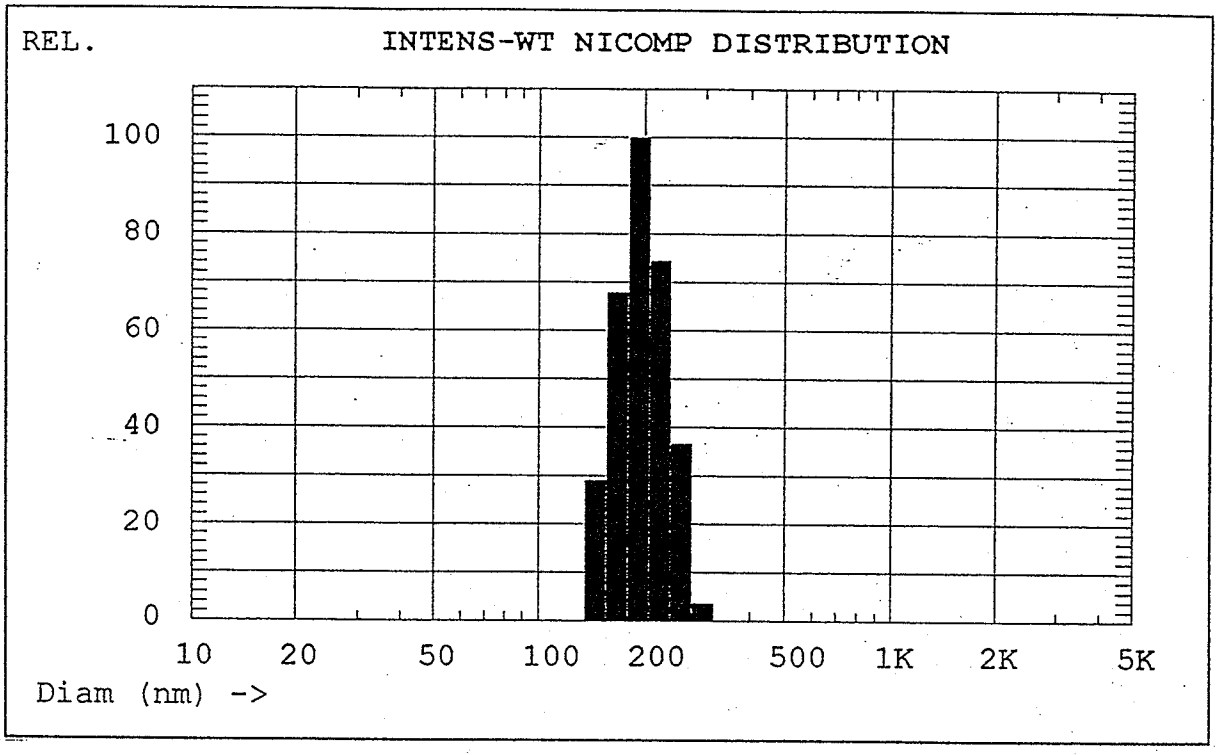

Figure 20. Particle size analysis of negatively charged lipid vesicles (-veLUVs) performed using Nicomp 380 ZLS Submicron Particle Sizer / Zeta Potential Analyzer. The intensity-weighted distribution plot shows a uni-modal peak. The mean diameter of the vesicles was 199 ± 37 nm (mean ± SD).

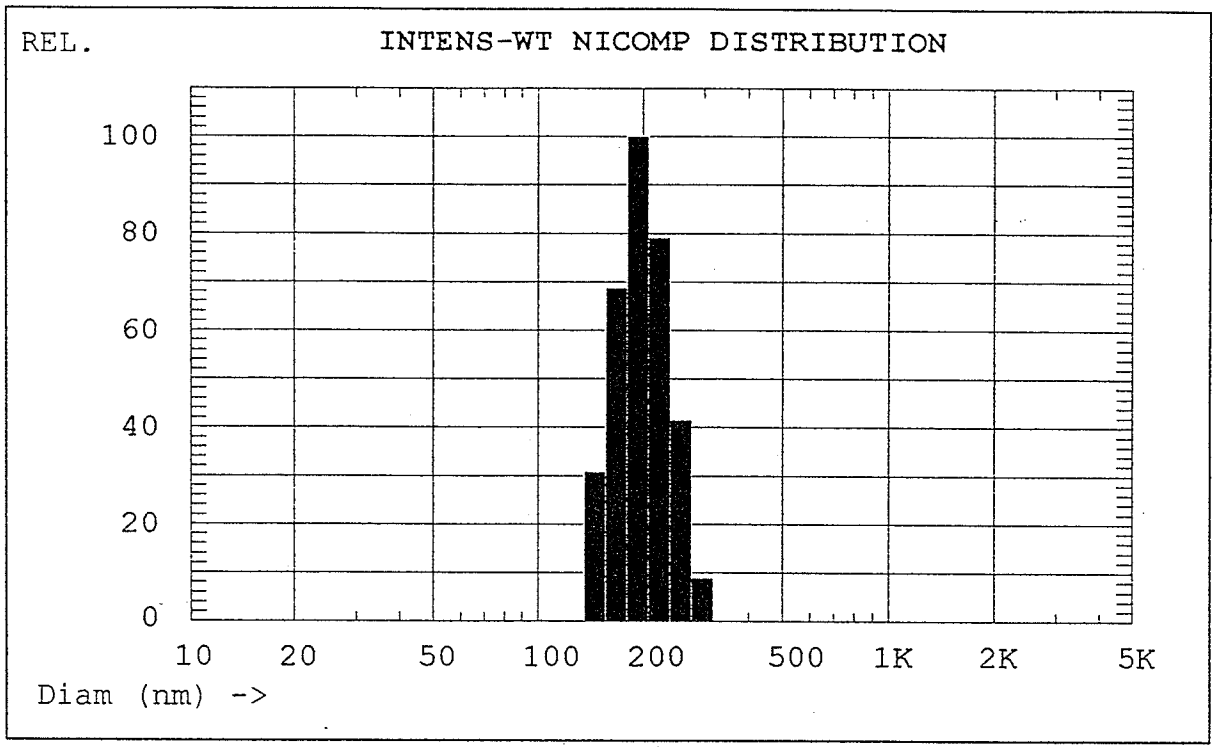

Figure 21. Particle size analysis of neutral lipid vesicles (neuLUVs) performed using Nicomp 380 ZLS Submicron Particle Sizer / Zeta Potential Analyzer. The intensity-weighted distribution plot shows a uni-modal peak. The mean diameter of the vesicles was 200 ± 39 nm (mean ± SD).

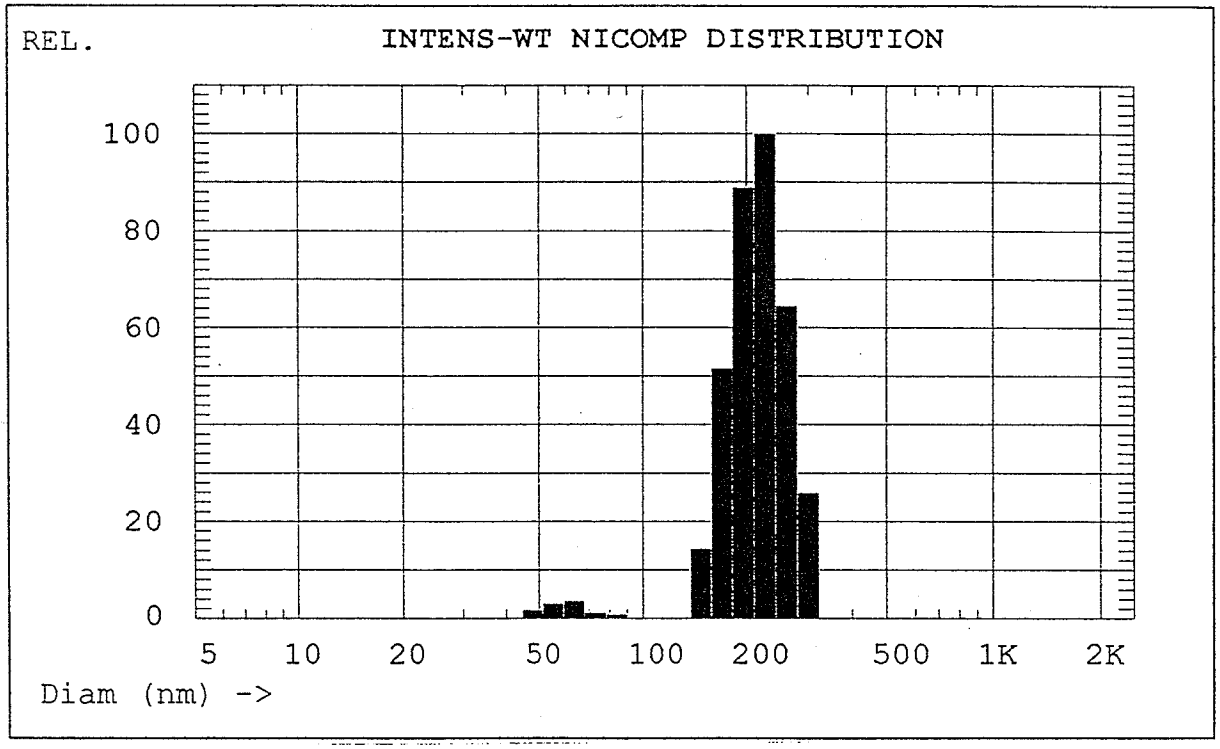

Figure 22. Particle size analysis of positively charged lipid vesicles (+veLUVs) performed using Nicomp 380 ZLS Submicron Particle Sizer / Zeta Potential Analyzer. The intensity-weighted distribution plot shows a bi-modal peak. The main peak constituted the majority of the vesicles (96.5%; 222 ± 35 nm) while a minor peak with mean diameter of (61.3 ± 8.7 nm) constituted only 3.5% of the total vesicles. Data are mean ± SD.

D.4.3. AOPA protein binding

Fig. 23 shows the fluorescence intensity of AOPA in the presence of ALB, ALB_{E1}, and PBS. Binding of AOPA to ALB and ALB_{E1} is shown in Figure 24 and was analyzed according to the method of Cogan et al. [130]. The apparent number of binding sites for ALB and ALB_{E1} was calculated to be 1.7. The calculated apparent dissociation constant (K_d) for ALB and ALB_{E1} was 0.024 μM and 0.016 μM, respectively ($p>0.05$). The data show that ALB and ALB_{E1} bind AOPA with comparable affinities. Based on these K_d values, the protein:ligand molar ratio used in all transfer assays was 10:1, a ratio at which more than 99% of the AOPA was bound to ALB or ALB_{E1}.

D.4.4. Partitioning of AOPA between binding proteins and lipid vesicles.

The relative distribution of AOPA between ALB or ALB_{E1} and lipid vesicles was determined by measuring the equilibrium fluorescence intensity before the addition of vesicles and the remaining fluorescence intensity after the addition of vesicles and applying equation 5. Data in Table 8 are presented as the partition ratio of AOPA between binding proteins and lipid vesicles. While partitioning of AOPA between the positive and negative lipid vesicles was highly significant ($p<0.0001$), there was no statistical difference in the partitioning of AOPA between ALB or ALB_{E1} and the neutral lipid vesicles. AOPA had the greatest preference for positively charged lipid vesicles followed by neutral LUVs and lastly negative LUVs. In all cases partitioning favored the binding proteins over vesicles. The result also implies that vesicle membrane surface charge has a

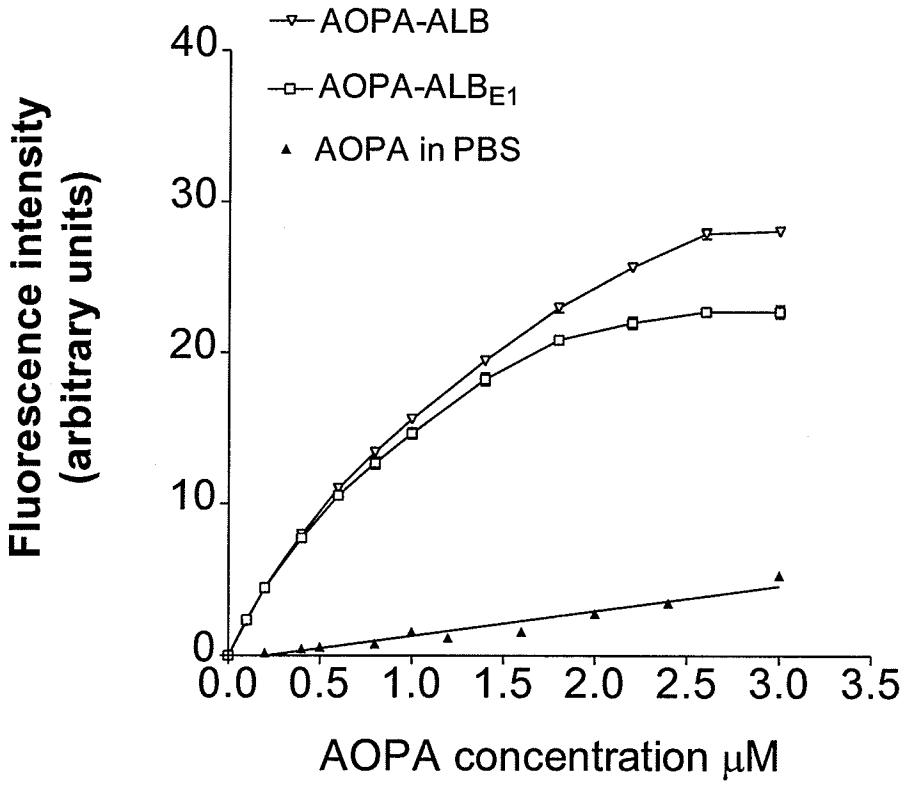

Figure 23. Binding of AOPA to ALB or ALB_{E1}. An increase in fluorescent intensity and saturation of 1 μM ALB (▽) or ALB_{E1} (□) when titrated with an increasing concentration of AOPA. Fluorescence intensity of AOPA alone in PBS (▲).

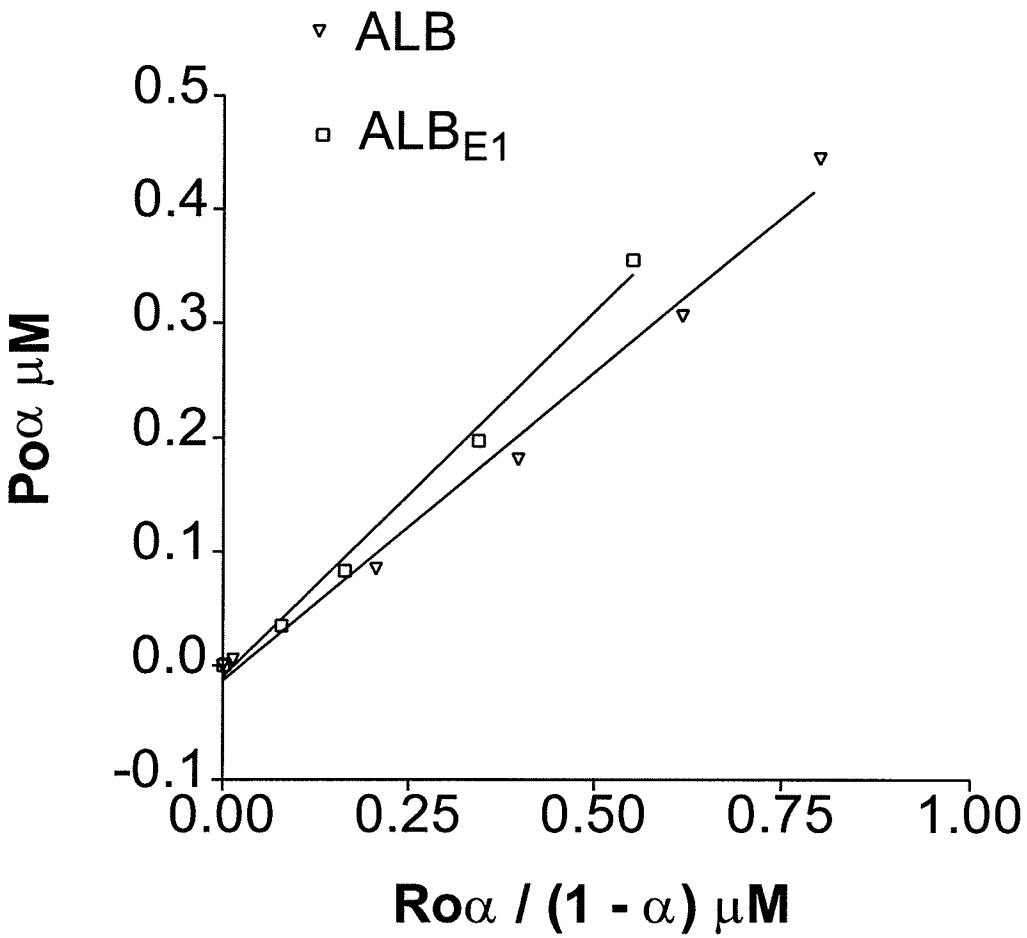

Figure 24. Binding data of AOPA to ALB or ALB_{E1} were analyzed as described in Materials and Methods. Po is the total protein concentration, Ro is the total AOPA concentration, and α is the fraction of free binding sites on protein molecule. The apparent K_d for ALB and ALB_{E1} were 0.024 and 0.016 μM, respectively.

Relative partitioning of AOPA between protein and lipid vesicles.

Protein	Negatively charged vesicles (-veLUVs)	Neutral vesicles (neuLUVs)	Positively charged vesicles (+veLUVs)
ALB	*270 ± 9	229 ± 9	*43 ± 9
ALB_e	*360 ± 37	219 ± 3	*66 ± 1.3

Table 8. Proteins (1 μM) were incubated with 0.1 μM AOPA at pH 7.4 and 37° C, as described in Materials and Methods. The fluorescence intensity was measured and the protein-AOPA complex was mixed with neutral, negatively, or positively charged lipid vesicles. At equilibrium, the remaining fluorescence reflected only the AOPA, which remained bound to the protein. The relative distribution of AOPA between protein and vesicles was then calculated using equation 5. Values are mean ± SEM, n = 4 to 8. Statistical comparisons were made between ALB and ALB_{E1}, * $p < 0.0001$.

remarkable effect on the partitioning of AOPA between protein and lipid vesicles.

D.4.5. Effect of lipid vesicle concentration on AOPA transfer to neuLUVs.

To discriminate between AOPA transfer occurring by aqueous diffusion and that occurring through a collisional interaction of protein and acceptor membrane, we examined AOPA transfer from binding protein as a function of increasing acceptor membrane concentration. Fig. 25 shows the transfer of AOPA from ALB or ALB_{E1} to neuLUV. Prior to the addition of vesicles, there was no difference in the maximum fluorescence intensity between the two proteins. Over a range of phospholipid:protein (mol/mol) of 20:1 to 100:1, the rate of transfer from both proteins increased linearly as the lipid vesicle concentration increased, suggesting that one possibility for the mechanism of fatty acid transfer from proteins is through a collisional interaction of the protein-fatty acid complex with the phospholipid membranes. If transfer occured solely through aqueous diffusion, we should not expect to see a change in the transfer rate as the number of acceptor vesicles was increased [117]. Interestingly the Y-intercepts for the regression lines in Figure 25 were 0.013 ± 0.001 sec^{-1} and 0.009 ± 0.0003 sec^{-1} for ALB and ALB_{E1}, respectively ($p>0.05$). The transfer rates at zero lipid vesicles concentration were estimated to be equivalent to the dissociation of AOPA into an aqueous phase (K_{off}) [118]. The values were much lower than those values reported using other techniques [36, 52].

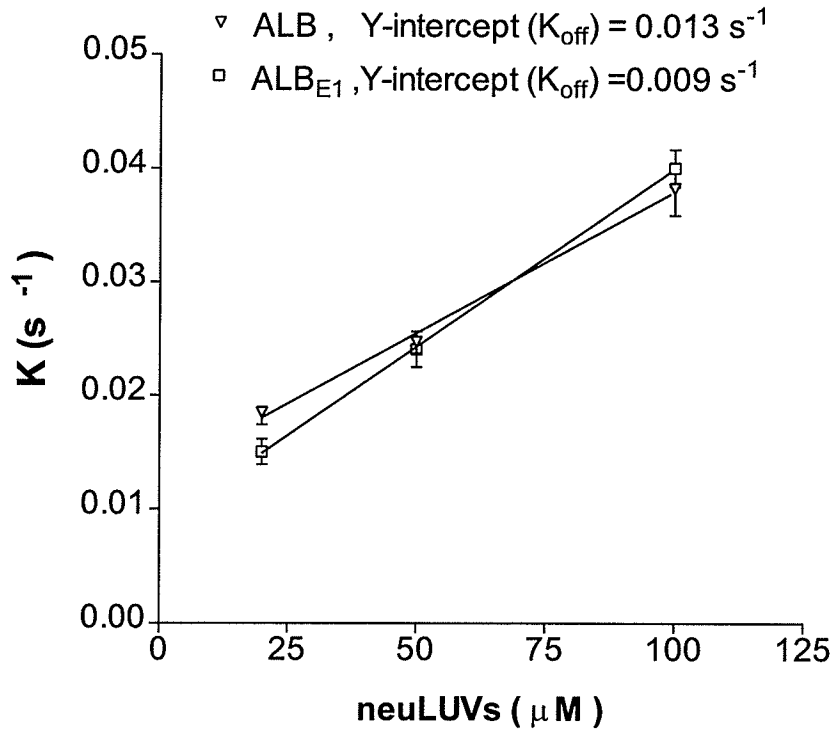

Figure 25. Effect of acceptor membrane concentration on AOPA transfer from binding proteins. The transfer of 0.1 μ M AOPA from 1.0 μ M ALB (▽) or ALB_{E1} (□) to neutral acceptor vesicles. Transfer was monitored at 37° C. The estimated K_{off} (Y-intercept at zero lipid vesicles concentration) for ALB and ALB_{E1} were 0.013 ± 0.001and 0.009 ± 0.0003 s^{-1}, respectively. Data are mean ± SEM, n = 4.

D.4.6. Effect of ionic strength on AOPA transfer to neuLUVs.

If transfer of AOPA from extracellular binding proteins to acceptor vesicles occurred through aqueous diffusion, then the rate of transfer may be affected by changing the aqueous solubility of the ligand [118]. Conversely, if transfer occurred solely by a collisional interaction, then the transfer rate ought to be unaffected by changes in ligand solubility. Fig. 26 shows that an increase in sodium chloride concentration resulted in a nonlinear decrease in the rate of AOPA transfer from ALB or ALB_{E1}. The decrease in transfer rates was linear up to 540 mM sodium chloride. At higher concentrations (>540 mM), the decrease in transfer rate appeared to reach a nadir. Although the results indicate that some AOPA transfer must be occurring through diffusion, the observed decrease in the transfer rates due to possible changes in protein binding and/or lipid vesicles integrity by increasing ionic strength must not be ruled out (see discussion).

D.4.7. Effect of pH on AOPA transfer to neuLUVs

To determine the effect of ionization state on fatty acid transfer between binding protein and neuLUV, the transfer of AOPA was studied as a function of pH (Figure 27). At pH 4.0, AOPA transfer rate from both proteins to lipid vesicles was significantly lower ($p<0.0001$) than at neutral pH. The transfer rate of AOPA from ALB and ALB_{E1} decreased slightly at pH 8.5 compared to pH 7.4 ($p>0.05$). The relative binding of AOPA to either ALB or ALB_{E1} (measured as the maximum fluorescence intensity of AOPA bound to ALB or ALB_{E1}) was similar at pH 7.4

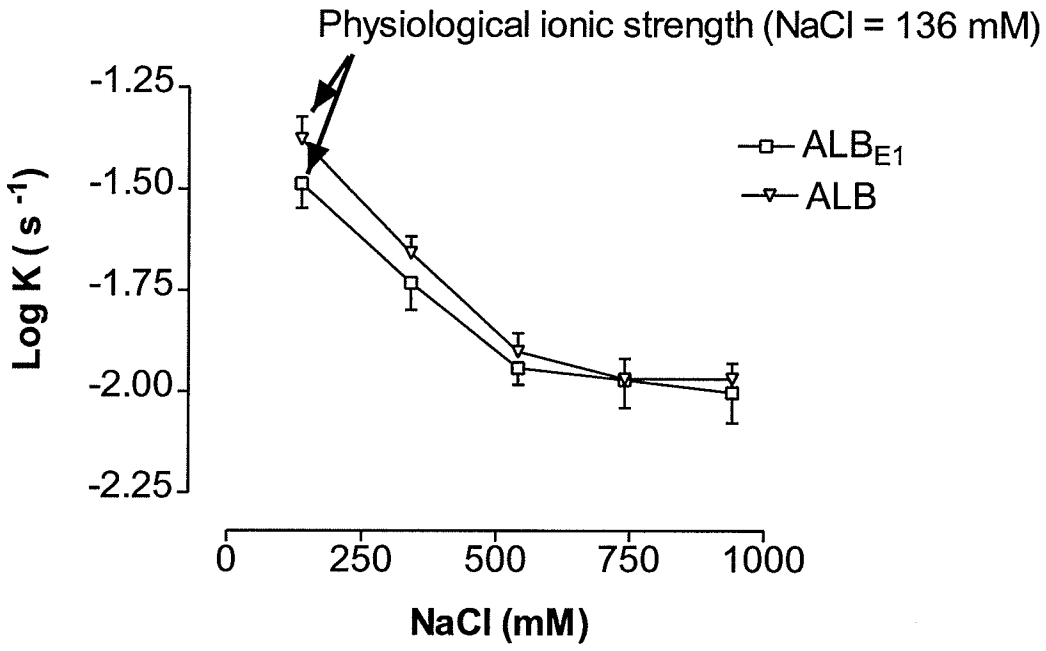

Figure 26. Effect of ionic strength on AOPA transfer from binding proteins. Transfer of 0.1 μM AOPA from 1.0 μM ALB (▽) or ALB_{E1} (□) to 100 μM neutral acceptor vesicles. Sodium chloride concentration of lipid vesicles and ligand-protein solutions were adjusted before mixing. Data are mean ± SEM, n = 4.

$Fmax_{pH} / Fmax_{7.4}$

pH	4.0	7.4	8.5
ALB	0.50	1.0	1.0
ALB_{E1}	0.47	1.0	0.96

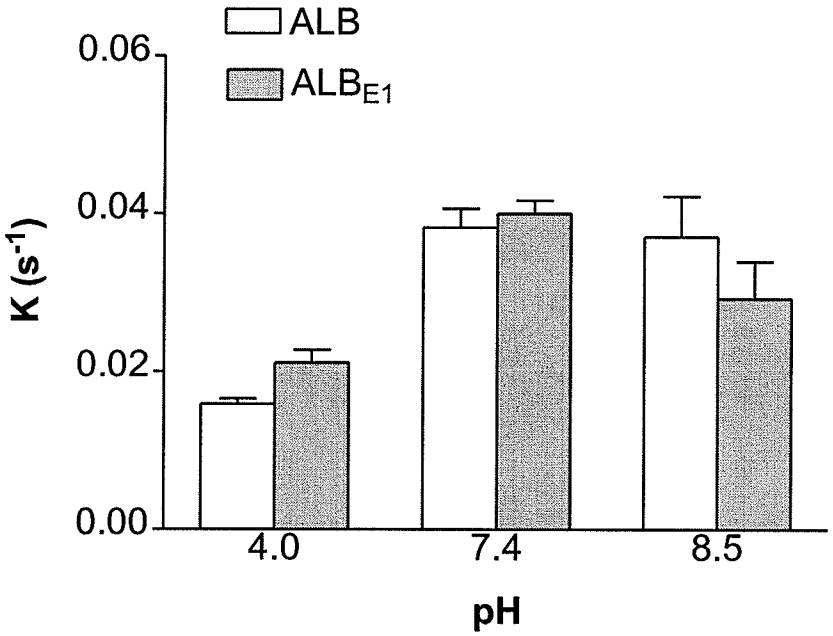

Figure 27. Effect of pH on AOPA transfer and protein binding. Transfer of 0.1 μM AOPA from 1.0 μM ALB (light bars) or ALB_{E1} (dark bars) to 100 μM neutral lipid vesicles at 37°C and at different pH values. Ligand-protein solutions and lipid vesicles were incubated at each pH before assay. Inset: $Fmax_{pH}$ is the maximum observed fluorescence intensity at designated pH; $Fmax_{7.4}$ is the maximum observed fluorescent intensity at pH 7.4. Data are mean ± SEM, n =4.

and 8.5 but significantly lower at pH 4.0 (see Fig. 27, inset). This result suggests that ionization of AOPA alone is not an important determinant of the transfer process as expected if AOPA transfer was solely through diffusion. In addition, the data suggest that maximum binding to protein accompanies faster transfer rates.

D.4.8. Effect of phospholipid surface charge on AOPA transfer.

To explore the effect of membrane properties on the transfer rate of AOPA from ALB or ALB_{E1}, we measured the AOPA transfer rates to acceptor membranes of different surface charges. Figures 28 and 29 show the transfer rate results of AOPA from ALB and ALB_{E1} to negatively and positively charged vesicles. Transfer of AOPA from ALB_{E1} to negative LUV was significantly greater than ALB ($p<0.01$). Conversely, transfer of AOPA from ALB_{E1} to positive LUV was significantly lower than in the presence of ALB ($p<0.0001$). Also, the AOPA transfer rate to negatively charged vesicles in the presence of ALB was significantly lower than that to positively charged vesicles ($p<0.001$). In contrast, the AOPA transfer rate in the presence of ALB_{E1} was significantly higher when negatively charged vesicles were used as acceptor membranes as compared to positively charged vesicles ($p<0.001$).

D.4.9. Effect of ALB concentration on AOPA transfer rate

To investigate further the role of ALB in AOPA transfer to model membranes, we measured the transfer rate of AOPA to +veLUVs in the

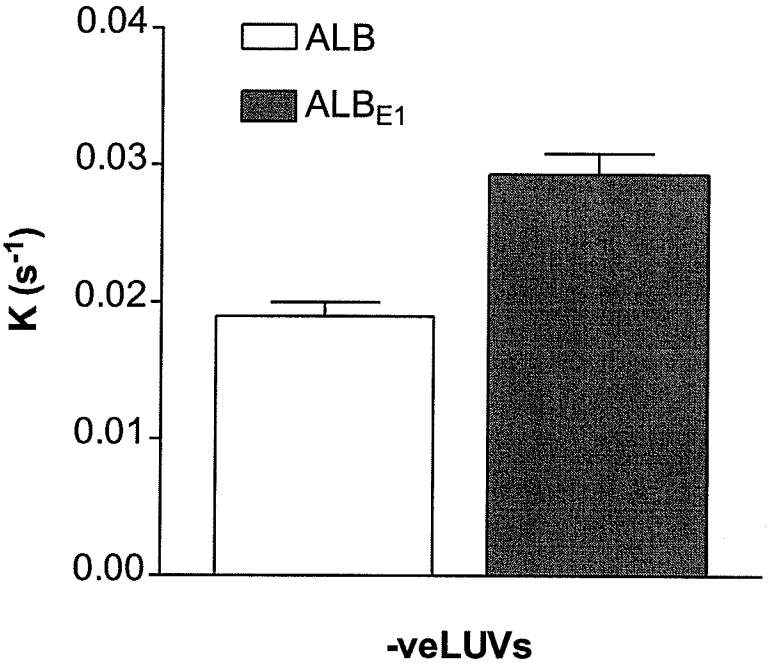

Figure 28. Effect of vesicle surface charge on AOPA transfer. Transfer of 0.1 μM AOPA from 1.0 μM ALB or ALB_{E1} to 100 μM -veLUVs. Rates were 0.019 ± 0.01 s^{-1} and 0.029 ± 0.0015 s^{-1} from ALB and ALB_{E1}, respectively. Data represent the mean ± SEM, n = 4 to 8. P= 0.0024

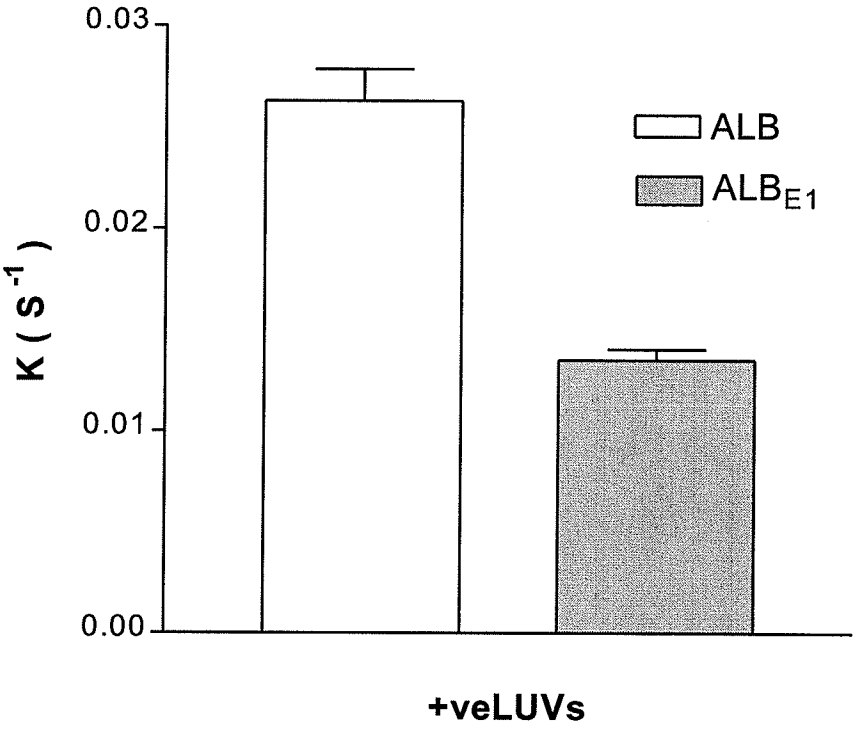

Figure 29. Effect of vesicle surface charge on AOPA transfer. Transfer of 0.1 μM AOPA from 1.0 μM ALB or ALB_{E1} to 100 μM +veLUVs. Rates were 0.026 ± 0.0015 s^{-1} and 0.014 ± 0.0005 s^{-1} from ALB and ALB_{E1}, respectively. Data represent the mean ± SEM, n = 4 to 8, P< 0.0001

presence of 1.0, and 10.0 μM ALB and at low AOPA to ALB molar ratio e.g. 0.1. Using these protein concentrations and low AOPA to ALB molar ratio, the free AOPA concentration is predicted to be unchanged and independent on ALB concentration [34]. Figure 30 shows that the transfer rate of AOPA from 10 μM ALB was significantly higher than from 1.0 μM ALB ($p<0.0001$). These data imply that the AOPA-ALB bound fraction is an important determinant in transfer.

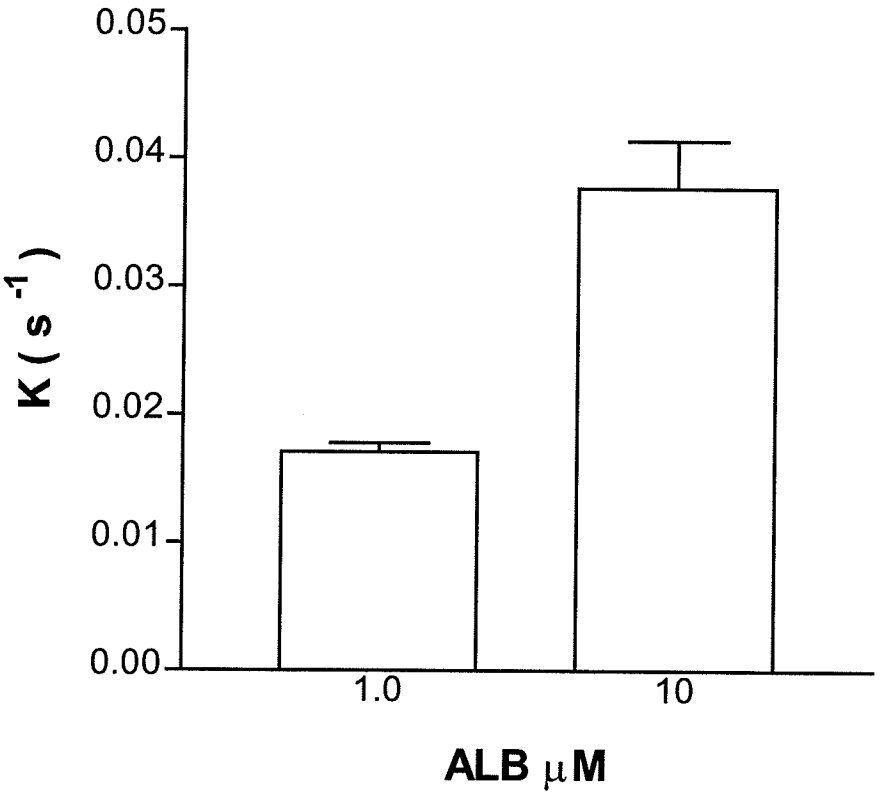

Figure 30. Effect of ALB concentration on AOPA transfer rate. Transfer of AOPA from 1.0 and 10.0 μM ALB to 63 μM +veLUVs. For the two protein concentrations, AOPA-to-ALB molar ratio was 0.1. Data represent the mean ± SEM, n = 4. P is < 0.0001.

D.5. Discussion

One of the first barriers that long-chain fatty acids must overcome prior to entry into the cytoplasm is binding to the outer plasma membrane leaflet followed by transmembrane flux. Traversing the lipid bilayer has been argued to occur by either diffusion through the lipid bilayer [131] or transport via a fatty acid binding protein resident on the plasma membrane of hepatocytes [42]. Investigating the role of extracellular binding proteins on the hepatic uptake of protein-bound palmitate, our group has published evidence supporting the notion that an ionic interaction between the protein-ligand complex and the hepatocyte cell surface is likely to be responsible for supplying ligand from the protein-bound fraction to the cell [52]. In those reports we showed that hepatocyte uptake of [^{3}H]-palmitate was greatest when the binding protein contained a net positive charge at physiological pH compared with the binding proteins contained a net negative charge.

To further explore the uptake process, we used liposomes as model membranes. Liposomes or lipid vesicles are widely accepted as model membranes in variety of biological, physiological, and pathological studies. This model system is of great benefit in various studies by providing more experimental freedom. However, because of their structural versatility, their physical properties such as vesicle size, phospholipid composition, surface charge, bilayer fluidity, and lamellarity are important factors to be considered in any study. Such variables could significantly affect the interpretation of

experimental results and may potentially lead to misleading conclusions. Thus for accurate and precise interpretation of our data, we tested the physical characteristic of our lipid vesicle preparations to ensure reproducibility. We used three lipid vesicle preparations that were similar in their phospholipid composition / concentration, vesicle size, unilamillarity and transition temperature but differed in their net surface charge at physiological pH (Table 7).

We examined the initial transfer rate of AOPA from ALB (pI=4.8) and ALB_{E1} (pI=7.5) to neutral as well as charged LUVs. The results show that; (a) AOPA transfer rate is a first order process and best described by monoexponential equation plus a constant; (b) the mechanism of transfer involves two steps occurring concomitantly, an aqueous-diffusion mediated process and a collisional mediated process; (c) FFA transfer by a specific or nonspecific membrane-protein interaction provides the possibility of regulating the movement of these substrates by changes in membrane composition and structure. Figure 31 provides a useful view about the proposed kinetic model for the transfer process.

Partitioning of anthroyloxy labeled long-chain fatty acid between protein and lipid membranes is known to be affected by pH, site of attachment of anthroyloxy moiety on acyl fatty acid chain and, lipid vesicle surface charge [121, 123]. The relative partitioning of AOPA between binding protein and lipid vesicle (Table 8) depicts the highest partitioning was for negatively charged vesicles in the presence of ALB (negatively charged), followed by neutral, and

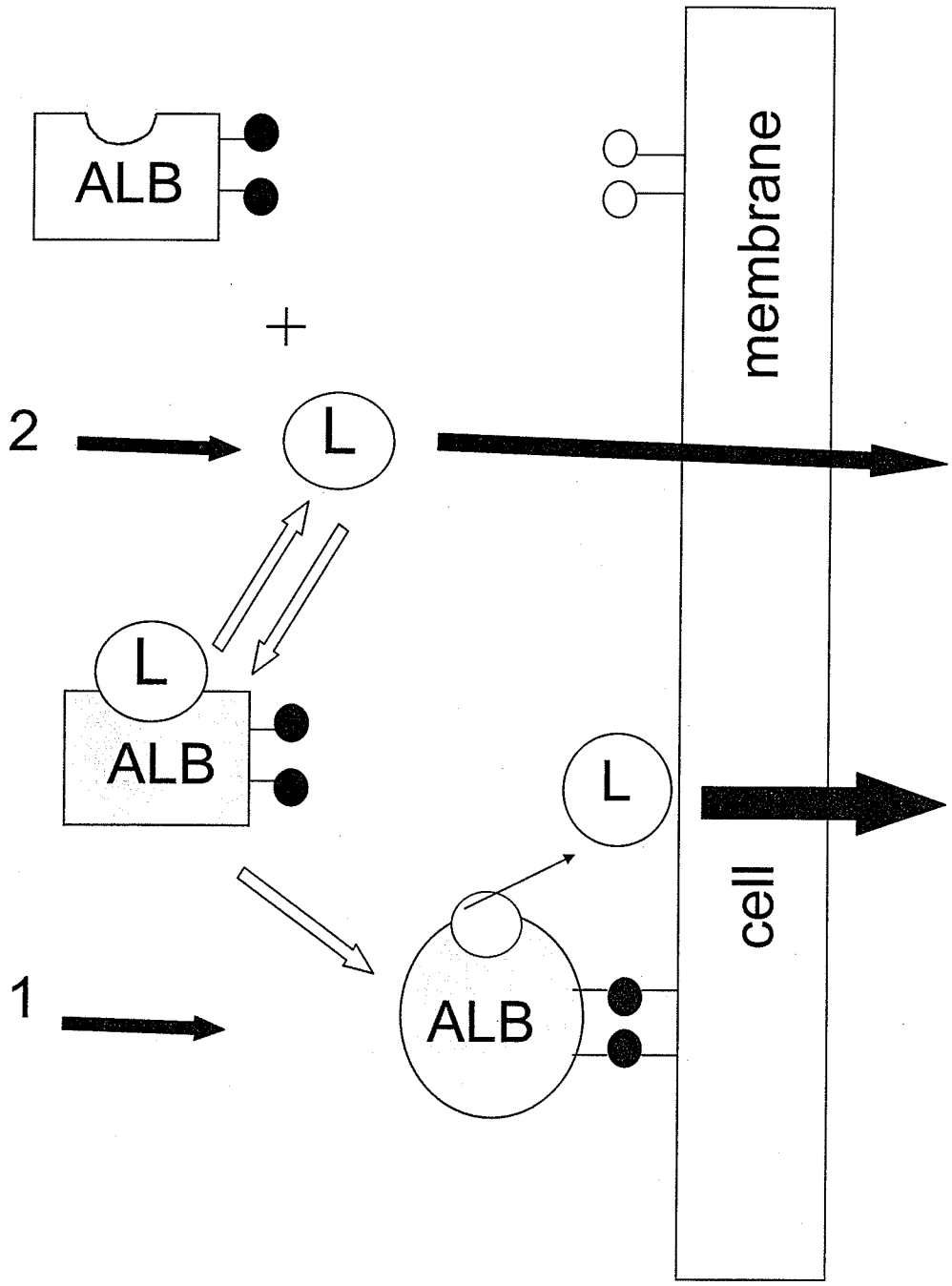

Figure 31. Schematic representation of albumin-mediated transfer. Transfer of ligand to the cell membrane could be in two ways. One pathway is bound form (➔). Second pathway is unbound form (→).

lastly positively charged vesicles. Greatest partitioning of AOPA between binding protein and vesicle favored the neutral binding protein ALB_{E1}. Similar profiles have been reported for the cationic drugs propranolol, tetracaine, and procaine (pKa values 9.5, 8.5, 9.0, respectively) binding to negative and neutral liposomes [132]. In that case, however, highest partitioning was reported to be with the negatively charged liposome surface. Because partitioning of AOPA favored the binding proteins rather than vesicles by approximately two orders of magnitude, it was necessary to use higher acceptor to donor ratios in the transfer assay experiments to ensure that unidirectional transfer was monitored (final molar ratio of lipid vesicles to protein was 100).

There was no statistical difference in the equilibrium binding constant for AOPA:ALB ($4.2x10^7$ M^{-1}) and AOPA:ALB_{E1} ($6.2x10^7$ M^{-1}). Values were much lower than those reported using radiolabeled long-chain fatty acids, e.g., [^{3}H]-palmitate:ALB – ($2.2x10^8$ M^{-1}) [133] and [^{3}H]-palmitate:ALB_{E1} – ($1.49x10^8$ M^{-1}) [133], using the fluorescent probe ADIFAB ($1.2x10^8$ M^{-1}) [63] or using red cell ghosts and [^{3}H]-oleate:ALB ($1.3x10^8$ M^{-1}) [134]. The difference in values may be attributed to the bulky fluorescent group attached to the palmitic acid molecule. This group could be expected to hinder proper AOPA binding to the ALB binding site. Also, the molar ratio of AOPA:protein used in the present study was much higher (range 0.1-3.0) than those using tracer concentrations of radiolabeled long-chain fatty acid such that some binding may occur to the secondary sites leading to a lower overall equilibrium binding constant. Because the equilibrium

binding constants for AOPA to ALB or ALB_{E1} were similar, the unbound AOPA fraction also was similar in the presence of ALB and ALB_{E1} in the transfer studies.

The Y-intercept for the data shown in Figure 25 using neutral vesicles allow us to estimate a dissociation rate constant (K_{off}) for the AOPA:binding protein complexes. Transfer rate at zero lipid vesicles concentration was suggested to be equivalent to the dissociation of AOPA into an aqueous phase (K_{off}) [118]. Interestingly the Y-intercepts for the regression lines were 0.013 $\pm$ 0.001 s^{-1} and 0.009 $\pm$ 0.0003 s^{-1} for ALB and ALB_{E1}, respectively. The observed transfer rates were estimated to be equal to the dissociation rates of AOPA from binding proteins into water plus collision-mediated transfer rates (see below). The K_{off} values were much lower than those determined using [^{3}H]-palmitate and ALB (0.070 sec^{-1}) or ALB_{E1} (0.070 sec^{-1}). The latter values were determined by transfer rate measurements of [^{3}H]-palmitate from binding proteins to a solid phase acceptor such as albumin-agarose (see chapter three) [133]. Weisiger et al. reported higher results for [^{3}H]-oleate dissociating from albumin, 0.14 sec^{-1} [36]. If part of the transfer, however, involved a direct collisional transfer of ligand, the observed dissociation rate may be an overestimate of the true rate.

The possibility that AOPA transfer occurred via a collisional mechanism (protein-vesicle) was examined by increasing the concentration of the acceptor membrane. If direct transfer was an important process in the overall uptake process, then we expect to observe an increase in the AOPA transfer rate as the

acceptor membrane concentration is increased [118, 121]. Figure 25 showed that there was an increase in the quenching of AOPA fluorescence, which reflected a higher AOPA transfer rate to the lipid vesicle membrane. Similar results were shown to occur with AOFA transfer from I-FABP to lipid vesicles (egg phophatidylcholine) but not from L-FABP [118] or bilirubin transfer from ALB to model membranes [126].

To further examine the mechanism(s), diffusion and/or direct transfer, through which AOPA is transferred to lipid vesicles, we altered the aqueous solubility by increasing the solution ionic strength through the addition of NaCl. It has been postulated that if the transfer process was dominated by diffusion (direct transfer being not important) then by increasing the solution ionic strength, the transfer rate would be expected to decrease linearly as solution ionic strength is increased. Conversely, if no change occured in the transfer rate then this would indicate that a direct transfer mechanism was involved in the transfer process [118]. The data in Figure 26 show that transfer initially decreased with an increase in ionic strength. However, at higher ionic strengths (>500 mM NaCl) the AOPA transfer remains constant. This type of relationship between transfer rate and ionic strength is consistent with the kinetic salt effect on electrostatic interactions (in this case the dissociation process) [118]. This means that the aqueous solubility of AOPA may be an important factor in the transfer process. Another possibility for the observed initial decrease in AOPA transfer rate was that the hydrophobic and electrostatic protein-membrane

interactions were disrupted by high salt concentrations [124, 135]. Thus, the collisional AOPA transfer from ALB or ALB_{E1} would decrease as ionic strength increased. A similar profile has been observed with the effect of ionic strength on the transfer of anthroyloxy labeled palmitic acid from rat adipocyte fatty acid binding protein to zwitterionic small unilamellar vesicles. This protein was thought to transfer ligand through collisional interaction with membranes [124].

We further examined the possibility that increasing salt concentration might affect the lipid bilayer structure and / or lipid vesicle mean size. Increasing NaCl concentration causes vesicle fusion, as indicated by the increase in vesicle mean size and a broader particle size distribution compared to the same vesicles at physiological ionic strength (Table 7). The changes in physical structure of the lipid vesicles may, in part, explain the decrease in the transfer rate of AOPA from ALB or ALB_{E1}. It has been shown that fluorescence polarization of 1,6-diphenyl-1,3,5-hexatriene (DPH) incorporated into SUVs was increased as ionic strength increased, indicating an increase in the phospholipid acyl chain order and a decrease in the lipid motional freedom [125]. If lipid motional freedom is important for an effective collisional interaction between ALB or ALB_{E1} and lipid membranes then, we might expect to observe a decrease in AOPA transfer rate.

Another possible effect of increasing phospholipid acyl chain order was that the orientation of charged groups in phospholipids e.g. negative charge on phosphate group and positive charge on choline group could be altered in such

way that hydrophobic and / or electrostatic interaction of ALB or ALB_{E1} with lipid membranes is reduced and thus affecting the AOPA transfer rate [125, 136].

The possibility that the binding of AOPA to ALB or ALB_{E1} was affected by increasing NaCl concentration is unlikely, since the observed relative maximum fluorescence intensity at each NaCl concentration compared to the maximum fluorescence intensity at physiological ionic strength was similar.

The effect of pH on AOPA binding and transfer from both proteins to neuLUVs was examined in order to investigate the role of AOPA ionization and aqueous solubility. The maximum fluorescence intensity of AOPA in the presence of ALB and ALB_{E1} and the transfer rate decreased significantly at low pH, suggesting that ionization of the fatty acid carboxyl group is an important determinant of transfer. Interestingly, a small but not statistically significant decrease of AOPA transfer from both proteins was observed at pH 8.5, in contrast to the maximum transfer rate observed at neutral pH. Overall, our data show that higher ligand binding to protein accompanies faster transfer rate and both processes are optimal at neutral pH.

These results further demonstrate that ionization alone is not the only determinant of the transfer process, the extent of AOPA binding to protein is also an important determinant of this process. It is important to note that structural changes in the albumin molecule (Neutral-Fast and Neutral-Base transitions) may be partially responsible for the observed pH effect on AOPA binding and

transfer. Such conformational changes (unfolding) in albumin affect the intrinsic ligand properties and may also affect its interaction with membranes [137].

This study showed that transfer of AOPA bound to ALB (pI=4.8-5.0) was significantly faster to positively charged LUVs than to negatively charged LUVs. In contrast, the transfer of AOPA bound to ALB_{E1} (pI=7.0-7.5) was significantly faster to negatively charged LUVs than to positively charged LUVs. The observed transfer dependence upon surface charge may reflect an electrostatic interaction between charged phospholipid head groups in the membrane and opposite charges on the AOPA-protein complex. Another potential explanation is that presence of charged head groups on the membrane phospholipids which might cause secondary changes in the membrane bilayer structure e.g. phospholipid head group packing order in the membrane. These secondary changes could increase or decrease the accessibility of binding protein to the lipophilic site of the membrane. The observed differences in AOPA transfer rates to charged LUVs are unlikely due to differences in vesicle size and / or lamellarity since the particle size measurement (Table 7) and electron micrographs showed no difference in the three vesicle preparations. Similar dependence on transfer of ligands to negatively charged liposomes was shown by Wootan and Storch [117]. They reported enhanced transfer of AOPA to negatively charged liposomes but in the presence of adipocyte and heart fatty acid binding proteins. These proteins have pI values similar to ALB_{E1} [138]. They also reported that transfer likely involved a collisional interaction between

binding protein and liposome surface. The dependence on surface charge also has been reported by Sugawara et al. [139] for the uptake of the anionic compounds ceftixime, benzyloxyindoleacetic acid, ceftibuten and S-1006 by large unilamellar vesicles. Investigating the role of surface charge on the transfer process in the presence of ALB has not been reported to our knowledge.

In an attempt to elucidate the role of ALB in the transfer process, we measured the AOPA transfer rate in the presence of two low ALB concentrations at a fixed AOPA to ALB molar ratio. Under this condition, the free AOPA concentration is predicted to be unchanged. [34]. The protein-bound AOPA concentration was increased with increasing protein concentration. If the transfer process occurred solely from the unbound AOPA fraction and independent of ALB concentration, we would not expect to see a difference in the measured transfer rates. Data in Figure 30, however, show that the transfer rate increased significantly with increasing ALB concentration. This result leads us to suggest that transfer of AOPA occurred from both the free and protein-bound fractions.

In summary, the present study shows that the transfer process of LCFA from ALB to model membranes may involve both diffusion to the membrane surface and a direct collisional effect. In contrast to the known aqueous diffusion mechanism observed for transfer of lipophilic compounds such as cholesterol and phospholipids, bovine serum albumin does not only function as an extracellular buffer for FFA levels but also as a delivery vehicle via its direct interaction with membranes. Our results support other reports on the effect of

albumin binding on cellular uptake [71, 140] as well as our previous reports that electrostatic interactions between the albumin-ligand complex and hepatocyte or myocyte surfaces modulate the kinetics of free fatty acid uptake [52, 133].

Chapter five

Summary and conclusions

Summary and conclusions

1- Most literature values of fatty acids partition ratios determined using heptane-buffer portioning technique appear to be underestimated because of the presence of radiolabeled impurities in the manufacturer-supplied radiolabeled ligand.

2- The reported low values of high affinity binding constants (K_a) of albumin for fatty acids need to be readjusted.

3- The apparent dependence of K_a on the albumin concentration was most likely due to the presence of radiolabeled artifacts. The equilibrium binding constant for ALB-palmitate complex is independent of protein concentration.

4- Presence of radiolabeled impurities can lead to overestimation of the radiolabeled-ligand cellular uptake thus leading to misinterpretation of the uptake study.

5- The unbound palmitate concentration is ONLY constant at low ALB concentrations (< 10 uM) and at low ALB-palmitate molar ratio (1:1 and 1:2). Cellular uptake studies using high ligand-protein molar ratio must not be interpreted based on the assumption that the unbound ligand concentration is constant.

6- Using heptane-buffer partitioning technique, the determined value of unbound palmitate concentration at physiological albumin concentration is comparable to the literature values ($\approx$ 7.5 nM).

7- Hepatocytes and cardiac myocytes can directly utilize ALB-complexed fatty acids as substrates for uptake. This process requires the interaction between the complex and cell surface.

8- The positively charged residues on the surface of proteins are important for the formation of protein-membrane complex. Most if not all plasma membranes of eukaryotic cells have a net negative charge thus a ligand-protein complex having a net positive charge at physiological pH is likely to deliver its cargo faster than a ligand-protein complex having a net negative charge.

9- It is reasonable to expect that hepatic or cardiac drug uptake from physiological proteins (albumin, α_1-acid glycoprotein, conalbumin) is different and depends on the protein net surface charge. For example drug bound to conalbumin may have higher cellular uptake than if it is bound to albumin. This becomes clinically important in a condition where there is a disturbance and / or deficiency in plasma binding proteins.

10- With a better understanding of the role of cell surface in the uptake of protein-bound ligand, future research work could be directed at uncovering the molecular mechanism of the uptake process.

References

1. Evans, J.R., Lionel H. Opie, and Joseph C. Shipp, *Metabolism of palmitic acid in perfused rat heart.* Am. J. Physiol, 1963. **205**(4): p. 766-770.

2. Neely, J.R., and Howard E. Morgan., *Relationship between carbohydrate and lipid metabolism and energy balance of heart muscle. Ann Rev Physiol.* Vol. 36. 1974. p. 413-459.

3. Marks, D.B., Allan D. Marks, and Collen M. Smith, *Basic Medical Biochemistry. A Clinical Approach.* 1996, Maryland: Williams & Wilkins.

4. Amri, E.Z., G. Ailhaud, and P.A. Grimaldi, *Fatty acids as signal transducing molecules: involvement in the differentiation of preadipose to adipose cells.* J Lipid Res, 1994. **35**(5): p. 930-7.

5. Yamashita, A., T. Sugiura, and K. Waku, *Acyltransferases and transacylases involved in fatty acid remodeling of phospholipids and metabolism of bioactive lipids in mammalian cells.* J Biochem (Tokyo), 1997. **122**(1): p. 1-16.

6. Jackson, C.S., P. Zlatkine, C. Bano, P. Kabouridis, B. Mehul, M. Parenti, G. Milligan, S.C. Ley, and A.I. Magee, *Dynamic protein acylation and the*

regulation of localization and function of signal-transducing proteins. Biochem Soc Trans, 1995. **23**(3): p. 568-71.

7. Mundy, D.I., *Protein palmitoylation in membrane trafficking.* Biochem Soc Trans, 1995. **23**(3): p. 572-6.

8. Anderson, M.P. and M.J. Welsh, *Fatty acids inhibit apical membrane chloride channels in airway epithelia.* Proc Natl Acad Sci U S A, 1990. **87**(18): p. 7334-8.

9. Ordway, R.W., J.J. Singer, and J.V. Walsh, Jr., *Direct regulation of ion channels by fatty acids.* Trends Neurosci, 1991. **14**(3): p. 96-100.

10. Philipson, K.D. and R. Ward, *Effects of fatty acids on Na+-Ca2+ exchange and Ca2+ permeability of cardiac sarcolemmal vesicles.* J Biol Chem, 1985. **260**(17): p. 9666-71.

11. Ordway, R.W., J.V. Walsh, Jr., and J.J. Singer, *Arachidonic acid and other fatty acids directly activate potassium channels in smooth muscle cells.* Science, 1989. **244**(4909): p. 1176-9.

12. Amri, E.Z., B. Bertrand, G. Ailhaud, and P. Grimaldi, *Regulation of adipose cell differentiation. I. Fatty acids are inducers of the aP2 gene expression.* J Lipid Res, 1991. **32**(9): p. 1449-56.

13. Levay-Young, B.K. and S. Nandi, *Spermidine is necessary for, but not the only mediator of, linoleic acid-stimulated alpha-casein accumulation in mouse mammary epithelial cells.* Endocrinology, 1989. **125**(3): p. 1513-8.

14. Dulbecco, R., M. Bologna, and M. Unger, *Control of differentiation of a mammary cell line by lipids.* Proc Natl Acad Sci U S A, 1980. **77**(3): p. 1551-5.

15. Grimaldi, P.A., S.M. Knobel, R.R. Whitesell, and N.A. Abumrad, *Induction of aP2 gene expression by nonmetabolized long-chain fatty acids.* Proc Natl Acad Sci U S A, 1992. **89**(22): p. 10930-4.

16. Keler, T., C.S. Barker, and S. Sorof, *Specific growth stimulation by linoleic acid in hepatoma cell lines transfected with the target protein of a liver carcinogen.* Proc Natl Acad Sci U S A, 1992. **89**(11): p. 4830-4.

17. Bihain, B.E., R.J. Deckelbaum, F.T. Yen, A.M. Gleeson, Y.A. Carpentier, and L.D. Witte, *Unesterified fatty acids inhibit the binding of low density*

lipoproteins to the human fibroblast low density lipoprotein receptor. J Biol Chem, 1989. **264**(29): p. 17316-21.

18. Kang, J.X. and A. Leaf, *Effects of long-chain polyunsaturated fatty acids on the contraction of neonatal rat cardiac myocytes.* Proc Natl Acad Sci U S A, 1994. **91**(21): p. 9886-90.

19. Pepe, S., K. Bogdanov, H. Hallaq, H. Spurgeon, A. Leaf, and E. Lakatta, *Omega 3 polyunsaturated fatty acid modulates dihydropyridine effects on L-type Ca2+ channels, cytosolic Ca2+, and contraction in adult rat cardiac myocytes.* Proc Natl Acad Sci U S A, 1994. **91**(19): p. 8832-6.

20. Amri, E.Z., L. Teboul, C. Vannier, P.A. Grimaldi, and G. Ailhaud, *Fatty acids regulate the expression of lipoprotein lipase gene and activity in preadipose and adipose cells.* Biochem J, 1996. **314**(Pt 2): p. 541-6.

21. Clark, A.B. and S.H. Quarfordt, *Apolipoprotein effects on the lipolysis of perfused triglyceride by heparin-immobilized milk lipase.* J Biol Chem, 1985. **260**(8): p. 4778-83.

22. Sammett, D. and A.R. Tall, *Mechanisms of enhancement of cholesteryl ester transfer protein activity by lipolysis.* J Biol Chem, 1985. **260**(11): p. 6687-97.

23. Civelek, V.N., J.A. Hamilton, K. Tornheim, K.L. Kelly, and B.E. Corkey, *Intracellular pH in adipocytes: effects of free fatty acid diffusion across the plasma membrane, lipolytic agonists, and insulin.* Proc Natl Acad Sci U S A, 1996. **93**(19): p. 10139-44.

24. Hamilton, J.A., V.N. Civelek, F. Kamp, K. Tornheim, and B.E. Corkey, *Changes in internal pH caused by movement of fatty acids into and out of clonal pancreatic beta-cells (HIT).* J Biol Chem, 1994. **269**(33): p. 20852-6.

25. Legaspi, A., M. Jeevanandam, H.F. Starnes, Jr., and M.F. Brennan, *Whole body lipid and energy metabolism in the cancer patient.* Metabolism, 1987. **36**(10): p. 958-63.

26. Brown, R.E., R.W. Steele, D.J. Marmer, J.L. Hudson, and M.A. Brewster, *Fatty acids and the inhibition of mitogen-induced lymphocyte transformation by leukemic serum.* J Immunol, 1983. **131**(2): p. 1011-6.

27. Tomita, T., Y. Yamasaki, M. Kubota, R. Tohdo, M. Katsura, M. Ikeda, I. Nakahara, Y. Shiba, M. Matsuhisa, and M. Hori, *High plasma free fatty acids decrease splanchnic glucose uptake in patients with non-insulin-dependent diabetes mellitus.* Endocr J, 1998. **45**(2): p. 165-73.

28. Reaven, G.M., C. Hollenbeck, C.Y. Jeng, M.S. Wu, and Y.D. Chen, *Measurement of plasma glucose, free fatty acid, lactate, and insulin for 24 h in patients with NIDDM.* Diabetes, 1988. **37**(8): p. 1020-4.

29. Luostarinen, R., M. Boberg, and T. Saldeen, *Fatty acid composition in total phospholipids of human coronary arteries in sudden cardiac death.* Atherosclerosis, 1993. **99**(2): p. 187-93.

30. Glickman, R.M., and S.M. Sabesin, *Lipoprotein metabolism-In: the liver. Biology and pathobiology*, ed. W.B.J. I.M. Arias, H. Popper, D. Schachter and D.A. Shafritz. 1988, New York: Raven Press, Ltd. 331-354.

31. Skipski, V., *Lipid composition of lipoproteins in normal and diseased states. In: Nelson Gj, ed. Blood lipids and lipoproteins: Quantitation, compostion, and Metabolism.* 1972, New York, NY: Wiley-Interscience. 471-583.

32. Pickart, L., *Increased ratio of plasma free fatty acids to albumin during normal aging and in patients with coronary heart disease.* Atherosclerosis, 1983. **46**(1): p. 21-8.

33. Levak-Frank, S., H. Radner, A. Walsh, R. Stollberger, G. Knipping, G. Hoefler, W. Sattler, P.H. Weinstock, J.L. Breslow, and R. Zechner, *Muscle-specific overexpression of lipoprotein lipase causes a severe myopathy characterized by proliferation of mitochondria and peroxisomes in transgenic mice.* J Clin Invest, 1995. **96**(2): p. 976-86.

34. Elmadhoun, B.M., G.Q. Wang, J.F. Templeton, and F.J. Burczynski, *Binding of [3H]palmitate to BSA.* Am J Physiol, 1998. **275**(4 Pt 1): p. G638-44.

35. Stremmel, W., G. Strohmeyer, and P.D. Berk, *Hepatocellular uptake of oleate is energy dependent, sodium linked, and inhibited by an antibody to a hepatocyte plasma membrane fatty acid binding protein.* Proc Natl Acad Sci U S A, 1986. **83**(11): p. 3584-8.

36. Weisiger, R.A. and W.L. Ma, *Uptake of oleate from albumin solutions by rat liver. Failure to detect catalysis of the dissociation of oleate from albumin by an albumin receptor.* J Clin Invest, 1987. **79**(4): p. 1070-7.

37. Weisiger, R., J. Gollan, and R. Ockner, *Receptor for albumin on the liver cell surface may mediate uptake of fatty acids and other albumin-bound substances.* Science, 1981. **211**(4486): p. 1048-51.

38. Rose, C.P. and C.A. Goresky, *Constraints on the uptake of labeled palmitate by the heart. The barriers at the capillary and sarcolemmal surfaces and the control of intracellular sequestration.* Circ Res, 1977. **41**(4): p. 534-45.

39. Spitzer, J.J., *Effect of lactate infusion on canine myocardial free fatty acid metabolism in vivo.* Am J Physiol, 1974. **226**(1): p. 213-7.

40. Ballard, F.B., William H. Danforth, Siegfried Naegle and Richard J. Bing, *Myocardial Metabolism of Fatty Acids.* J Clin Invest, 1960. **39**: p. p. 717-723.

41. Glatz, J.F., J.J. Luiken, F.A. van Nieuwenhoven, and G.J. Van der Vusse, *Molecular mechanism of cellular uptake and intracellular translocation of fatty acids.* Prostaglandins Leukot Essent Fatty Acids, 1997. **57**(1): p. 3-9.

42. Berk, P.D. and D.D. Stump, *Mechanisms of cellular uptake of long chain free fatty acids.* Mol Cell Biochem, 1999. **192**(1-2): p. 17-31.

43. Burczynski, F.J. and Z.S. Cai, *Palmitate uptake by hepatocyte suspensions: effect of albumin.* Am J Physiol, 1994. **267**(3 Pt 1): p. G371-9.

44. Pond, S.M., C.K. Davis, M.A. Bogoyevitch, R.A. Gordon, R.A. Weisiger, and L. Bass, *Uptake of palmitate by hepatocyte suspensions: facilitation by albumin?* Am J Physiol, 1992. **262**(5 Pt 1): p. G883-94.

45. Burczynski, F.J., Z.S. Cai, J.B. Moran, and E.L. Forker, *Palmitate uptake by cultured hepatocytes: albumin binding and stagnant layer phenomena.* Am J Physiol, 1989. **257**(4 Pt 1): p. G584-93.

46. Burczynski, F.J., Z.S. Cai, J.B. Moran, T. Geisbuhler, and M. Rovetto, *Palmitate uptake by cardiac myocytes and endothelial cells.* Am J Physiol, 1995. **268**(4 Pt 2): p. H1659-66.

47. Samuel, D., S. Paris, and G. Ailhaud, *Uptake and metabolism of fatty acids and analogues by cultured cardiac cells from chick embryo.* Eur J Biochem, 1976. **64**(2): p. 583-95.

48. Paris, S., D. Samuel, Y. Jacques, C. Gache, A. Franchi, and G. Ailhaud, *The role of serum albumin in the uptake of fatty acids by cultured cardiac cells from chick embryo.* Eur J Biochem, 1978. **83**(1): p. 235-43.

49. Horie, T., T. Mizuma, S. Kasai, and S. Awazu, *Conformational change in plasma albumin due to interaction with isolated rat hepatocyte.* Am J Physiol, 1988. **254**(4 Pt 1): p. G465-70.

50. Reed, R.G. and C.M. Burrington, *The albumin receptor effect may be due to a surface-induced conformational change in albumin.* J Biol Chem, 1989. **264**(17): p. 9867-72.

51. Srivastava, D.K. and S.A. Bernhard, *Metabolite transfer via enzyme-enzyme complexes.* Science, 1986. **234**(4780): p. 1081-6.

52. Burczynski, F.J., G.Q. Wang, and M. Hnatowich, *Effect of binding protein surface charge on palmitate uptake by hepatocyte suspensions.* Br J Pharmacol, 1997. **120**(7): p. 1215-20.

53. Wadhwani, K.C., M. Shimon-Hophy, and S.I. Rapoport, *Enhanced permeabilities of cationized-bovine serum albumins at the blood-nerve*

and blood-brain barriers in awake rats. J Neurosci Res, 1992. **32**(3): p. 407-14.

54. Nishida, M., A. Ookubo, Y. Hashimura, A. Ikawa, Y. Yoshimura, K. Ooi, T. Suzuki, Y. Tomita, and J. Kawada, *Interaction of bovine serum albumin with the surface of a microcrystalline aluminum oxide hydroxide compound: a possible new type of phosphate adsorbent.* J Pharm Sci, 1992. **81**(8): p. 828-31.

55. Ghitescu, L., M. Desjardins, and M. Bendayan, *Immunocytochemical study of glomerular permeability to anionic, neutral and cationic albumins.* Kidney Int, 1992. **42**(1): p. 25-32.

56. Norde, W. and J. Lyklema, *The Adsorption of Human Plasma Albumin and Bovine Pancreas Ribonuclease at Negatively Charged Polystyren Surfaces.* Journal of Colloid and Interface Science, 1978. **66**(2): p. 257-265.

57. Galis, Z., L. Ghitescu, and M. Simionescu, *Fatty acids binding to albumin increases its uptake and transcytosis by the lung capillary endothelium.* Eur J Cell Biol, 1988. **47**(2): p. 358-65.

58. Raicu, M., D. Alexandru, A. Fixman, and N. Simionescu, *Albumin binding sites are expressed on the abluminal plasma membrane of capillary endothelium.* J Submicrosc Cytol Pathol, 1991. **23**(1): p. 1-8.

59. Park, C.H. and T. Maack, *Albumin absorption and catabolism by isolated perfused proximal convoluted tubules of the rabbit.* J Clin Invest, 1984. **73**(3): p. 767-77.

60. Wall, D.A. and T. Maack, *Endocytic uptake, transport, and catabolism of proteins by epithelial cells.* Am J Physiol, 1985. **248**(1 Pt 1): p. C12-20.

61. Smith, K.R. and R.T. Borchardt, *Permeability and mechanism of albumin, cationized albumin, and glycosylated albumin transcellular transport across monolayers of cultured bovine brain capillary endothelial cells.* Pharm Res, 1989. **6**(6): p. 466-73.

62. Sorrentino, D., R.B. Robinson, C.L. Kiang, and P.D. Berk, *At physiologic albumin/oleate concentrations oleate uptake by isolated hepatocytes, cardiac myocytes, and adipocytes is a saturable function of the unbound oleate concentration. Uptake kinetics are consistent with the conventional theory.* J Clin Invest, 1989. **84**(4): p. 1325-33.

63. Richieri, G.V., A. Anel, and A.M. Kleinfeld, *Interactions of long-chain fatty acids and albumin: determination of free fatty acid levels using the fluorescent probe ADIFAB.* Biochemistry, 1993. **32**(29): p. 7574-80.

64. Demant, E.J. and M. Sehested, *Recognition of anthracycline binding domains in bovine serum albumin and design of a free fatty acid sensor protein.* Biochim Biophys Acta, 1993. **1156**(2): p. 151-60.

65. Burczynski, F.J., J.B. Moran, Z.S. Cai, and E.L. Forker, *Beta-lactoglobulin enhances the uptake of free palmitate by hepatocyte monolayers: the relative importance of diffusion and facilitated dissociation.* Can J Physiol Pharmacol, 1990. **68**(2): p. 201-6.

66. Moran, J.B., F.J. Burczynski, R.F. Cheek, T. Bopp, and E.L. Forker, *Protein binding of palmitate measured by transmembrane diffusion through polyethylene.* Anal Biochem, 1987. **167**(2): p. 394-9.

67. Burczynski, F.J., J.B. Moran, and Z.S. Cai, *Facilitated dissociation of albumin-fatty acid complexes by rat hepatocytes.* J Pharmacol Exp Ther, 1993. **267**(2): p. 714-9.

68. Spector, A.A., J.E. Fletcher, and J.D. Ashbrook, *Analysis of long-chain free fatty acid binding to bovine serum albumin by determination of stepwise equilibrium constants.* Biochemistry, 1971. **10**(17): p. 3229-32.

69. Burczynski, F.J., G.Q. Wang, and M. Hnatowich, *Effect of nitric oxide on albumin-palmitate binding.* Biochem Pharmacol, 1995. **49**(1): p. 91-6.

70. Pond, S.M., R.A. Gordon, A.L. Simi, and D.J. Winzor, *Further observations on the measurement of fatty acid incorporation by erythrocyte ghosts to quantify unbound palmitate concentration in albumin-palmitate mixtures.* Anal Biochem, 1996. **237**(2): p. 232-8.

71. Fleischer, A.B., W.O. Shurmantine, B.A. Luxon, and E.L. Forker, *Palmitate uptake by hepatocyte monolayers. Effect of albumin binding.* J Clin Invest, 1986. **77**(3): p. 964-70.

72. Burczynski, F.J., S.M. Pond, C.K. Davis, L.P. Johnson, and R.A. Weisiger, *Calibration of albumin-fatty acid binding constants measured by heptane-water partition.* Am J Physiol, 1993. **265**(3 Pt 1): p. G555-63.

73. Cai, Z.S., F.J. Burczynski, B.A. Luxon, and E.L. Forker, *On the design and interpretation of experiments to elucidate albumin- dependent hepatic uptake.* Am J Physiol, 1992. **262**(6 Pt 1): p. G1127-37.

74. Borgstrom, B., *Investigation on Lipid Separation Methods. Separation of Cholesterol Esters, Glycerides and Free Fatty Acids.* Acta. Physiol. Scand., 1952. **25**: p. 111-119.

75. Goodman, D.S., *The distribution of fatty acids between n-heptane and aqueous phosphate buffer.* J. Am. Chem. Soc., 1958. **80**: p. 3887-3891.

76. Smith, R., and C. Tanford., *Hydrophobicity of long chain n-alkyl carboxylic acida, as measured by their distribution between heptane and aqueous solutions.* Proc. Natl. Acad. Sci., 1973. **70**: p. 289-293.

77. Bolton, S., *Pharmaceutical Statistics. Practical and Clinical Applications.* 1990, New York: Marcel Dekker.

78. Simpson, R.B., J.D. Ashbrook, E.C. Santos, and A.A. Spector, *Partition of fatty acids.* J Lipid Res, 1974. **15**(4): p. 415-22.

79. Mukerjee, P., *Dimerization of anions of long-chain fatty acids in aqueous solutions and hydrophobic properties of the acids.* J. Phys. Chem., 1965. **69**: p. 2821-2827.

80. Bojesen, I.N. and E. Bojesen, *Water-phase palmitate concentrations in equilibrium with albumin-bound palmitate in a biological system.* J Lipid Res, 1992. **33**(9): p. 1327-34.

81. Spector, A.A., K. John, and J.E. Fletcher, *Binding of long-chain fatty acids to bovine serum albumin.* J Lipid Res, 1969. **10**(1): p. 56-67.

82. Trigatti, B.L. and G.E. Gerber, *A direct role for serum albumin in the cellular uptake of long-chain fatty acids.* Biochem J, 1995. **308**(Pt 1): p. 155-9.

83. Klapper, M.H., and I. M. Klotz, *Acylation with Dicarboxlic Acid Anhydrides.* Methods. Enz., 1972. **25**: p. 531-536.

84. Hoare, D.G. and D.E. Koshland, Jr., *A method for the quantitative modification and estimation of carboxylic acid groups in proteins.* J. Biol. Chem., 1967. **242**(10): p. 2447-53.

85. Butler, P.J.G., and B. S. Hartley, *Maleylation of Amino Groups.* Methods. Enz., 1972. **25**: p. 191-199.

86. Moore, S., and W. H. Stein, *A Modified Ninhydrin Reagent for the Photometeric Determination of Amino Acids and Related ompounds.* J. Biol. Chem., 1954. **211**: p. 907-913.

87. Islam, M., S. Qamar, and S. Tayyab, *Involvement of lysine residues of goat serum albumin in high-affinity binding of bilirubin.* Biochim Biophys Acta, 1994. **1205**(2): p. 171-7.

88. Verentchikov, A.N., W. Ens, and K.G. Standing, *Reflecting time-of-flight mass spectrometer with an electrospray ion source and orthogonal extraction.* Anal Chem, 1994. **66**(1): p. 126-33.

89. Fasman, G.D., *CRC Handbook of Biochemistry and Molecular Biology. 3 rd edition, Proteins.* Vol. 2. 1970, Boca Taton, Florida, USA: CRC Press, Inc.

90. Bradford, M.M., *A rapid and sensitive method for the quantitation of microgram quantities of protein utilizing the principle of protein-dye binding.* Anal Biochem, 1976. **72**: p. 248-54.

91. Stoscheck, C.M., *Quantitation of protein.* Methods Enzymol, 1990. **182**: p. 50-68.

92. Hillier, A.P., *Human thyroxine-binding globulin and thyroxine-binding pre-albumin: dissociation rates.* J Physiol, 1971. **217**(3): p. 625-34.

93. Glatz, J.F. and J.H. Veerkamp, *A radiochemical procedure for the assay of fatty acid binding by proteins.* Anal Biochem, 1983. **132**(1): p. 89-95.

94. Burczynski, F.J. and B.A. Luxon, *Is there facilitated uptake of fatty acids by the liver? Interpretation and analysis of experimental data.* Can J Physiol Pharmacol, 1995. **73**(4): p. 409-20.

95. Kirshenbaum, L.A. and D. de Moissac, *The bcl-2 gene product prevents programmed cell death of ventricular myocytes.* Circulation, 1997. **96**(5): p. 1580-5.

96. DeSante, D.C., L. Little, D.E. Peavy, and F. Vinicor, *Insulin-responsive cultured foetal-rat hepatocytes. Their preparation and characterization.* Biochem J, 1984. **223**(1): p. 39-46.

97. Burgaya, F., J. Peinado, S. Vilaro, M. Llobera, and I. Ramirez, *Lipoprotein lipase activity in neonatal-rat liver cell types.* Biochem J, 1989. **259**(1): p. 159-66.

98. Popov, D., M. Hasu, N. Ghinea, N. Simionescu, and M. Simionescu, *Cardiomyocytes express albumin binding proteins.* J Mol Cell Cardiol, 1992. **24**(9): p. 989-1002.

99. Collins, M., *Electrokinetic properties of dissociated chick embryo cells. I. pH- surface charge relationships and the effect of calcium ions.* J Exp Zool, 1966. **163**(1): p. 23-37.

100. Woo, J. and D.B. Cater, *A study of the cell surface of tumour, foetal and lymph-node cells by cell electrophoresis after antibody and enzymic treatment.* Biochem J, 1972. **128**(5): p. 1273-84.

101. Alberts, B., Bary, D., Lewis, J., Raff, M., Robert, K. and Watson, J., *Molecular Biology of the Cell, 3rd edn.* 1994, New York: Garland Publishing,.

102. Walter, H., E.J. Krob, and D.E. Brooks, *Membrane surface properties other than charge involved in cell separation by partition in polymer, aqueous two-phase systems.* Biochemistry, 1976. **15**(14): p. 2959-64.

103. Rivory, L.P., S.M. Pond, and D.J. Winzor, *The influence of pH on the interaction of lipophilic anthracyclines with bovine serum albumin. Quantitative characterization by measurement of fluorescence quenching.* Biochem Pharmacol, 1992. **44**(12): p. 2347-55.

104. Shiau, Y.F., R.J. Kelemen, and M.A. Reed, *Acidic mucin layer facilitates micelle dissociation and fatty acid diffusion.* Am J Physiol, 1990. **259**(4 Pt 1): p. G671-5.

105. Bos, O.J., J.F. Labro, M.J. Fischer, J. Wilting, and L.H. Janssen, *The molecular mechanism of the neutral-to-base transition of human serum albumin. Acid/base titration and proton nuclear magnetic resonance studies on a large peptic and a large tryptic fragment of albumin.* J Biol Chem, 1989. **264**(2): p. 953-9.

106. Carter, D.C. and J.X. Ho, *Structure of serum albumin.* Adv Protein Chem, 1994. **45**: p. 153-203.

107. Hasinoff, B.B., *Flash Photolusis Reactions of Myoglobin and Hemoglobin with Carbon Monoxide and Oxugen at Low Temperatures. Evidence for a Transient Diffusion-Controlled Reaction in Supercooled Solvents.* J. Phys. Chem., 1981. **85**: p. 526-531.

108. Berg, O.G., *Orientation constraints in diffusion-limited macromolecular association. The role of surface diffusion as a rate-enhancing mechanism.* Biophys J, 1985. **47**(1): p. 1-14.

109. Bass, L. and S.M. Pond, *The puzzle of rates of cellular uptake of protein-bound ligands. In: Pharmacokinetics: Mathematical and Statistical Approaches to Metabolism and Distribution of Chemicals and Drugs, edited by A. Pecile and A. Rescigno. London: Plenum,*. 1988. 241-265.

110. Collins, M., *Electrokinetic properties of dissociated chick embryo cells. Calcium ion binding by neural retinal cells.* J Exp Zool, 1966. **163**(1): p. 39-47.

111. Blazquez, E., A. Perez Castillo, and J.G. de Diego, *Characterization of glucagon receptors in liver membranes and isolated hepatocytes during rat ontogenic development.* Mol Cell Endocrinol, 1987. **49**(2-3): p. 149-57.

112. Burgaya, F., J. Peinado, M. Llobera, and I. Ramirez, *Hepatic endothelial lipase activity in neonatal rat liver.* Biosci Rep, 1989. **9**(5): p. 559-64.

113. McLean, L.R. and M.C. Phillips, *Mechanism of cholesterol and phosphatidylcholine exchange or transfer between unilamellar vesicles.* Biochemistry, 1981. **20**(10): p. 2893-900.

114. Arvinte,T. and K. Hildenbrand, *N-NBD-L-alpha-dilauroylphosphatidyl-ethanolamine. A new fluorescent probe to study spontaneous lipid transfer.* Biochim Biophys Acta, 1984. **775**(1): p. 86-94.

115. Pownall, H.J., D. Hickson, A.M. Gotto, Jr., and J.B. Massey, *Kinetics of spontaneous and plasma-stimulated sphingomyelin transfer.* Biochim Biophys Acta, 1982. **712**(1): p. 169-76.

116. Doody, M.C., H.J. Pownall, Y.J. Kao, and L.C. Smith, *Mechanism and kinetics of transfer of a fluorescent fatty acid between single-walled phosphatidylcholine vesicles.* Biochemistry, 1980. **19**(1): p. 108-16.

117. Wootan, M.G. and J. Storch, *Regulation of fluorescent fatty acid transfer from adipocyte and heart fatty acid binding proteins by acceptor*

membrane lipid composition and structure. J Biol Chem, 1994. **269**(14): p. 10517-23.

118. Hsu, K.T. and J. Storch, *Fatty acid transfer from liver and intestinal fatty acid-binding proteins to membranes occurs by different mechanisms.* J Biol Chem, 1996. **271**(23): p. 13317-23.

119. Hamilton, J.A. and D.P. Cistola, *Transfer of oleic acid between albumin and phospholipid vesicles.* Proc Natl Acad Sci U S A, 1986. **83**(1): p. 82-6.

120. Daniels, C., N. Noy, and D. Zakim, *Rates of hydration of fatty acids bound to unilamellar vesicles of phosphatidylcholine or to albumin.* Biochemistry, 1985. **24**(13): p. 3286-92.

121. Storch, J. and N.M. Bass, *Transfer of fluorescent fatty acids from liver and heart fatty acid- binding proteins to model membranes.* J Biol Chem, 1990. **265**(14): p. 7827-31.

122. Wootan, M.G., D.A. Bernlohr, and J. Storch, *Mechanism of fluorescent fatty acid transfer from adipocyte fatty acid binding protein to membranes.* Biochemistry, 1993. **32**(33): p. 8622-7.

123. Kim, H.K. and J. Storch, *Mechanism of free fatty acid transfer from rat heart fatty acid-binding protein to phospholipid membranes. Evidence for a collisional process.* J Biol Chem, 1992. **267**(28): p. 20051-6.

124. Herr, F.M., J. Aronson, and J. Storch, *Role of portal region lysine residues in electrostatic interactions between heart fatty acid binding protein and phospholipid membranes.* Biochemistry, 1996. **35**(4): p. 1296-303.

125. Storch, J. and A.M. Kleinfeld, *Transfer of long-chain fluorescent free fatty acids between unilamellar vesicles.* Biochemistry, 1986. **25**(7): p. 1717-26.

126. Zucker, S.D., W. Goessling, and J.L. Gollan, *Kinetics of bilirubin transfer between serum albumin and membrane vesicles. Insight into the mechanism of organic anion delivery to the hepatocyte plasma membrane.* J Biol Chem, 1995. **270**(3): p. 1074-81.

127. Campos, B., Y.D. Mo, T.R. Mealy, C.W. Li, M.A. Swairjo, C. Balch, J.F. Head, G. Retzinger, J.R. Dedman, and B.A. Seaton, *Mutational and crystallographic analyses of interfacial residues in annexin V suggest direct interactions with phospholipid membrane components.* Biochemistry, 1998. **37**(22): p. 8004-10.

128. MacDonald, R.C., R.I. MacDonald, B.P. Menco, K. Takeshita, N.K. Subbarao, and L.R. Hu, *Small-volume extrusion apparatus for preparation of large, unilamellar vesicles.* Biochim Biophys Acta, 1991. **1061**(2): p. 297-303.

129. Ames, B.N., *Assay of Phosphate and Phosphatase*. Methods in Enzymology. Vol. 8. 1966, New York: Academic Press Inc. 115-117.

130. Cogan, U., M. Kopelman, S. Mokady, and M. Shinitzky, *Binding affinities of retinol and related compounds to retinol binding proteins.* Eur J Biochem, 1976. **65**(1): p. 71-8.

131. Kleinfeld, A.M., *Lipid phase fatty acid flip-flop, is it fast enough for cellular transport?* J Membr Biol, 2000. **175**(2): p. 79-86.

132. Schlieper, P. and R. Steiner, *The effect of different surface chemical groups on drug binding to liposomes.* Chem Phys Lipids, 1983. **34**(1): p. 81-92.

133. Elmadhoun, B.M., G.Q. Wang, L.A. Kirshenbaum, and F.J. Burczynski, *Palmitate uptake by neonatal rat myocytes and hepatocytes Role of extracellular protein.* Eur J Biochem, 2001. **268**(11): p. 3145-53.

134. Bojesen, I.N. and E. Bojesen, *Oleic acid binding and transport capacity of human red cell membrane.* Acta Physiol Scand, 1996. **156**(4): p. 501-16.

135. Jones, J.D. and T.E. Thompson, *Mechanism of spontaneous, concentration-dependent phospholipid transfer between bilayers [published errata appear in Biochemistry 1990 May 15;29(19):4746 and 1991 Nov 5;30(44):10818].* Biochemistry, 1990. **29**(6): p. 1593-600.

136. Kim, H.K. and J. Storch, *Free fatty acid transfer from rat liver fatty acid-binding protein to phospholipid vesicles. Effect of ligand and solution properties.* J Biol Chem, 1992. **267**(1): p. 77-82.

137. Peters, T.J., *All about Albumin : Biochemistry, Genetics, and Medical Applications.* 1996, San Diego, California: Academic Press, Inc.

138. Glatz, J.F., R.J. Paulussen, and J.H. Veerkamp, *Fatty acid binding proteins from heart.* Chem Phys Lipids, 1985. **38**(1-2): p. 115-29.

139. Sugawara, M., A. Hashimoto, M. Kobayashi, K. Iseki, and K. Miyazaki, *Effect of membrane surface potential on the uptake of anionic compounds by liposomes.* Biochim Biophys Acta, 1994. **1192**(2): p. 241-6.